THE ROLE OF TRIGGER WAVES IN CANCER ANGIOGENESIS

by

Birses Debir

B.S., Astronomy and Space Sciences, Ege University, 2011

M.S., Physics, Boğaziçi University, 2015

Submitted to the Institute for Graduate Studies in
Science and Engineering in partial fulfillment of
the requirements for the degree of
Doctor of Philosophy

Graduate Program in Physics

Boğaziçi University

2022

ACKNOWLEDGEMENTS

To begin with I would like to thank Bowie, Queen, Epictetus, and Aurelius, Chagall, the sky upon the shores of my homeland where I've been watched over by the stars and welcomed by the sea. All of these keep me motivated to finish my PhD, and look beyond.

I would like to thank my advisor Prof. Burçin Ünlü for his enthusiasm on sharing endless supply of coffee, extra visionary ideas and his attempts of enduring my ideas by rubbing his face in an overly expressive way. I would also like to thank Prof. Kohandel and Cameron Meaney for their guidance and their patience during our collaboration.

I thank Natali Çizmeciyan and Emine Ertuğrul for their wonderful ideas, questions, and their support. During early years of PhD, I also have the chance to collaborate with Assoc. Prof. Levent Akant and Asist. Prof. Can Kozcaz, I learn many things from our interactions. Today I believe, I walk on the road that is newly paved and for that I would like to express my sincere gratitude to them for their help on finding this route.

Of course no PhD acknowledgements is complete without thanking to friends and family. I thank all my family and friends. Their affection, and honesty is my token of luck. I wrote this page for myself, so no names are given. I am forever in dept, for their support, and their laughter. My dark days were warmer, and sun beams were kinder with you. Finally I wanted to thank myself. Wonderful job finishing the thesis, now go get some fresh air. By the way, best of luck to anyone who wishes to write their thesis.

ABSTRACT

THE ROLE OF TRIGGER WAVES IN CANCER ANGIOGENESIS

This study includes mathematical modeling of biological observations and numerical solutions of these models. Our study focused on different phenomenons, including; vessel formation, intracellular calcium ion concentration, traveling wave solutions, and cytosol elasticity. Understanding signaling in diseases is essential for a proper response. For this reason, understanding the secondary messenger signaling that mechanisms often prefer to use and their interaction with the mechanisms enables the system's response to be better understood. This study examined the interaction of angiogenesis, a mechanism that contributes to tumor growth, and cytosolic calcium ion, an intracellular secondary messenger. Therefore, we simulated a mathematical model involving essential angiogenesis and calcium homeostasis elements using previously used models. In our simulations, we developed two and multiple cell scenarios and examined the results of our system in distributions of different angiogenic stimulus uptake. Since angiogenesis requires the cell to move in a specific direction, we simulated the cytosolic gelation-solution mechanism, inspired by another model used in the literature. We examined the condition under which the wave direction persists in the traveling wave configuration.

ÖZET

TETİK DALGALARININ KANSER ANJİOJENEZİNDEKİ ROLÜ

Bu çalışma biyolojik gözlemlerin matematiksel olarak modellenmesiyle ve bu modellenlerin nümerik çözümlerini içerir. Çalışmamızda yeni damar oluşumunu, hücre içi kalsiyum iyonu konsantrasyonunu, yürüyen dalga çözümlerini ve sitozol elastisitesini beraber inceledik. Hastalıklardaki hücre içi iletişimi anlamak onlara doğru şekilde müdehale etmek için önemlidir. Bu nedenle sistemlerin sıklıkla kullanmayı tercih ettiği ikincil elçi sinyallerini ve onların mekanizmalarla olan etkileşimini doğru kavramak, sistemin vereceği tepkinin daha iyi anlaşılabilir olmasını sağlar. Bu çalışmada, tümörün büyümesini sağlayan bir mekanizma olan anjiojenezin, hücre içi ikincil bir elçi olan kalsiyum iyonu ile olan etkileşimini inceledik. Bu nedenle anjiojenezin ve kalsiyumun homeostazının önemli elemanlarını içeren matematiksel bir modeli daha önce kullanılmış elemanları kullanarak simüle ettik. Simülasyonlarımızda iki ve çoklu hücre senaryoları geliştirip, farklı anjiojenik uyarıcı alımına ait dağılımlarda sistemimizin verdiği sonuçları inceledik. Anjiojenez hücrenin belirli bir yönde ilerlemesini gerektirdiği için, sitozolik jelasyon-solusyon mekanizmasını yine literatürde kullanılan bir başka modelden esinlenerek simüle ettik ve yürüyen dalga konfigurasyonunda dalganın hangi koşullarda bir yöne sahip olduğunu inceledik.

TABLE OF CONTENTS

LIST OF FIGURES

LIST OF TABLES

LIST OF SYMBOLS

b	The basal current of IP3R
c_i	Calcium Concentration of the ith cell
D	Diffusivity of Ca2+
D_0	Diffusivity of Ca2+
DLL_i	DLL4 concentration of the ith cell
$dllnotch_i$	DLL4-Notch concentration of the ith cell
HE_i	HE concentration of the ith cell
k_1'	The half-maximum of Ca2+ pumping
k_2'	The reactivation rate
k_1	Maximum total Ca2+ flux through IP3R
k_2	Maximum rate of Ca2+ pumping from the cytosol
k_3	Half maximum rate of Ca2+ pumping from the cytosol
k_4	Half maximum rate of DLL4 production
k_5	Association rate for dn complex
k_6	Disassociation rate for dn complex
k_7	Degradation rate of proteins
k_8	Catalyses rate for dn complex
k_9	Half maximum rate of NICD production
k_{10}	Mechanochemical autofeedback
k_{11}	Strength of calcium contribution
k_{flux}	The maximum $Ca2+$ flux from all IP3Rs
k_γ	The half maximum of Ca2+ pumping from the cytosol
$nicd_i$	NICD concentration of the ith cell
$notch_i$	Notch concentration of the ith cell
$R2_i$	R2 concentration of the ith cell
u_i	Dilation of the ith Cell
v_i	DLL4 concentration of the ith Cell
V_1	The rate of IPRs activated by $Ca2+$ binding

$VEGF_i$	VEGF concentration of the ith cell
w_i	Notch concentration of the ith Cell
x_i	DLL4-Notch concentration of the ith Cell
y_i	NICD concentration of the ith Cell
z_i	HE concentration of the ith Cell
β	Basal gene expression of proteins
β'	The rate of $Ca2+$ influx coming from the outside
γ	Maximum rate of pumped Ca2+
λ	Mechanochemical contribution to calcium
μ	IP3 concentration in the IP3R site
τ_n	The time constant
θ	Production rate of NICD
Θ	Production rate of DLL4
ζ	Negative feedback rate of HE on Calcium

LIST OF ACRONYMS/ABBREVIATIONS

AU	Arbitrary Units
Ca2+	Calcium Ion
CICR	Calcium Induced-Calcium Release
DLL4	Delta-Like Ligand 4
EC	Endothelial Cell
EMT	Epithelial-to-Mesenchymal Transition
ER	Endoplasmic Reticulum
ERK	extracellular Signal-Regulated Kinase
FA	Focal Adhesion
HE	Hairy and Enhancer-of-split Family
IP3	Inositol 1,4,5-trisphosphate
IP3R	Inositol 1,4,5-trisphosphate Receptor
NICD	Notch intracellular domain
NO	Nitric Oxide
PM	Plasma Membrane
SERCA	Sarco/Endoplasmic Reticulum Ca2+-ATPase
Tmem33	Transmembrane protein 33
TRPMC	Transient Receptor Potential Cation Channels
VEGF	Vascular Endothelial Growth Factor
VEGFR	Vascular Endothelial Growth Factor Receptor

1. INTRODUCTION

This thesis is written for two groups: first, the few who are interested in learning the matters of the topic, and second, the few who are interested in testing the issues of the thesis. I hope the reader, who belongs to either of these groups, will enjoy reading a part of the thesis. The thesis resides on the intersection between specific topics, and by its multidisciplinary nature, requires a certain level of knowledge on those. This dissertation will begin with a biological background including the main pillars of the problem: cancer, angiogenesis, calcium signalling, cell movement, signal transport. We will conclude the biological background chapter by giving a brief introduction to the problem from a biological perspective. Later, the mathematical background chapter will begin by a brief comment on mathematical modelling, and introduce the models we have used in construction of our models. Trigger wave, angiognecity, calcium oscillation and cell movement models will be introduced on this context. In the following two chapters, we will be discussing our models in a course following as biological motivation, introduction, established model, its results and discussion. Finally we will confine the thesis with an overall conclusion chapter.

2. BIOLOGICAL BACKGROUND

2.1. Cancer

An overall presentation of cancer disease is depicted with introducing some key terminology.

Cancer is a general term for sicknesses that occur due to abnormalities in cells leading them to grow unnaturally and invade different organs [6]. World Health Organization denotes cancer as being the leading cause of death worldwide [7].

According to the Global Cancer Statistics more than 19 million people added to the number of existing cancer patients yearly, and nearly 10 million people deceased from cancer [8]. In 2040, however, the number of cases is foreseen as 29.5 million and deaths as 16.4 million [9].

However, not all abnormally growing population of tissue, tumor is lethal. These mass of cells might also be benign tumors that do not spread to other tissues and are not classified as cancer. Only malign tumors which have the potential to spread to other tissues are called cancer, and this process is called metastasis [10].

Even though it comes about in different tissues and might go through various steps, all cancerous tissues join in some central traits, which are defined as hallmarks of cancer [1, 2, 11]. These innate features enable proliferative signaling, immortality, diversity creating mutations, angiogenesis, evading the immune system, uncontrollable in-cell energetics, inflammation, and resistance to cell death and invasion.

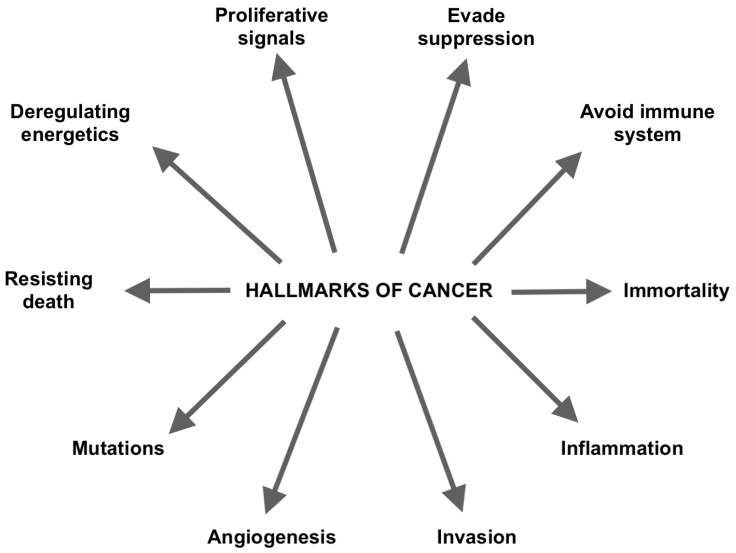

Figure 2.1. Hallmarks of cancer. Adapted from [1, 2].

Due to different characteristic features, hallmarks have been criticized, and Fouad and Aanei [11] redefine them in terms of similar but more inclusive properties.

Cancer treatment types are various since it is not a disease but a group of diseases. Cancer can be treated with one or more methods. Chemotherapy, a treatment option that is based on a single or a combination of drugs, is also preferred to be applied together with other methods, including radiation therapy, surgery, immunotherapy, electrical applications, or surgery [12]. However, these techniques are causing collateral damage and an economic burden to the patient. For that reason, new low-cost techniques are deeply needed.

Although cancer requires expensive treatment, some novel methods have been developed like calcium-electroporation are promising for being economically sustainable [13]. This selective drug effect the calcium homeostasis of the cell by electrifying the calcium injected region [13]—another novel treatment involving a change in the extracellular pH in the environment of the tumor. pH is particularly important in terms of metastasis. It alters cancer cell migration and invasion of remote tissues and

causes patient death [14, 15]. Calcium carbonate, a low-cost material that has been found in limestone, has been used for changing the local pH level of surrounding tissues of tumor by a new calcium carbonate nano-material [16]. In contrast with the other toxic agents, when the substance dissolves in the low pH environment, it dissolves into two non-toxic materials that the body is familiar with. This promising new nano-material is shown to affect tumor growth in a recent study [16]. Like these novel treatments, other new methods are needed for curing cancer.

2.2. Initial Angiogenesis

Here, we point out the parts of the pathway essential for understanding our mathematical model and its application.

Angiogenesis is a biological process by which existing vasculature sprouts new vessels to alleviate areas of oxygen deficiency. It is essential for the development, maintenance, and survival of tissues [17]. It also plays an essential role in many disorders [18]. For completion of angiogenesis several stages should be followed in order. In the initial steps, which comprises the topic of this thesis, the endothelial cells are budding from the already existed vessel. Then this budded cells moves towards the oxygen deficient area creating a thin branch of cells. Finally the vessel begins to form a lumen and strengthens and stabilizes the vessel the gap [19].

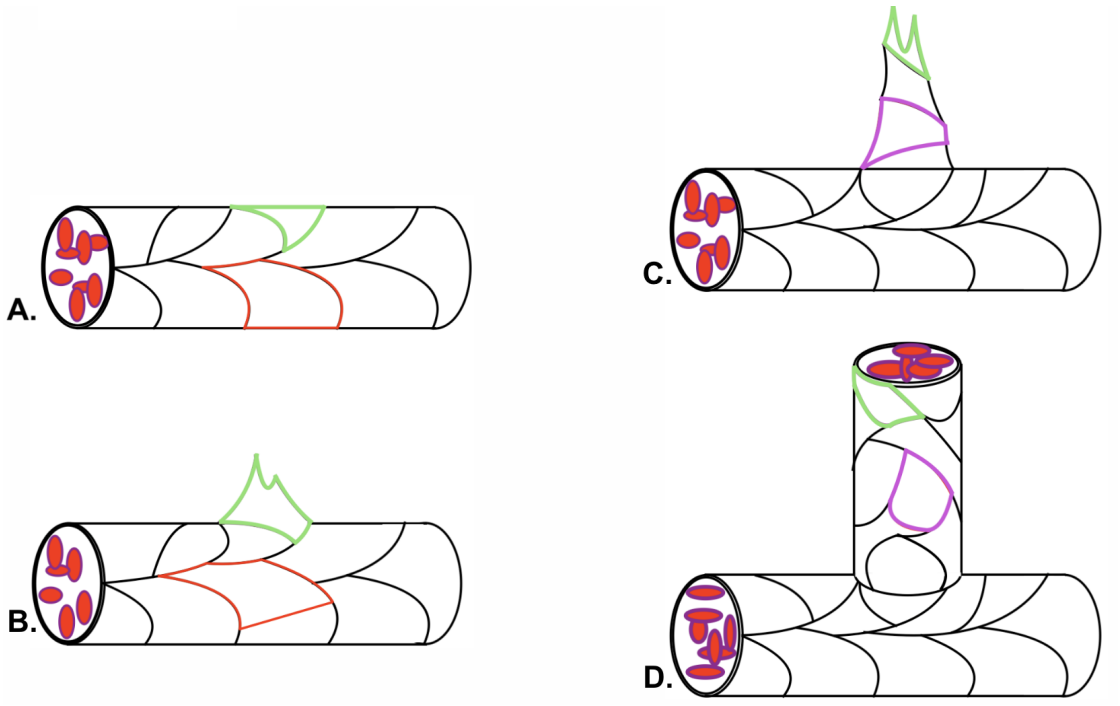

Figure 2.2. Different stages of angiogenesis. In **A.,** two cells are labeled with different colors. In **B.,** the green cell has shown unusual morphological behaviour due to activated protein cascades and therefore gains migration abilities (phenotype is differentiated). The green cell is budded from the vessel. In **C.,** the migratory green cell moves away from the vessel forming a branch of cells. The red cell follows the green cell. In **D.,** the vessel is fully formed and cells gain their usual behaviour.

In particular, the mechanisms governing angiogenesis are frequently dysfunctional in cancerous tissues, leading to improper cell-to-cell angiogenic signaling and an abnormal vascular network [20].

Cells which are in close range of the vessel periphery can intake the oxygen that diffused from blood to the surrounding area. Due to the gradient of oxygen cells in the closer proximity of the vessel receive more oxygen than others in more distant position. For that reason, the range of oxygen diffusion sets which tissue can get oxygen and how dense the vasculature has to be [21].

When a tumour tissue grows, it finally reaches to a diameter that it needs more oxygen and therefore extra blood vessels. Because, the cells within the center of the tumor cannot take up enough oxygen and therefore they cannot proliferate. Due to this low-in-oxygen (hypoxic) conditions the tumor it initiates angiogenic processes by secretion of proangiogenic factors from tumor environment, this is considered as activation of the angiogenic switch [22]. For that, tissues around the vessel, called extra-cellular matrix, is disrupted by proteins secreted from tumor cells such that the inner-most vessel cells, endothelial cells, can be activated by proangiogenic factors [23].

When the tumor vascularization is completed by following steps of normal angiogenesis, tumor cells can continue to proliferate. With the additional vasculature, a higher blood supply secures the needed oxygen and nutrients for the tumor. The changed environmental conditions do more than feed the tumor, and they also provide an escape route for the metastasic cells [24]. The specialized tumor cells (which undergo another phenotype differentiation called epithelial to mesenchymal) gain access to the vascular system and metastasize to the secondary sites [24].

As already mentioned, angiogenesis is a part of our survival, and it has to be run due to several balances. Tumor cells secrete proangiogenic factors in an unbalanced manner, and with regard to tumor-induced angiogenesis, the newly formed blood vessels become torturous. This is because they lack protecting tissues surrounding the vessel structure. This tendency is related to permeability. In fact, VEGF is initially referred to VPF (vascular permeability factor) [22, 25, 26].

Deregulated angiogenic signaling is accepted as one of the fundamental hallmarks of cancer [1, 2], and many modern anticancer treatments or studies are designed to target aspects of this dysfunctional vasculature [27–30].

The treatment is mainly based on inhibition of the most prominent proangiogenic factor VEGF and its receptors. Antibodies binding VEGF can block VEGF to binding receptors residing on endothelial cells. One of the well-known antibodies is Be-

vacizumab (Avastin) [31]. Similar to antibodies, soluble receptors are also a treatment option where altered receptors bind to VEGF, creating an inhibitor effect. Another treatment option is blocking a crucial protein in the cascade of VEGFR. For example, Lenvatinib can connect to inhibit Protein Kinase [32]. However, these inhibit features also play a role in tumor unrelated biological events, and since drugs are dispersed through the body, they also cause unwanted results.

We need to increase our knowledge of angiogenesis-related pathways and the key factors in modulating the working dynamics to regulate them with better precision. For these reasons, we wanted to model angiogenesis together with calcium, with the motivation that this study might inspire models for testing treatment options that calcium can also be used in angiogenesis-related procedures.

When signals secreted from the oxygen-deficient area reach nearby vessels, they awaken the dormant vessels and initiate some molecular pathways in these cells [30]. After a while, only a few cells but not all begin to move normal to the vessel surface [33, 34]. This selection process is vital to maintaining the integrity of the vessel, and we will also be focusing on this phenomenon in the primary model. When cells of the same type activate different pathways and consequently gain different specialties helping them to change their shape and gain different roles, they are called different phenotypes [35]. The moving cells are followed by others who form the main vessel. The motile cells are referred to different phenotypes: tip and stalk cells [19, 36].

Growth factors, such as VEGF (vascular endothelial growth factor), are secreted from cells in low oxygen environments, acting as signals which can cause quiescent, unpatterned endothelial cells (ECs) to activate, begin vessel formation, and pattern their selected cells [37,38]. However, the participating ECs must undergo a competition process for each sprouting vessel to decide which will lead the new vessel and which will follow along.

The before-mentioned selection process of cells is called lateral inhibition, and as the name suggests, it is based on inhibiting the migratory features of neighboring cells on the lateral base of the vessel [39, 40]. Since neighbors are involved in this process, the critical role belongs to transmembrane proteins residing on the cell membrane, communicating with the neighbor cell's transmembrane proteins.

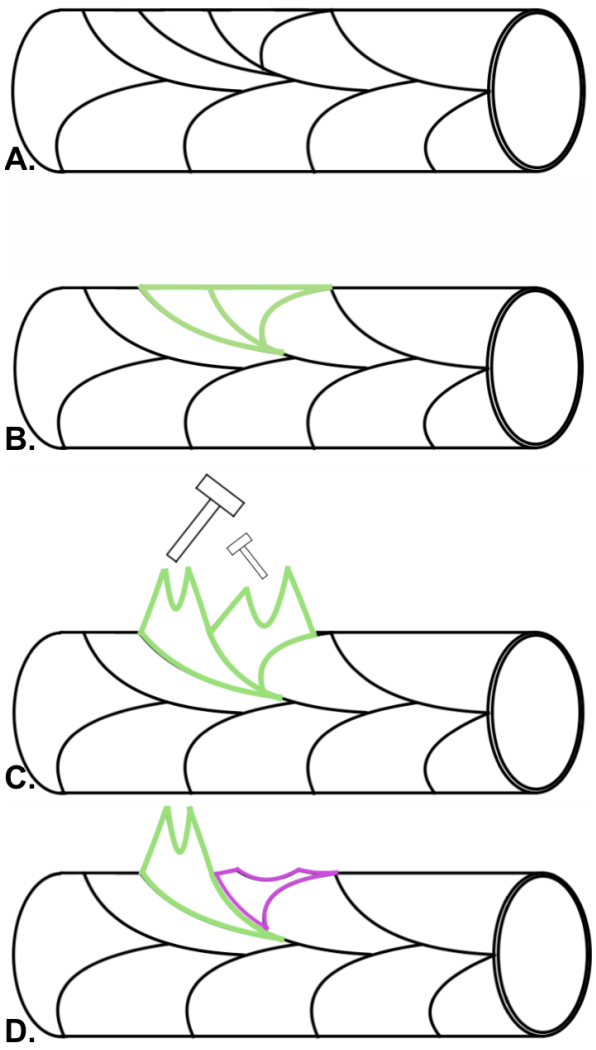

Figure 2.3. An illustration for lateral inhibition processes. **A.,** dormant cells resides on the vessel. **B.,** cells activated by VEGF (in green) changes to tip phenotype. **C.,** tip cells compete through ligand-receptor interaction (DLL4-Notch pathway). **D.,** inhibited cells become Stalk phenotype (in pink), others remain in Tip fate (in green).

In more detail, the angiogenesis signaling pathway is complex and interconnected with other cellular signaling pathways. VEGF signaling triggered by oxygen-deficient cells. VEGF is captured by VEGFR (vascular endothelial growth factor receptor) of endothelial cells residing in the vessel, and causes an upregulation of intracellular PLCγ, which in turn increases levels of inositol 1,4,5-trisphosphate (IP3) [41]. IP3 upregulation causes the IP3 receptors (IP3R) present on the surface of the endoplasmic reticulum to open, leading to a rapid increase in cytosolic Ca2+ (Calcium ion). Cellular homeostasis of calcium ions is maintained through various exchangers and pumps as part of the extracellular signal-regulated kinase (ERK) pathway, which also causes the secretion of delta-like ligand 4 (DLL4) as a byproduct [42,43]. DLL4 is a transmembrane protein that interacts with the Notch protein on the surface of neighboring cells. If DLL4 of a neighbouring cell dimerizes Notch, it releases Notch intracellular domain (NICD) into the cytoplasm, which inhibits the VEGF pathway through the Hairy and Enhancer-of-split (HE) family of proteins [44]. Here, Notch target factors (Hes, Her, Hey) are gathered as HE family for expressing all proteins that results the VEGFR cascade repressors together [45–47]. This process of cells activating their VEGF pathways while simultaneously inhibiting neighbouring pathways gives rise to the previously mentioned competition model where a few cells emerge from the many, leading to the formation of the new vessel branch.

The EC phenotypic selection process is achieved through lateral inhibition of the VEGF signaling pathway between neighboring ECs on the mother vessel through DLL4-Notch interaction on cell surfaces. In theory, cells with a high level of DLL4 tend toward the expression of a tip phenotype with increased mobility features such as filopodia, and cells with a lower level of DLL4 tend to express the stalk phenotype [43, 48, 49]. In reality though, the temporal dynamics of this phenotypic separation are not this simplistic and can be linked to other initiators as well, such as oscillating intracellular signals.

Different angiogenic factors triggers different signalling pathways, but Notch receptor and its ligand DLL4 is known to be evoked by VEGF signalling transduction [50].

As an angiogenic therapy, anti VEGF drugs resulted pruned vessels, however inhibiting DLL4-Notch signalling resulted increased sprouting [51]. Even though Notch/DLL4 is one of many molecules secreted of the VEGF initiated the pathway, this converse effect might be resulted by the nuanced role of Notch-DLL4 signalling in endothelial phenotype regulation [52].

Calcium oscillations are present in this cellular competition and are key players in determining which cell will begin to bud from the existing vessel. As the cell-to-cell competition progresses, ECs become distinguished based on the activation of VEGF downstream factors. Cells with inactive downstream factors will attach and follow the other cells with active factors, proliferating and migrating away from the vessel. This characterization brings about two distinct phenotypes: the 'tip' phenotype - proliferative and migratory cells at the tip of the new branch - and the 'stalk' phenotype - proliferating but follower cells at the base of the new vessel branch. In addition to the behavioral differences between tip and stalk cells, tip cells can also be distinguished by their prominent and dynamic filopodia [25]. These long thin actin protrusions exist in higher quantities in tip cells, increasing their migratory abilities and ability to sense the direction of enhanced signaling [40]. Furthermore, tip and stalk cells are patterned such that neighboring cells cannot both display the tip phenotype. Under extracellular VEGF, all cells initially exhibit a tip phenotype but later readjust their phenotype following an inhibitory process. [39] This fact will be reflected to our model by a three different phases: initial tip cell duration where DLL4 level increases in all cells, the quiescent duration when DLL4 decreases in all, and finally the selection phase where only tip cells increase their DLL4s.

Here in this thesis, we will inspect possible effects created on the vessel initiation by a secondary messenger, calcium. We will claim that due to lateral inhibition, calcium oscillation might be ceased, then consequently calcium down path molecule DLL4 (Delta-like Ligand 4) would be expressed in a lower level, and as a result phenotype of a cell would be altered similar to the experiments. [42].

2.3. Calcium Signalling

Here, we illustrate the key points of the mechanism for calcium ion signalling in intracellular cytoplasm of the cells.

Calcium is the metal element that has been concentrated in the highest amount within the human body. It has a highly reactive nature, hence it is found as ionized in the body (for this reason it is commonly abbreviated as Ca^{2+}).

Calcium is known to be a widely used element of cell communication for a long time. The reason behind it's wide preference is open to debate [53]. Since it is widely used, different organelles interacts with calcium by their own means. Due to many years of experience, an organelle's calcium interaction can be modeled mathematically by certain terms (this concept is often referred to as "calcium toolbox" [53]). These terms are nonlinear, consequently, we can describe how calcium levels are changing in cell cytoplasm with a mathematically interesting equation.

Calcium distribution in the body and cell is quite variant. Approximately 1% of the total calcium in our body is inside the cells (99% is stored in the bones), 0.1% is in the extracellular fluid. However the 1% inside the cell is distributed between organelles and the cytoplasm [53]. The difference in calcium density among the calcium in extracellular fluid (1 mM), cytoplasm (0.1 μM when cell is functioning) and organelles (higher than cytoplasm) are in orders of magnitude. Low Ca^{2+} concentration in the cytoplasm ensures even a small increase of the calcium cause changes in the concentration profile and forms signals [53].

Signal in biology, also called agonists, is different from what we understand signal in physics. Here, the signal is a molecule often a protein or an ion, and ions transmission is an initiation of an event either by an interaction between the signal molecule and a receptor molecule or by the signal itself. Signals can also originate from outside or the inside of the cell. There are localized signals, usually resides on the mouth of a

gate or a receptor. Sometimes organelles bound themselves to the other organelles or to the plasma membrane, creating "microdomains" where calcium is much higher in concentration comparing to the other parts of the cytosol [54]. These inner sections provides direct calcium transport therefore the cell avoid global raise in the calcium levels. Another signal type is the global signals, where levels can oscillate, and show a gradient. Oscillating signals may differ in the frequency, and regarding to it they would trigger different cellular mechanisms. On the other hand, gradients are giving cell a direction which is much needed in orientation based actions such as cell movement [55].

Most signals received by the cell, through receptors residing on the cellular boundary, trigger the calcium pathway [53]. In a possible signal-dependent activation, these stores transmit the signal using the appropriate elements. The diversity in temporal and spatial signal forms allows for analytical examination of calcium. The same diversity makes it possible for calcium to play different roles in nearly every cell type [21, 53, 56, 57]. Thanks to the common organelles and cellular functions on different cell types, it has become a common communication tool (a second messenger) that can be used by many cells.

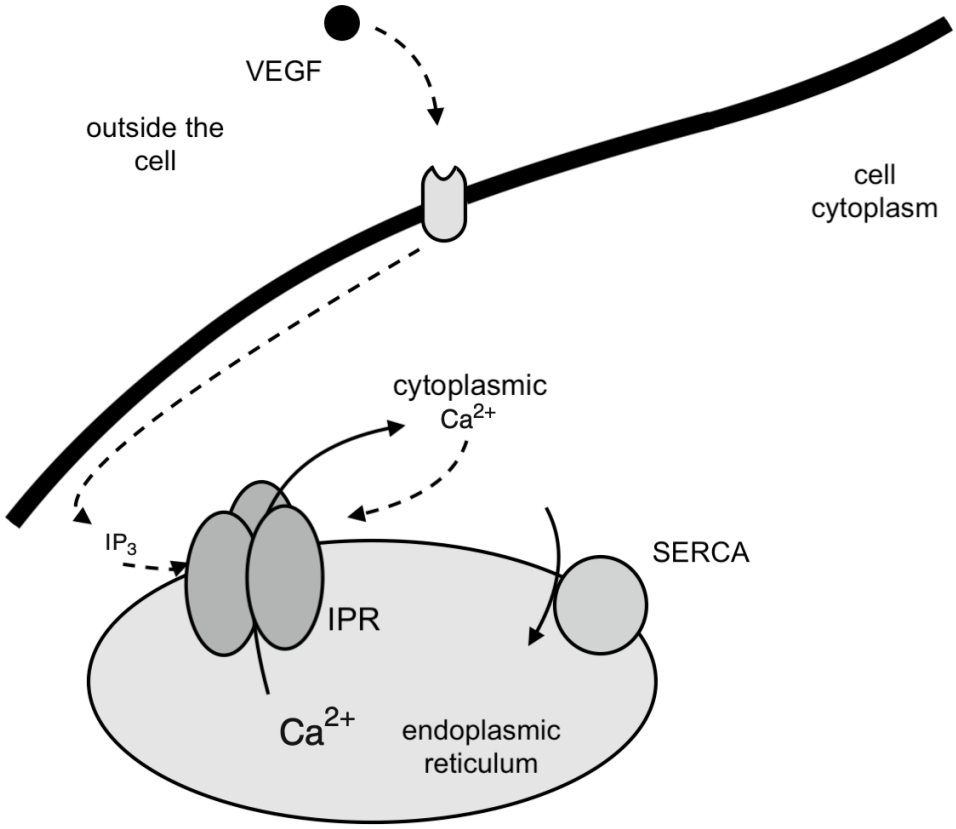

Figure 2.4. Calcium pathway used in this model.

As well as changing concentration levels of different chemicals, another way of sending external cues might be stretching the cell. Some channels of calcium is sensitive to stretching and under mechanical force they become activated. Ca2+ channels are spread to the cell nearly homogeneously, in addition to the cell membrane, they are also resided on a huge organelle ER (endoplasmic reticulum) and multiple mitochondria. When stretching activates plasma membrane (PM) channels, like TRPM7, they increase Ca2+ concentration in nanoscale regions, which further perturbs other channels inside the cytoplasm [58]. When PM channels are activated with a spatiotemporal direction the result is a calcium activation wave in the cytoplasm which bring a notion of direction to the cell [59].

Due to the wide usage of calcium, you may think it is harmless for the cell, however, this friend is also a foe. Organelles contain calcium in concentrations much higher than the cell cytoplasm when contained in organelles, cytoplasmic concentration

level is harmless. However when concentration is kept in a higher level for a duration of time, it kills the cell [53]. For this reason cells regulates calcium levels with the utmost care. When calcium is secreted from organelles it is quickly buffered (connected to free particles in the cytosol), so that the risen levels can be gauged, and the excessive load of calcium can be taken off from the system [53].

Treatment options with calcium is also become a current issue recently. Electrochemotherapy is a method for increasing the chemotherapy intake level to the tumor, also studied in relation to calcium. The tumour, under short pulses evokes the plasma membrane for opening the pores, leading a faster drug intake in levels higher than usual. Calcium electroporation is a method developed from electrochemotherapy. In this method electric pulses are applied to a previously calcium solution injected area of tumor. Interestingly, healthy cells have a better efflux mechanism, such that they can survive the high Ca2+ intake and cancer cells cannot [60]. Also, this procedure is shown to interfere the migrational capacity of endothelial cells and slowdown angiogenesis [61]. Besides not only endothelial cells but also mesenchymal cells shows calcium oscillations during the treatment. In a recent study it is also proven that short electric pulses can also generate calcium oscillations in mesenchymal cells [62]. Considering the lethal impact of metastasis in human generation, it can be seen how calcium modelling and its further applications might be essential in future.

2.4. Cell Movement

In this section, we aimed to explain the general mechanisms of cell cytoskeleton and movement. Later, we depicted how calcium is related with these processes.

Migration is a multilayered event, and one of the key elements calcium, has different roles in every step of cell motility [63–67]. It is vital for the survival of an organism especially during development, and recovery. Some cell types like leukocytes are always in the move, and patrol the body against problematic cells. However, many cell types need to be stimulated by external cues to awaken their ability to move. In health, em-

bryo development, wound healing, angiogenesis, and in sickness, malignant mutations, or cancer activates dormant cells to turn them into mobile cells [55]. Cell migration has a major role in deadly hallmarks of cancer including; angiogenesis, invasion into surrounding tissue, or metastasis. For example, without cell migration a tumour cannot exceed a certain radius, invade the tissue, and metastasize into secondary sites [1,2,55].

Cells have mainly three cytoskeleton structures, referred as filaments. These structures are fibers that can be formed strengthened and disintegrated if necessary (a good visualization aid might be cooked spaghetti, when it is heated it turns to be bendable however when it is cold it is rigidified.) These can modulate transportation of intracellular factors or organelles, along with the structure and movement of the cell itself [67]. There are type of three filaments. Microtubules organize location of organelles. Intermediate filaments increase the mechanical support of one or a group of cells [68]. And finally, actin filaments residing inside the cytoplasm regulates the overall shape of the cell and it's mobility (these can be thought as mikado sticks inside a balloon). Cell regulate the orientation and the length of actin filaments to create membrane protrusions including microvilli (leads increased cell surface), lamellopodia (leading edge for a direction of the cell), and filopodia (thinner extensions can be elongated further away from a lamellopodia) [67–69].

Cytoskeleton is highly dynamic and regulated according to current needs of the cell. Some cell types requires to be more stable their shape like neurons and bone cells, however, others needs to be more agile like immune cells. On the other hand, phenotype differentiation of a cell can also change the reorganization pace of its cytoskeleton [70]. For instance, endothelial cells are stable when they are dormant. On the contrary, when the angiogenic switch is turned on the cells reorganize to be a tip cell with increased reorganization features. These new abilities are beneficial for altering their routes according to VEGF gradient.

The filaments can associate and disassociate due to polymerization of the actin by actin-myosin interplay [71]. When the polymerization occur the once soluble cytoplasm become more gel-like, and cell has a firmer overall shape. This process is called solation-gelation process, and can be modulated in relation to calcium homeostasis.

A cell moves as a result of several events. Extended in the direction of the movement, the cell creates focal adhesion (FA) points in the front and releases such points in the back. Then, by retracting, the rear part of the cell moves towards the front due to released FAs [70, 72, 73]. These processes require multiple structures like protrusions, cytoskeleton, or FA points to play different roles with a specific chronological order. Protrusions, like filopodia, or lamellipodia, are actin-based elongated frontal features of the cell [70]. These dynamic structures elongate toward the external cues with their actin-myosin structures and stretch the membrane activating certain channels. On the other hand, the actin cytoskeleton also enables the cell to change shape and to move further by creating retractions or dilations [70]. During these processes the cell simultaneously creates new FA points on the front called as nascent FA's and releases mature FA's on the rear [74, 75].

Actin polymerization requires presence of calcium in the medium, however their relation and the mechanisms stressing polymerization is not well understood [76]. Filopodia and other types of podia are related with spatial orientation of actin polymerization in the cell since they are extensions of cytoskeleton [77, 78]. The biological importance of spontaneous actin polymerization waves might spatially organize cell architecture during cell locomotion, inducing cytoskeleton shape changes. Waves of actin filament polymerization are related with protrusions of the cell [76, 79, 80]. For that reason, we extend our phenotypic model by including an element where travelling waves play a crucial role in the orientation of the cell.

Cell cytoplasm contains cytoskeleton and cytosol which is the liquid compound filling the cell for providing some medium for second messengers and other signals to disperse. Cytoplasm is shown to demonstrate gelation/solation behaviour from the

early studies [81]. We now know that, due to the actin-myosin compounds connectivity of the gel changes accordingly with the calcium concentration on the cytosol, and this relation is investigated in multiple studies [4, 82, 83]. Under low calcium concentration polymerization aligns fibres, stiffs the material and gelates the cytosol in a denser solute. However, when concentration increases the material becomes looser due to breaking links actin fibers and solated cell occupies more domain. Naturally, there are limits for a cell's dilatency and contraction. Since the cell is a solid substance in this model, it cannot be contracted lower then and cannot be extended (membrane would tear down) higher than a value. On the other hand, this model runs in a range away from these undesired effects [21, 84, 85]. The model assumes that the cell is isotropic unless the spatial perturbation. This might not be the case for a living cell but for our simple extension we leave sophistication of the model for a future work.

By integrating an actin-myosin gelation to our calcium angiogenesis relation we are aiming to to model the processes of an migrating tip cell in a more realistic way.

2.5. Coordinated Waves in Biology

Here, we emphasized the trigger/travelling wave phenomenon, its importance in signalling and we mentioned some examples.

Many well-known facts of one discipline might not be known to scientists working in other spheres of science. When combined with the fact that scientists prefer to use the terminology belonging to their disciplines, many phenomena may have been rediscovered and given different names. Trigger waves are an example of this situation in nomenclature. Traveling wave phenomenon can be seen in any field having wave dynamics, including electromagnetic, ultrasonic motors, water waves, or chemical solutions [86]. Non-dispersive traveling waves were also examined by many in chemical set ups [87, 88]. Since a non-dispersive traveling wave should contain a spatial perturbation from its initial steady-state conditions, due to this perturbed trigger, it is given the name of "trigger wave" for non-dispersive traveling waves. Although chemical

and biological societies commonly use the "trigger wave" term, the "traveling wave" is well accepted in mathematics and physical sciences. We will use both of the names interchanging for the rest of the thesis.

Different means of transport has been used by living organisms. From slowly diffusing ions to instantly beating heart, the time for signal coordination is arranged according to the needs of the creature. Diffusion is ineffectively slow process for distances above micrometer. For example, one meter like travel of a particle would last thousands of years [89]. Microtubules are a biological alternative to diffusion however, it is again incredibly slow such that it takes approximately ten days to transport signals [90]. On the other hand, circulatory systems (like blood or lymph) is significantly faster with meter per minute speeds [91].

However, by using these signal transport alternatives no one can catch a ball thrown or can be tickled. We feel events nearly simultaneously with their occurrence. What sets our limit in perception is traveling/trigger waves which can travel a meter around 0.01 seconds [92]. This special type of travelling wave is called an action potential, and it occurs in the nervous system due to the interplay between different ions [93]. Not all travelling waves are quick as the action potential. Many examples including spread wave of state for mitoses, or calcium ion wave in-between cells are travelling waves but they have slower velocities [94, 95]. Without the need of an extra tube, or a filament system travelling waves can be seen in all mediums where coordinates waves can arise.

Besides, diffusion and circulatory systems can create some loss in the intended signal with events such as dispersion or leakage. In addition to their decreased signal transportation time, non-dispersive traveling waves do not disperse and hence protect their signal and conserve its energy during their travel [86]. This can induce constructive or destructive results according to the nature of the wave. For example, a non-dispersive nerve signal helps the brain command other parts of the body quickly and effectively; however, a tsunami wave can wipe out a village.

In this thesis, we observe traveling waves due to a phenomenological calcium model, where calcium concentration wave is moving across the cell. Traveling wave dynamics will play an essential role in setting out an orientation for the cell. For the angiogenesis part, a cell's phenotype is defined according to temporal changes, and the spatial distribution of the protein is irrelevant for our purposes. On the other hand, angiogenic cells migrate towards the source of the stimulant, which is very much related to the orientation of the cell [96]. Calcium being also a prominent player in cell migration [97], we extend our calcium-angiogenesis model for cell elasticity. Here, we observe how the cell has been gelated according to the change in calcium concentration on the cell and how the initial trigger sets a direction for stretching/pulling of the cell cytosol. Moreover, our traveling waves will not be perfect (non-dispersive) traveling waves. In our problem, we want the wave to be objected to external couplings, like angiogenesis, and lose its neat traveling wave feature, and we will be focused on what makes the cell lose its orientation in our model.

2.6. Unveiling the Problem

Here, we try to give an overall biological explanation for the problem of our model.

When the tumor tissue grows, it finally reaches a limit radius that it needs more nutrients to exceed. The tumor needs additional vessels that will sustain the blood flow for continual growth to get nutrients. For that, stimulant proteins are secreted from the tumor surrounding and diffuse to signal nearby vasculature to initiate proangiogenic pathways [98, 99].

When the stimulants awaken the endothelial cells (a cell type enveloping the innermost part of the vessel contacting with blood cells) for vascular endothelial growth, initiation happens through special receptors matching the stimulant. These receptors residing on the membrane of the cell initiate biochemical pathways via second messengers, like calcium, which later signals production of extracellular kinases (ERK) and map kinases (MAPKs) causing other down-path materials to induce certain cellular

events like mobilization, proliferation, etc. [100]. On the other hand, the stimulant, vascular endothelial growth factor, also causes the vessel to be more permeable allowing metastasic cells to reach blood flow with ease [101], along with triggering creation of a new vessel as seen in Figure 2.5.

Initiation of a new vessel requires secretion of many proteins by cells in different stages of the formation [100]. Intact vessel cells are first awakens by the stimulant, later they move towards the stimulant source. As a tree grows, the thinner branches moves towards their direction of the budded branch tip, while the root gets strengthen and thicker. Similarly, a vessel stars with a budded endothelial cell, as it can be seen at the green cell on the right-end of the vessel section at Figure 2.5. This cell will guide others (the pink cells) which will form the vessel tube. In this thesis we are focused only on this budded vessel stage.

Experiments show that after the stimulant intake the cells perform calcium oscillations [42]. They observed that some cells oscillate for longer duration of time and they end up having a special role for angiogenesis. These cells, depicted in green at Figure 2.5, move away from the vessel, orient other cells to a direction. However, for the other pink cells whose oscillations cease earlier, they follow the green cell and proliferate more often.

Creation of vasculature requires some restrictions, especially if the mother vessel needs to continue functioning. For that, neighbouring cells starts a selection process where the try to inhibit their neighbour's chances to become the cell type depicted in green at Figure 2.5. The end result is a pattern where no two green cells can be adjacent neighbours [25].

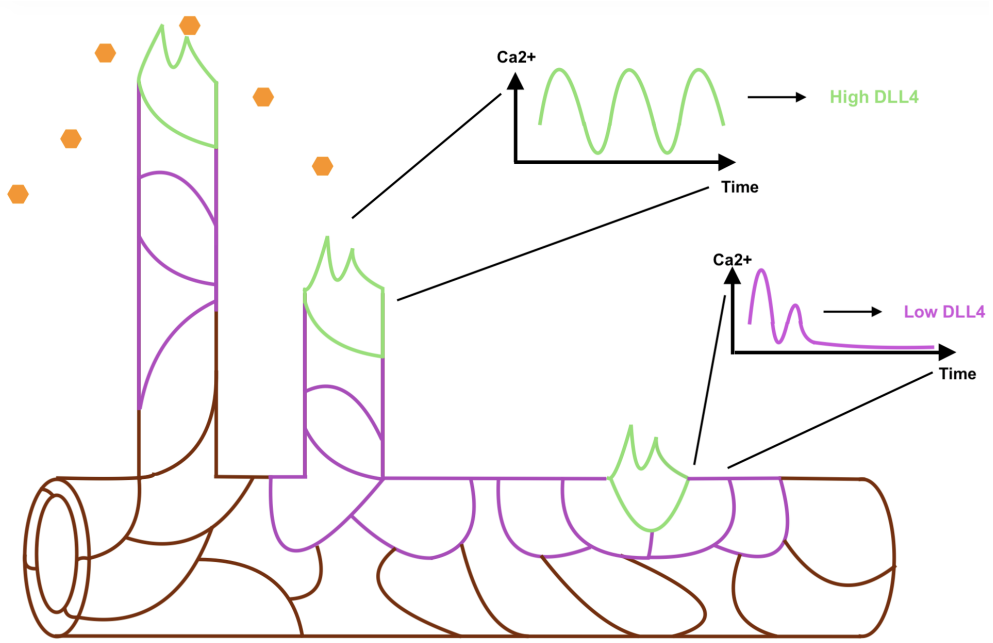

Figure 2.5. Angiogenesis stages. Each loop represents a cell. Orange hexagons shows the stimulant, green cells and pink cells are cells that are affected by their stimulant intake. Their long term calcium behaviours are depicted by the graphics in matching colors. Also, the most important protein in cells phenotype, DLL4, has been shown in relation to calcium behaviour. Red cells have no stimulant intake and they continue to keep the vessel intact.

In this thesis, we aim to connect these ideas, in a mathematical model by using various simulation techniques. In my first approach to this problem, due to the aforementioned pattern formation, I thought reaction-diffusion equations will be related with the subject. For that I wrongfully foresee that the cell-scale travelling/trigger waves plays a role in inter-cellular pattern formation. This was wrong due to the scaling of the model at hand (intracellular calcium oscillation) vs. the scale of inter-cellular pattern formation (phenotype selection). In this thesis, we will model phenotype selection without a significant effect from travelling wave dynamics, and later we will extend our model for inspection of an oriented polymerization wave (calcium related actin polymerization) for the purpose of fulfilling the title of the thesis.

3. MATHEMATICAL BACKGROUND

In this chapter, we introduce the models that has been used for modelling the biological phenomenons depicted in the prior chapter.

3.1. Trigger/Travel Wave Models

In this section, we will describe trigger/travelling waves. We will discuss typical features travelling waves and how nonlinearity plays a role in the shape of the wave. Later, we will examine dynamics of a typical example, and FitzHugh-Nagumo model.

Biological waves can occur in many living organisms. In humans the cases for a single agent like calcium many example events can be found. To state the few, from the wave seeping our fertilized eggs in the first moments of our existence, to our nerve signals transmitted constantly or our beating heart at any moment, travelling waves are at play. This wave phenomenon is widely studied for many years by various techniques and point of view. However before we delve more into the nature of a trigger/travelling wave, we should understand what do we understand when we mentioned a wave. A wave is a spreading disturbance from equilibrium, such as a water wave. The equation describing the waves is the following,

$$\partial_t^2 u(x,t) = \partial_x^2 u(x,t) + V(u(x,t)). \tag{3.1}$$

Here, let u denote the variable of the phenomenon in question. A trigger/travelling wave is a substance concentration wave come about from the solution of a reaction-diffusion equation as below,

$$\partial_t f(x,t) = D\partial_x^2 f(x,t) + R(f(x,t)). \tag{3.2}$$

Here f denotes the chemical reactant, as D, and the function R are the diffusion constant and the reaction for the reactant in question. Waves can be found in many areas of science. Along with electromagnetic waves, quantum mechanical waves, sound waves, etc. chemical waves is just an another kind of wave. However, at this point one can realize that equations 3.2 and 3.1 are not alike. Just like the Schrodinger equation, the reaction-diffusion equation in 3.2 is actually a heat equation rather than a wave equation.

When reactive agents are modeled with diffusion, these two effects compete. If the reaction is dominant, we observe an over all change in the whole domain, without any spatial difference. In this situation the reactant might not be diffusive enough, then a model that is solely temporal might be more proper to describe the mechanism. On the contrary, in a case where the diffusion is dominant we would observe a gradual alteration in the domain like if there is no reaction. However, in this wave type, the solution is a cooperation between the two components. We aim to observe the model with a diffusing reaction wave on the spatial domain. An easy-to-visualize example is a white paper set on fire from a corner. The fire (reaction) would travel (diffuses) across the paper (domain). Reaction in each spatial point initiates the reaction in the next step. By this spatial coupling the reaction moves with diffusion.

Dynamic or static pattern formation come into existence on the biological phenomenons including nonlinear reactions creating trigger/travelling waves (we briefly discussed the terminology on this matter on Section 2.5). It yields a spatially regular distribution, or synchronized function between the cells via chemical waves [102]. Especially, during events requiring spatial or temporal organization, for instance developing from a single-cell micro scale creature, to a meter scale multi-organ organism, travelling waves are invaluable. As an example, the synchronization of a protein in a Drosophlia egg which is famous for fast communication throughout the huge cell [103]. Both in intracellular or extracellular scales many examples of these interesting chemical waves exist, and in this thesis we will focus travelling waves when we discuss on an intracellular case relating calcium dynamics to cytoplasmic actin polymerization.

However, not all chemical waves are trigger waves. A trigger wave (or a travelling wave as this term is more widely being used) is a solution of a partial differential equation. This solution can be obtained in several ways [86]. The emergent wave solution is a wave moving with a fixed shape and velocity in a directed course. This wave solution is known to exist in fluid mechanics, high energy physics, chemical reactions, biology etc. [86, 104, 105].

There are two common way of investigating travelling waves in the literature. More theoretical works are focused on proving the existence of travelling waves [86]. In this case travelling waves are examined on a space-time domain and often starts with imposing a solution with a change of coordinates from change of reference from (t, x) to $(x - ct)$ argument. However here we will only focus on models which are known to contain travelling wave solutions already. For that reason, we will prefer to reveal this wave configuration with numerical solutions under a spatial perturbation.

In a system travelling waves occur when an excitable media (the reactants domain) in a homogeneous steady state f_0

$$\partial_t f(x,t) = 0 \tag{3.3}$$

$$f(x,0) = f_0 + \epsilon(x) \tag{3.4}$$

is objected to a small spatial perturbation $\epsilon(x)$. The perturbation is expanded via diffusion and forms regulated wave structures and in special cases where the velocity of the wave is zero form stationary waves, i.e. static patterns. In cases where activators and inhibitors is at play, reactions are objected to a self positive feedback for an activator along with synthesizing the inhibitor, and the inhibitor inhibits the activator [106]. For the wave to be form, a threshold must be overcame by a trigger mechanism (hence the name trigger wave) for the formation of the wave in an excitable medium. Trigger waves are named by Winfree [87] after the work of E. C. Zeeman on waves of trigger mechanism [107]. On this work he summarizes the co-features of an action in heart and nerve cells as,

- stable equilibrium
- an energy step/threshold to stimulate an action
- a returning/recovering phase to the equilibrium

As an addition to the wave's movement, the shape of the wave profile can be found from a nonlinearity inspection through the tools of nonlinear dynamics. For our aim, we want to be able to create travelling wave trains. These wave trains will emerge from a very specific parameter. Since, we are interested in oscillating concentration waves moving with diffusion, we will not fine tune our parameters since it will be biologically irrelevant for this specific problem at hand. However, for another problem like heart beat, signal should be fine tuned and even a slight change in the parameters might cause catastrophic problems, as heart attack [108]. The parameter controlling the dynamical behaviour of the system will correspond to stimulant intake. Also, a crucial feature of our problem depends on comparison between cells with configurations of intake. For that, we will seek a range of parameters that we can assign to the cells rather than finding the parameter for the perfect non-dispersive travelling wave. These parameters will correspond the interval between the points that system's stability changes and periodic oscillation arise.

For illustrating the aforementioned ideas we will now proceed with a famous example of excitable media.

3.1.1. An Example - FitzHugh-Nagumo Model

FitzHugh-Nagumo (FHN) model is used to model dynamic behaviour of electric activity of nerve cells [93,109]. It is a simplification of a more complex axon model called Hodgkin-Huxley [110]. However, this model is widely used due to its simple nonlinear nature originating from the self-excited v^3 term. One of the many representations of

dimensionless FHN system is the following

$$\frac{dv(t)}{dt} = -v(t)^3 + v(t) - w(t) + I, \tag{3.5}$$

$$\frac{dw(t)}{dt} = \epsilon(a - bw(t) + v(t)). \tag{3.6}$$

Above u and v represents fast action potential and slow recovery variable respectively and $a = 0.1$, $b = 1.5$, $\epsilon = 0.01$. Also, I is the voltage, and we will delve into that later. Between certain values system exhibits different behaviour and below the limits of change can be observed from Figure 3.1.

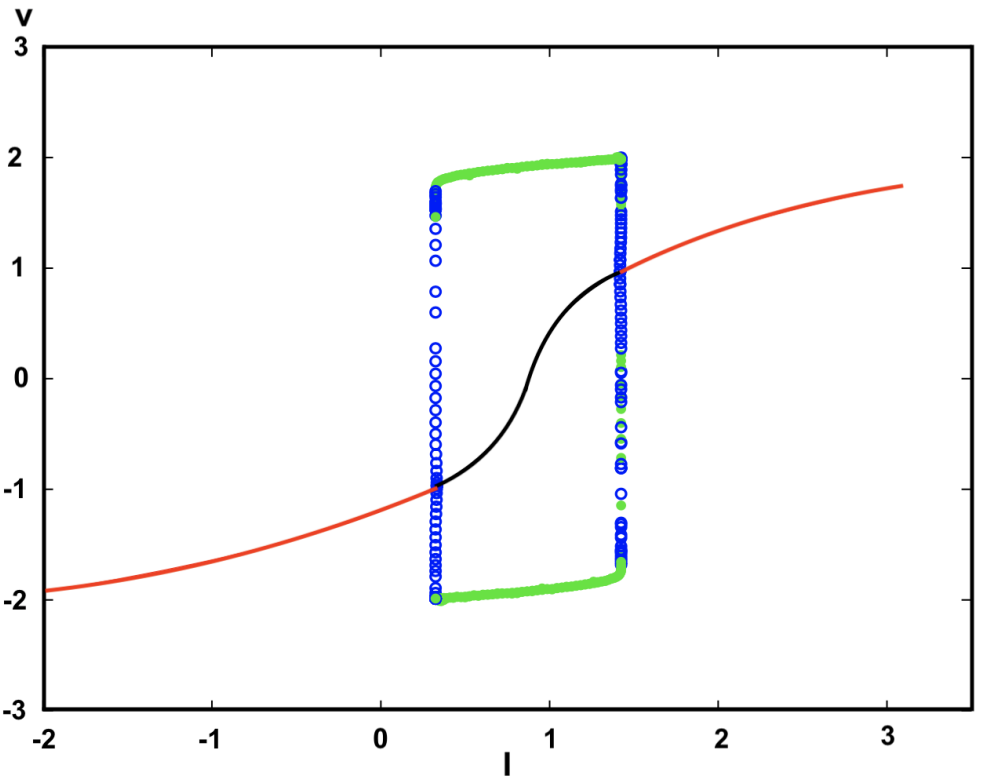

Figure 3.1. Bifurcation diagram for FHN system. Red line represents the unstable fixed points and the black line in between is for stable points. Blue and green points represents unstable and stable oscillation parameters.

Here one should emphasize that in the original experiment a voltage cable was infused inside the nerve axon for creating an artificial base for nerve stimulation. However mimicking the real life no such thing is required, hence we set $I = 0$.

Nerve cells creates an excitable medium for the signal to be transferred; if the initial stimulation is lower than a threshold, the signal has a different profile relative to the case in higher initial condition. In an excitable media, the system has two different types of behaviour before coming back to its rest state. This can be visualized on the phase plane as having a short and a long course. Beside to this threshold nature, excitability ensures one more important thing directionality both in time and space [111].

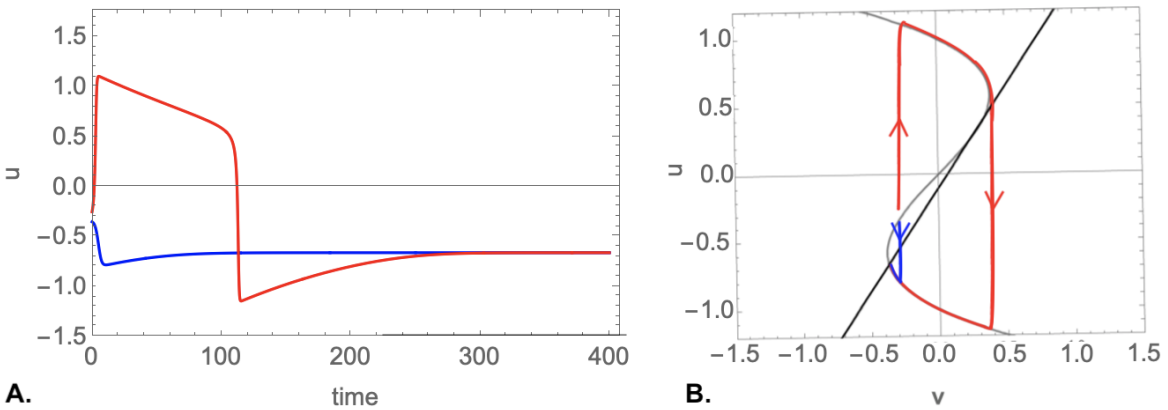

Figure 3.2. **A.,** time plots of FHN model under different initial conditions. As the red plot indicates behaviour for $u(0) = -0.25$, the blue one depicts the behaviour for $u(0) = -0.35$. The refractory phase can be seen between $t = 100$ and $t = 300$ seconds approximately. The signal surpassing the threshold evolves to an action pulse, on the contrary the signal evolves to the resting potential. **B.,** phase plots of the model with the same initial parameters as in the left figure. Reverse S shaped u nullcline intersects with v nullcline line. It can be seen that the red signal follows a longer path relative to the blue signal before reaching equilibrium.

Until now, we tried to understand the dynamics of temporal profile of the trigger wave mechanism but one detail is still missing, the spatial effects. As we mentioned before, together with nonlinear effects there is also the effect of diffusion which has an effect of the spreading the material to a larger spatial region with time.

3.2. Angiogenic Cell Phenotype Model

Here, we explain the angiogenesis model that we will use in combining our model. We will later use only the key elements for lateral inhibition part of this model.

VEGF is long-known as an angiogenesis trigger, however, the dynamical features of mediators of the process i.e., DLL4 and Notch was first investigated in [5]. With an ordinary differential equation model, they were able to examine the consequences of inner and surrounding status for the phenotype to switch and decide. In the work, Venkatraman et al. creates a set-up including two cells for investigating their collective behaviour. In contrast to our model they also include several different factors including filopodia, VEGF receptor and other internal signalling modulators [5].

Below, $VEGF$ represents the VEGF intake of the cell and is given in relation to the filopodia extension and retraction. Here, $filo$ is taken only as a temporal variable and used solely for feedback purposes

$$VEGF = VEGF(1 + \widetilde{k}_6 filo^n). \tag{3.7}$$

Below, subscript i represents one cell and, j represents the other cell being in contact with DLL4-Notch signalling pathway. The below model consists both of transmembrane proteins and in-cell proteins and deal with them in the equal footing in a solely temporal domain. Here, the model only includes trans-interactions (that occurs between the in-contact cells only) between the transmembrane proteins. On the other hand, delta like ligand 4 ligand and notch receptor can also reside and interact on the same endothelial cell as well. This interaction (called cis-interaction) can regulate the angiogenic cascade has not been elaborated in this study likewise. However, this model abstain from cis-interactions and only investigates modulatory effects of trans-interaction. For that reason, the subscripts in terms depicting the association of the transmebrane proteins and the disassociation of the emergent complex has both i and j subscripts.

In each equation there are degradation rate ϕ multiplied with the concentration term of the rate equation along with either the production rate γ or the basal gene expression β. Also the Hill coefficient, n, (also the power for the nonlinear feedback) is taken in this model as 2

$$R2_i = -\widetilde{k_1} VEGF_i \; R2_i + \widetilde{k_{-1}} VR2_i - \widetilde{k_3} R2_i \; HE_i^n - \phi \; R2_i + \gamma \tag{3.8}$$

$$VR2_i = \widetilde{k_1} VEGF_i \; R2_i - \widetilde{k_{-1}} VR2_i - \phi \; VR2_i + \gamma \tag{3.9}$$

$$DLL_i = \theta \frac{VR2_i^n}{1 + VR2^n{}_i} - \widetilde{k_2} DLL_i \; notch_j + \widetilde{k_{-2}} dllnotch_j - \phi \; DLL_i + \beta \tag{3.10}$$

$$notch_i = -\widetilde{k_2} DLL_j \; notch_i + \widetilde{k_{-2}} dllnotch_i - \phi \; Notch_i + \gamma \tag{3.11}$$

$$dllnotch_i = \widetilde{k_2} DLL_j \; notch_i - \widetilde{k_{-2}} dllnotch_i - \phi \; dllnotch_i \tag{3.12}$$

$$nicd_i = \widetilde{k_4} dllnotch_i - \phi \; nicd_i \tag{3.13}$$

$$HE_i = \theta \frac{nicd_i^n}{1 + nicd_i^n{}_i} - \phi \; HE_i + \beta \tag{3.14}$$

$$filo_i = \widetilde{k_5} VR2_i^n - \phi_f \; filo_i + \gamma. \tag{3.15}$$

In equation (3.8) VEGF receptor reacts with existing VEGFs for binding and reverse-reacting for disassociation. In the third term negative feedback of the HE family factors is activated. The VEGF-VEGFR complex is in forward reaction of ligand association and in reverse reaction for complex dissociation in equation (3.9). For equation (3.10), DLL4 gene expression in relation to VEGF is given by the Hill term. Also, the terms expressing binding between DLL4 and Notch factors, and breakage of DLL4-Notch complex follows the Hill term respectively. All coefficients will be given in the following chapters.

Due to the linear relation between DLL4 and Notch ligands, the terms following the Hill term creates the same effect on the rate equation of Notch, equation (3.11). In the rate equation for complex at equation (3.12) for the again shows the effect of ligand association and complex disassociation respectively. Here they assume that DLL4 of the cell reacts with Notch of the neighbour and creates a DLL4-Notch complex (*dllnotch*) belonging to the neighbouring cell. In equation (3.13) intracellular domain

of the notch protein (NICD) is released from cleavaged DLL4-Notch complex on the cell membrane therefore there is neither basal expression nor production rate term for NICD. HE rate equation (3.14) includes the production term due to NICD. Finally the cell's filopodia change is related with VEGF-VEGF receptor complex in equation (3.15)

In this model tip and stalk cells are simulated in a two cell setup, and are subjected to a competition between themselves, by being the cell with the highest DLL4 concentration. In their work Ubezio et al. [26] observed synchronized DLL4 oscillation among the cells. This model enables synchronization with the below nonlinear negative feedback term

$$-k_3 R2_i \; HE_i^n. \tag{3.16}$$

However, for our concerns we will not seek non-linearity in the negative feedback and continue with a linear feedback term instead as we will discuss in more detail in Section 4.6.

This model considers how the signal is received by the cell. It take account of a positive feedback between VEGF and VEGF dimer through filopodia. Filopodia, VEGF receptor, DLL4, and Notch are external elements presented in the model. Since their model is only on the temporal domain, there is no difference between transmembrane proteins, like DLL4, Notch and their complexes, and intracellular proteins, like HE or NICD. On the other hand, filopodia, and the VEGF receptor are directly related with received signal. For the purposes of our model presented in Chapter 4, we will not use all equations of the model and only focus on DLL4-Notch pathway and its negative feedback HE family proteins. We will assume that the system have already been triggered by the signal and it is steady.

3.3. Calcium Oscillation Model

Now we will focus on the calcium model that we can obtain oscillations similar to the ones observed on [42]. We will also illustrate receptor dynamics thoroughly.

As it has been stated before, what we want is the following: to depict calcium levels inside a cell. There are plenty of calcium models, therefore the decision must be given by deciding what do we want to consider. Models of calcium might be stochastic or deterministic: since we are aimed to combine the Ca^{2+} model with a deterministic angiogenesis model we picked a deterministic model that can be analyzed by tools of nonlinear dynamics. Another feature of calcium models is the number of compartments in the domain. If there are more than one compartments in the domain the boundaries should be set according to it, however we wanted to proceed with a single compartment model. The final decision is on the variables. Since multi-compartmental models are eliminated, calcium levels on the other organelles, endoplasmic reticulum being the most plausible, is out of questions.

Therefore we follow a common choice for variables, the cytosolic calcium, c, and the ratio of the Inositol tri-phosphat receptors (IP3R) that has not been inactivated by calcium negative feedback, n. Hence we proceed with the one of the most frequently worked on calcium class I model of Atri and Sneyd [3]. This is a minimal model exhibiting periodic oscillations in the calcium concentration. In minimal models [53, 112] oscillation dynamics can be obtained without varying the IP3 levels. It is originally modeled for stimulating the various wave dynamics observed on Xenopus Oocytes, it has also been successfully used to model different types of cells [4,113–116] and for that reason we will also prefer this model. Although the model has its shortcomings, that we will mention, it's results has been proven to be significantly close to experimental findings [117].

In the below system, biological events can be summarized as the following: in Equation 3.17 calcium in the cytoplasm diffuses, also secreted from IP3R with a maxi-

mum of k_{flux}, the Ca2+ efflux has an amplitude of γ and finally there is the static intake β (in the main model β will be negligible after nondimensionalization, and therefore will be disregarded) This model takes only the main calcium players into an account

$$\frac{\partial c(x,t)}{\partial t} = D\frac{\partial^2 c(x,t)}{\partial x^2} + \mu k_{flux} n(x,t)(b + \frac{V_1 c(x,t)}{k_1' + c(x,t)}) - \gamma \frac{c(x,t)}{k_\gamma + c(x,t)} + \beta' \quad (3.17)$$

$$\tau_n \frac{\partial n(x,t)}{\partial t} = \frac{{k_2'}^2}{{k_2'}^2 + c(x,t)^2} - n(x,t). \quad (3.18)$$

Except μ parameters of this equation can be seen from the parameter table 3.1, however the parameter representing IP3 level in the system, μ, should be chosen according to the desired dynamical effects. This system is highly nonlinear therefore it should be subject to linearization in the near vicinity of its equilibrium points such that the nature of its dynamics will be revealed. We will further focus on these analysis in the following sections.

This analyses is particularly important since that the calcium model is our main dynamical engine. Then we add complexity on top of this model, like angiogenesis or cytosolic gelation/solation, we will make some numerical arrangements for variables (for instance, when we add contraction/dilatation equation to the calcium angiogenesis model we will only set new initial values and change a single parameter from the old model, we will inspect the model in greater depth in later chapters.) In this model the biologically and dynamically more intricate term is the second term with μ. It sets the dynamical behaviour of the set up of non-linearity for the equilibrium system. We can set the model with the following parameters,

Table 3.1. All the parameters except k_{flux} were taken from [3]. k_{flux} is taken from [4].

Parameter	**Symb.**	**Value Unit**
Diffusivity of Ca2+	D	20 $\mu m^2 s^{-1}$
The maximum $Ca2+$ flux from all IP3Rs	k_{flux}	16.2 $\mu M s^{-1}$
The basal current of IP3R	b	0.111
The rate of IPRs activated by $Ca2+$ binding	V_1	0.889
The half-maximum of Ca2+ pumping	k_1'	0.7 μM
The half maximum of Ca2+ pumping from the cytosol	k_γ	0.1 μM
Maximum rate of pumped Ca2+	γ	2.0 $\mu M s^{-1}$
The rate of $Ca2+$ influx coming from the outside	β'	0-0.02 $\mu M s^{-1}$
The time constant	τ_n	2.0 s
The reactivation rate	k_2'	0.7 μM

This phenomenological model [3] portrays a scenario under several assumptions and processes are formulated according to experimental results rather than being build ground-up. There is a single compartment, the domain is ER covered homogeneously by IP3Rs. The domain seen on the figures contain more than one IP3Rs. Even though the boundaries are accepted as solid, the model also accepts, β', a constant level of Ca^{2+} ooze from outside. The cell is empty, there is no organelle, receptors and gates are shown as a function rather than a domain occupying element.

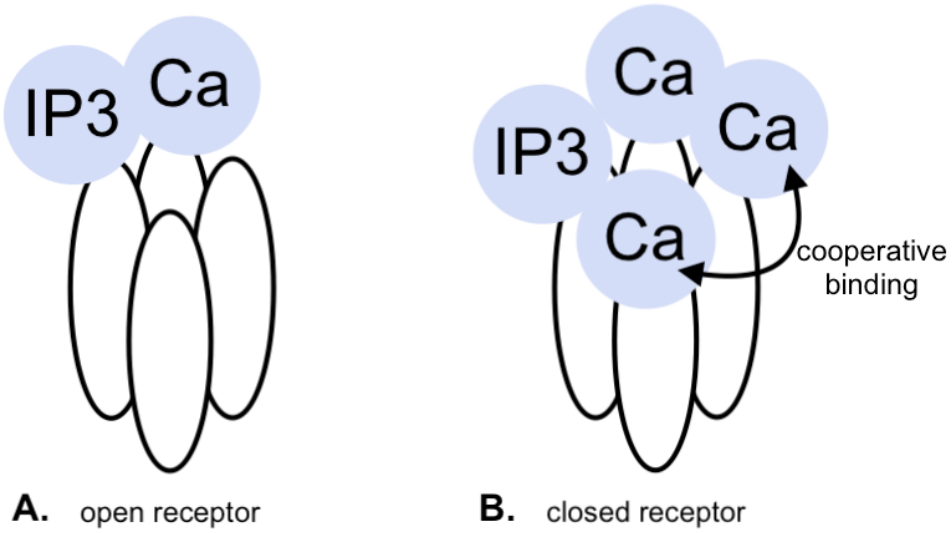

Figure 3.3. **A.,** sites rendering positive feedback -one, and two- are occupied by calcium ion and IP3. **B.,** the opposite effect of calcium when it is bind to sites three and four. Due to these intricate feedback mechanisms IP3R contribution is highly nonlinear.

In addition to the conjectures on the domain the model presumes that there are 4 domain sites of the receptor. These sites are not causally in relation. Site 1 connects with IP3 and the rest connects with Ca2+. Sites 1 (IP3 site) and 2 each can host one particle. Similarly, site 3 and 4 each can hos one calcium ion but they connect cooperatively. Hence there are 4 particles (1 IP3 and 3 Ca2+) when all sites are occupied. The calcium increase in cytosol will occur if an only if sites 1 and 2 will be full while site 3 and 4 are empty. The resulting effect of their cooperative binding is represented by a single term, p_3. Under this circumstances, calcium is able to turn on and turn off the efflux. Therefore the suitable conditions for probability a receptor to be open equal to

$$p_o = p_1 p_2 p_3. \tag{3.19}$$

Above p_1, p_2, and p_3 represents activation of first and second sites and inactivation of the third and fourth sites respectively.

In case IP3 and Ca2+ is zero, the existing basal current, b, makes sure that the current continues. Besides for all IP3Rs the flow of Ca2+ is fixed to the same value, i. Therefore, what changes calcium cytosol concentration levels inside the cell is only the number of open receptors. However, counting the number of open receptors is not possible, therefore the expression for concentration flux due to the IP3R is connected of the 3.19 and the number of open receptors

$$I = iNp_o \tag{3.20}$$

$$J_{IP3R} = \frac{iNp_0}{2\mathcal{F}U}. \tag{3.21}$$

Above Np_o gives the number of open receptors by multiplying the total number of receptors, N with the probability of openness, p_o. For computing the total steady state of the calcium current through the cytosol, I, each open receptor is multiplied with i. It is found experimentally as electrical charge per second, therefore for writing it in terms of calcium concentration, the number of calcium atoms should be found first. A single calcium atom ionizes to Ca^{2+} by losing two electrons and the charge of a mole of electrons is $\mathcal{F}$. Hence dividing I by $2\mathcal{F}$ will give the IP3R related calcium increase in the cytosol. Finally for expressing the flux of the Ca2+, total calcium concentration is divided by the volume, U

$$k_{flux} = \frac{iN}{2\mathcal{F}U} \tag{3.22}$$

$$J_{IP3R} = k_{flux}p_o. \tag{3.23}$$

p_o is an important source of nonlinearity in this equation, as mentioned earlier, this equation is based on experimental findings

$$p_o = \mu(b + \frac{V_1 c}{k_1 + c})(1 - \frac{c^2}{k_2^2 + c^2}). \tag{3.24}$$

Here, μ is the constant IP3 concentration. In the original study the dynamic IP3 concentration is also investigated. In terms of minimizing the calcium model, we pre-

ferred the static case in this study. When IP3 is taken static, it can be considered as a bifurcation parameter gauging the dynamics of the model. And when p is also a dynamical variable the system can even depicts spiral waves. Due to its nonlinear nature and varying speeds between variables, this model is very prosperous in terms of showing dynamical behaviours. Also, k_1 and k_2 have powers according to their Hill coefficients. It can be observed that the 2 Ca2+ bound site acts as a negative feedback mechanism for the flux. According to these grounds which domain dynamics is based on, the coefficients b and V_1 has a relation in between. Both of these represents the interaction of the domain that leads an opening in the IP3R. The parameter b is rate of the second domain activated with no calcium attached and V_1 is rate of the domain activated with calcium attached. Hence they are add to 1.

This model doesn't take into account of many realistic features of the underlying biology. In recent studies, it has been shown that dynamical behavior of receptor migration plays an important role in the dispersion of the concentration configuration in the cytosol [118, 119]. Cooperation between IP3Rs and trans-membrane gates is a proof for the effect of position of the receptors on calcium. Another neglected feature is how different and cooperative sub-types of IP3R work [120, 121]. A more dramatic deficit in the model is however the number of sub-units. IP3R has four sub-units, i.e., there are four sites of connection [122, 123]. Also the receptor requires binding of four IP3Rs to open the channel. Another important fact is that calcium is highly reactive and when it is secreted to the cytosol other intracellular factors (called buffers) acts to stabilize the existent calcium level to protect the calcium homeostasis, and hence the cell [124].

Since we will combine different models that working on different dimensions (for instance, Arbitrary Units in the angiogenesis model), in our model we will use non-dimensionalized versions of equations 3.17 and 3.18. We first non dimensionalize vari-

ables c and t as $k_1\bar{c}$ and $\tau_n\bar{t}$ respectively, then we will drop bars to obtain

$$\frac{\partial c_i}{\partial t} = D_0\ \nabla^2 c_i + K_1\ \mu_i\ n_i \left(\frac{b + c_i}{1 + c_i}\right) - K_2\ \frac{c_i}{K_3 + c_i} \tag{3.25}$$

$$\frac{dn_i}{dt} = 1 - \frac{c_i^2}{K_4 + c_i^2} - n_i \tag{3.26}$$

here

$$K_1 = \frac{k_{flux}\tau_n}{k_1'} \quad K_2 = \frac{\gamma\tau_n}{k_1'} \quad K_3 = \frac{k_\gamma}{k_1'}\ \ K_4 = \frac{k_2'}{k_1'}. \tag{3.27}$$

We will continue with these coefficients in the non-dimensionalized equations.

3.4. Mechanochemical Movement Model

Here, we will illustrate the mechano-chemical extention/contraction model that we will use in later chapters.

Cell migration is a complex event where calcium plays a role in nearly every step [64, 75, 125]. First and foremost, a cell moving on course needs polarization, and this requirement is met via stable or transient gradients of calcium [74, 126]. Also, orientation to an off-route direction is rendered possible with flickers originating from mechanosensitive calcium channels, like TRPM7, by stretched protrusions on membrane dynamically [59, 64]. In addition, adhesion points in the cell are spatially regulated by calcium. Interestingly, calcium dissemble rear focal adhesions (FA's) and strengthen frontal FA's. This relocation of FA's is related mostly to the overall calcium gradient across the cell cytosol. It is claimed that high levels of concentrations detach mature FA's, and nascent FA's are attached by low levels of calcium. Retraction behavior cannot be observed without released adhesion points, for this reason, cell contraction is observed in areas where adhesions are released [75]. However, these

and many other processes may create spatial perturbations in the cytosolic calcium. Yet, spatiotemporal coordination of the calcium wave should be maintained to have a polarized cell moving in a direction. Living organisms transform from small nuclei into large adults by the volume increase due to division of cells. In addition to the volume change, some specialized moving cells and tissues (a tip cell is one of those specialized mobile cells kinds) give a new shape to the growing tissue. While mobile movements can be the result of biological events, they can also be the cause of biological effects with elements/sensors such as receptors that are activated when stretched. As shown in the [127–130] models, the stretching of the cells can produce effects that can alter and at some limits even inhibit calcium release. If possible interventions that could change or turn off the signal should be included to the model, since angiogenesis requires cell mobilization this extension came natural.

The work of Kaouri et. al [4] preferred Atri et al. as well [3]. For that reason we preferred to include this model which is inspired heavily from other studies [21,82,131]. These models are using the visco-elastic gelation-solation argument where elastic materials can be modeled via their sheer and stress tensors. Under a viscoelastic assumption the same can be achieved for analysing the cell subjected to internal or external forces. (Assumptions and underlying parameter values can be determined by experiments.) Points in the solid can be displaced under such forces and it can be depicted as a displacement vector $\vec{u}(x,t)$. Displacement is easy to apply for circumstances where the set-up has clearly stated boundaries where the unstrained position is defined. However in the absence of those clear boundaries as in the case of cells, preferring another variable instead of displacement can be more practical. For this reason in this model dilatency/contraction θ is used for showing the viscoelastic status quo of the cell

$$\theta = \nabla.\vec{u}(x,t). \tag{3.28}$$

Mechano-stress sensitive channels triggers calcium intake when the channels are excited via stretching under a force. However, we are not going to assume and external source for any stress. By following [21, 131] the stress tensor and force balance equation for

visco-elastic material are

$$\vec{\sigma} = \zeta_1 \dot{\vec{e}} + \zeta_2 \theta_t \vec{I} + E'(\vec{e} + \nu' \theta \vec{I}\,) - T(c)\vec{I} \tag{3.29}$$

$$\nabla . \vec{\sigma} = 0 \tag{3.30}$$

where I is the unit tensor and the shear ζ_1 and bulk ζ_2 viscosities are taken as constants for linear cytosolic viscoelastic material. Above the strain tensor $e = \frac{1}{2}(\nabla \vec{u} + \nabla \vec{u}^T)$. Coefficients with Young modulus, E, and Poisson's ratio ν are

$$E' = \frac{E}{1+\nu}, \quad \nu' = \frac{\nu}{1+\nu}. \tag{3.31}$$

For the 1 dimensional case the strain tensor becomes the same as dilatation/contraction and the integration constant can be taken as 0 so that

$$0 = [(\zeta_1 + \zeta_2)\partial_t + E'(1+\nu')]\theta - T(c) \tag{3.32}$$

$$\partial_t \theta = \frac{E'(1+\nu')}{(\zeta_1 + \zeta_2)}\theta - \frac{T(c)}{(\zeta_1 + \zeta_2)}. \tag{3.33}$$

This equation should be coupled to the calcium equation before non dimensionalization. This coupling will gauge the influence on mechanical strength to the calcium dynamics. The coefficient should be closely related to the type of the stretch sensitive calcium channel, since we are not focused on a specific type of stretch sensitive channel but rather all channels, we will take this comparable to the other terms in calcium equation. Since we will solve these models in the same spatial and temporal domain what means as time and space should be the same for both equations. We nondimensionalized time in the prior sections as $t = \tau_n \bar{t}$ hence we cannot combine t and $\bar{t}$ by coupling a

nondimensionalized model to a dimensionful one

$$\begin{aligned}\frac{\partial c(x,t)}{\partial t} =& D\frac{\partial^2 c(x,t)}{\partial x^2} + \mu k_{flux} n(x,t)(b + \frac{V_1 c(x,t)}{k_1 + c(x,t)}) - \gamma \frac{c(x,t)}{k_\gamma + c(x,t)} \\ &+ \Lambda\theta(x,t)c(x,t) \qquad (3.34)\\ \tau_n \frac{\partial n(x,t)}{\partial t} =& \frac{{k_2}^2}{{k_2}^2 + c(x,t)^2} - n(x,t) \qquad (3.35)\\ \frac{\partial \theta(x,t)}{\partial t} =& \frac{E'(1+\nu')}{(\zeta_1+\zeta_2)}\theta(x,t) - \frac{T(c)}{(\zeta_1+\zeta_2)}. \qquad (3.36)\end{aligned}$$

after non-dimensionalization the equations we get

$$\begin{aligned}\frac{\partial c(x,t)}{\partial t} =& D_0\ \nabla^2 c(x,t) + K_1\ \mu_i\ n(x,t)\left(\frac{b + c(x,t)}{1 + c(x,t)}\right) - K_2\ \frac{c(x,t)}{K_3 + c(x,t)} \\ &+ \lambda\theta(x,t)c(x,t) \qquad (3.37)\\ \frac{dn(x,t)}{dt} =& 1 - \frac{c(x,t)^2}{K_4 + c(x,t)^2} - n(x,t) \qquad (3.38)\\ \frac{d\theta(x,t)}{dt} =& -\ k_\theta\theta(x,t) + \tilde{T}(c(x,t)) \qquad (3.39)\end{aligned}$$

where

$$\lambda = \frac{\Lambda\tau_n}{k_1}, \quad k_\theta = \frac{E'\tau_n(1+\nu')}{(\zeta_1+\zeta_2)}, \text{ and } \tilde{T}(c(x,t)) = \frac{\tau_n T(c(x,t))}{(\zeta_1+\zeta_2)}. \qquad (3.40)$$

Parameter values will be given at the following chapter. Since in the main model at Chapter 4, we denote only the estimated parameters with greek letters, we will denote $\theta(x,t)$ with $u(x,t)$.

3.5. A Brief Comment on Mathematical Modelling

In this section, we try to illustrate the overall situation of mathematical modelling in biology and emphasize its current shortcomings and future possibilities.

As it can be realized from hallmarks of the cancer, this disease requires a strategical treatment planning attacking it from different frontiers, which makes mathematical modelling very handy in terms of cancer studies [132, 133]. Mathematical models provides valuable mechanistic insights by analysing both the parameters and the long term results on variables. It also gives the opportunity of combining different therapies or optimize strategies all together in many diseases including human immunodeficiency virus [134]. Also dynamical features of the system allows for future behavioural perceptivity, for instance, number of cells in tumour mass might be oscillating or reach to a stable point for a variable in different ranges. Besides mathematical modelling can be utilized for finding better treatment agents by predicting the key elements determining the dynamics resulting the observed biological behaviours [132].

Zeitgeist of the science changes through ages, however, changing methodological norms even for the most scientific minds could be challenging. For many years animal testing is the norm of medical investigations, and against the accumulating evidence of its ineffectiveness and the scientific community [135] is reluctant to set the new norm. However, without spending resources (time/money) or increase suffering (for test animals) mathematical modelling have the potential to make prediction for analyses of the real-time optimization problems for biological circumstances [136, 137]. From lab grown mini brains [138], machine learning software, organs-on-a-chip methods [139], to mechanic biosimulations, novel in silico techniques are arising. Nowadays, big pharmaceutical companies like Pfizer, Novartis, Takeda etc. are working with biosimulation companies (Certara, In Silico Biosciences etc.) working on models similar to the ones you will see in this thesis (but much more extensive models with thousands of variables) it is very important for us to follow the recent studies and keep up with the times.

Today more realistic deterministic models are used in pharmacological models with systems biology approach in drug development. Our model, on the other hand, can be considered as a toy model in comparison to the (monstrous) models (including hundreds of variables) used in private sector. Mathematical models of nature are constructed in order to uncover some hidden mechanism or to use well known mechanisms

to optimize the event under inspection. We ask questions to solidify the assumption according to the resulting simulations of the mathematical model created based on the underlying assumptions. In the mathematical scenarios, gates, receptors, pumps are usually modeled related to their domains (with regard to the medium or contents of the domain) [140]. Hill functions are used to mathematically depicting the chemical reactions, and gates are usually regarded in a similar fashion, the number of bounded sites and their cooperativeness effects the concentration difference [140]. However these are naturally hard to measure by experiments and this results to different approaches on the same issue. Usually, a vast spectrum of biological experiments provides some halfway tactable hints (it is halfway due to the usual crowded scenery of the nature of biological events often involving a harmonical interplay between many pathways) but in combination with proper assumptions they can produce realistic results.

4. THE EFFECT OF CALCIUM IN PHENOTYPE SELECTION

In this chapter, we create a model by combining two aforementioned ideas calcium oscillation and phenotype selection. Then, we test our model in various set-ups including spatio-temporal and temporal two cell models, followed by a multi cell model for mimicking an in-silico vessel.

4.1. Biological Motivation

Temporal analysis is crucial in complex processes, and this is especially true in the context of angiogenesis which includes multiple processes such as cell migration, proliferation, and phenotype selection. Recent works have inspected the temporal scales of angiogenic decision-making in this context. Venkatraman et al. [5] designed a two-cell model coupled through VEGF-Notch-DLL4 system where they investigate the variations of time spent in phenotype identities. They examined how the temporal decisions on cellular identities are affected by local conditions. They built a two-cell model having positive feedback with rate equations for intracellular VEGF, VEGFR, DLL4, Notch, DLL4- Notch complex, NICD, HE, and filopodia. By using time-lapse imaging of zebrafish embryos, Yokota et al. [42] showed VEGF-dependent Ca2+ oscillations during endothelial phenotype selection. They observed that all VEGF-activated ECs contained oscillations in their concentration of Ca2+, but that these oscillations survived only in the budding cells, which took on the tip cell phenotype. Savage et al. [141] proposed that Transmembrane protein 33 (Tmem33) was required for cytosolic calcium oscillation in activated ECs. They showed that Tmem33 knockdown reduced ERK phosphorylation and Notch expression in zebrafish and human ECs. They also observed that calcium oscillations maintain filopodia extension and migration. Also, Ca2+ signaling is modulated in mammalian cells with dose-dependent VEGF signaling network [142]. Various cellular responses are thought to be conveyed by temporal Ca2+ dynamics; however, the precise outcome of angiogenic calcium signaling on endothelial

populations requires further investigation. In this model our main ambition to inspect this intricate relation, and further extend the idea in the upcoming chapter.

4.2. Introduction

As a second messenger, calcium has a multi-functional role in cell communication. For cancer specifically, calcium plays a crucial role in relevant pathways involved in angiogenesis, metastasis, and local cancer progression [143,144]. Recent experiments have more thoroughly investigated the link between cytosolic calcium oscillations in endothelial cells (ECs) and the proangiogenic molecule vascular endothelial growth factor (VEGF), [42,141] revealing the importance of Ca2+ oscillations to cell differentiation in the early stages of angiogenesis. Since positive regulators of angiogenesis are still under investigation [44], calcium should also be investigated as a spatio-temporal signalling modulator.

Temporal regulation of the DLL4/Notch pathway modulates the vascular architecture [5, 26, 36]. In their experimentally validated early angiogenesis model, Venkatraman et al. [5] investigated tip cell competition by VEGFR-mediated DLL4/Notch interaction. In their model, two adjacent cells compete against each other by negative lateral inhibition feedback and positive feedback with an arbitrary feedback parameter.

Here, a summary of the assumptions we have:

- Cytoplasmic calcium is known to signal (oscillate) during the phenotype selection.
- DLL4-Notch pathway is known inhibit neighbouring cells and lead to phenotype selection.

Then, we had the following basic questions:

- Can we mimic the observed behaviour of the cells in a Calcium - DLL4-Notch model?

- Would dynamical features of the wave create a significant difference in cell guidance?

Originating from the observations of Yokota et al. [42], we exclude the early factors of DLL4 and connect DLL4 concentration directly to cytosolic calcium by following the below schema.

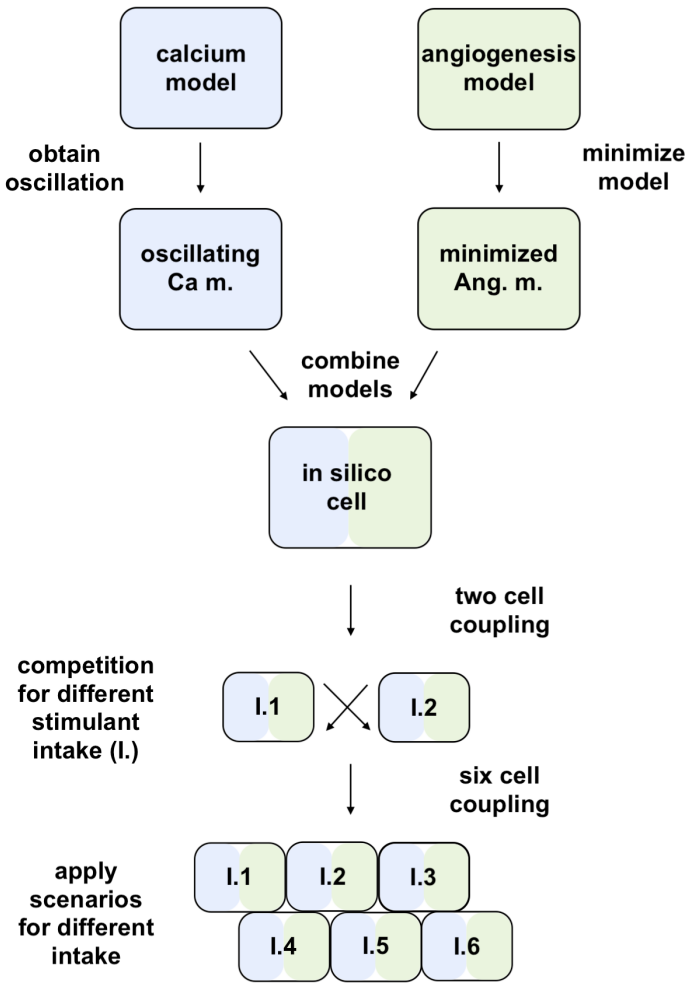

Figure 4.1. Design chart of the model.

In this model we aim to model single-cell size biological effects with rate equations where not all coefficients are well known. For that we need to able to set limits to those unknown variables and change them according to mathematical reasoning for getting a biologically sensible outcome. For that, before combining the models, we focused on the dynamical properties of the calcium model in the previous chapter. This model is

oscillating engine of our model, and even though the oscillation period is short termed (3rd order in time relative to DLL4 dynamics) it sets the outcome of the model. Then, we select the variables reasonable for our question, and finally combined the models. After that point, we apply our model with two- and multi- coupled cell set ups with different configurations on stimulant intake.

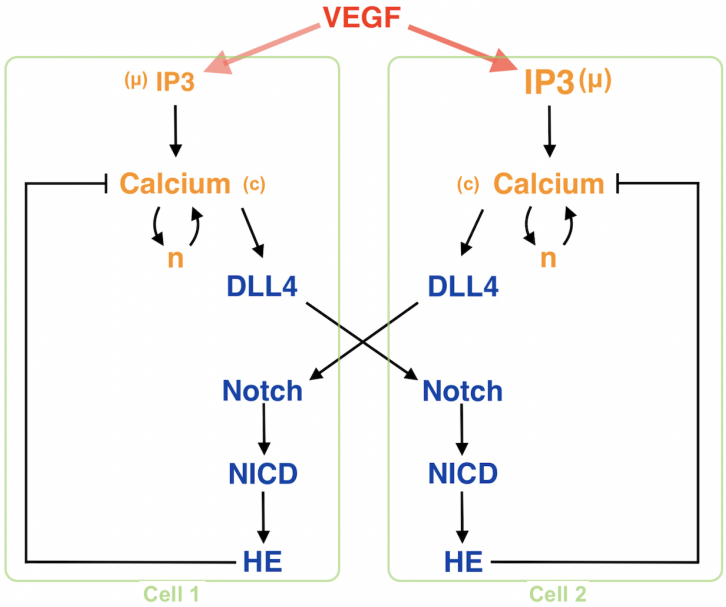

Figure 4.2. Schematic representation of the two cell model explaining the relevant factors and the interactions between them. Here, each cell is illustrated as green boxes including VEGF downstream pathways. VEGF resides in the extracellular space and is included through cellular IP3 concentration through PLCγ. redIn this model, we are aiming to compare the effect of varying VEGF intakes on a cell's angiogenesis dynamics. For this reason, we keep every variable and the initial conditions the same except for VEGF levels. Since IP3 levels are associated with VEGF over PLCγ, the only difference between the cells is accepted as being IP3 levels. Calcium related factors (yellow) are cytosolic calcium, c, the proportion of IP3 receptors not inactivated by calcium, n, and IP3 concentration, μ. The Ca2+ model includes the interplay between IP3R and SERCA pump. Additionally, angiogenesis-related factors (blue) are DLL4, Notch, NICD, and HE. Being trans-membrane proteins, DLL4 and Notch interact with each other to generate a DLL-Notch complex which is also included in the model. Furthermore, while HE family factors mediate Ca2+ by negative feedback, DLL4 secretion is connected to calcium concentration.

The cellular pathway presented in Figure 4.2 is a cytoplasmic calcium-based tip cell model that defines tip cell phenotype as high DLL4 concentration in the overall cell. The spatial configuration of DLL4 is not relevant. Cells are represented spatially

by a one-compartment model and a temporal model.

Selection of the tip cell phenotype activates migratory features within a cell. In addition to the usage of Ca2+ in cellular communication, Ca2+ is also involved in multiple other parts of cell migration. To avoid unnecessary complexity, our model contains the model in Atri et al. [3], representing calcium dynamics only via the IP3R and Sarco/endoplasmic reticulum Ca2+-ATPase (SERCA) dynamics on the Endoplasmic Reticulum (ER). The model takes advantage of the calcium induced-calcium release (CICR), which creates Ca2+ transients when the model includes a diffusion term for Ca2+. This non-excitable cell model is used for displaying calcium dynamics in different cell types for a wide range of problems [4, 113–116, 145, 146]. Wide usage of the model is based on its effectiveness and simple logic. IP3 receptors interact with dynamic cytosolic calcium and IP3 μ which is adapted as a parameter for gauging oscillations. For a range of μ values, oscillatory behavior in Ca2+ concentration can be generated in the system. The rich wave dynamics produced by the model are enabled by the different timescales between activation and inactivation of receptor dynamics.

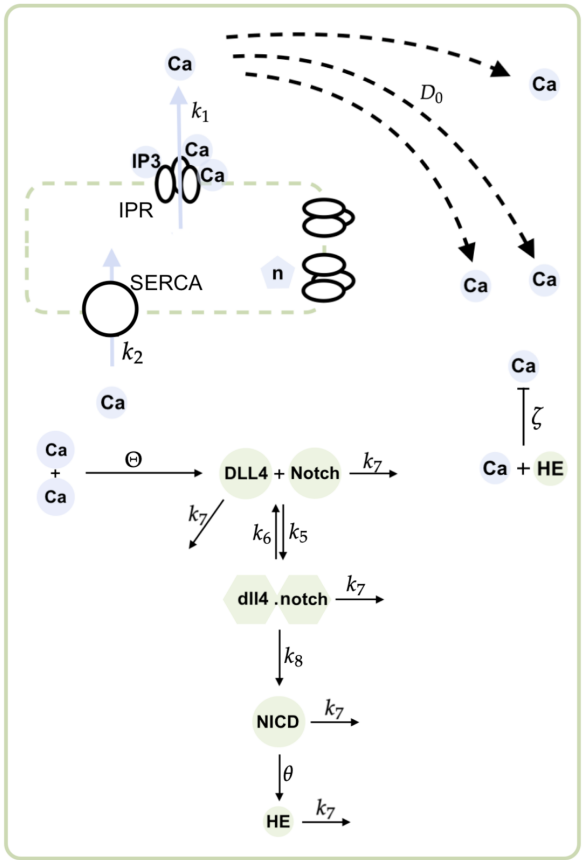

Figure 4.3. Model related events in cellular domain. Color labeled factors are in blue (calcium) and green (angiogenesis). Dashed green line represents ER and the grouped ovals are receptors. The big black circle illustrates SERCA pump. Dashed arrows indicate diffusion for calcium in cytosol. The green factors are represented in-cell even though they include trans-interactions.

4.3. Calcium Driven Phenotype Selection Model

Using in silico models in this model, we attempt to reproduce the results observed in the experiments detailed above. In particular, we aim to create a model capable of describing calcium oscillations coupled with angiogenic processes based on a lateral inhibition mechanism involving DLL4/Notch interaction. Since inhibition is contact-dependent, we propose several set-ups for cell domains: (i) a two-cell spatial configuration for inspection of Ca2+ distribution, (ii) a two-cell model with temporal dynamics, and (iii) a 6-cell set-up for investigation of neighboring dynamics. We also

consider the interaction of the lateral inhibition mechanism with HE-calcium negative feedback to inhibit oscillatory dynamics in the cell. Studies investigating angiogenic Ca2+ oscillations [42, 142], and VEGF signalling network [5] use procedurally-defined arbitrary units. Here, the model is also combined and presented using arbitrary units. So far, experiments looking at early angiogenesis have not reported cellular concentrations of relevant molecules. Therefore, in their absence, cell phenotypes can be assumed based on other traits: for example, in the experiment by Yokota et al. [42], tip cells are defined according to their shape rather than their DLL4 concentration.

Our model includes two already existed models one has variables in units of molar concentrations the other was in AU (Arbitrary Unit) for that we first nondimensionalized the calcium model then combined with already nondimensionalized angiogenesis model with $t\tau_n$. The nondimensionalization procedure helps to diminish the number of measured coefficients by making reasonable space-time assumptions. When the procedure has followed, some parameters might become negligible relative to others (for that reason we did not include cytosolic calcium leakage to our model). All the nondimensionalized parameters, including the ones from the aforementioned angiogenesis model, (Table 4.1) and coefficients in the below are in arbitrary units (AU) as we seek to model the qualitative, rather than quantitative, dynamics.

Table 4.1. Parameters used in the model were taken from [3–5] as indicated above. Since there is a lack of experimental data on cytosolic ion and protein concentrations, we use Arbitrary Units (AU) for the qualitative, rather than quantitative portrayal of relative concentrations.

Parameter	**Symbol**	**Value**	**Ref.**
Diffusivity of Ca2+	D_0	0.1	[3]
Basal gene expression of proteins	β	0.001	[5]
Production rate of NICD	θ	0.1	[5]
Production rate of DLL4	Θ	1.5	Est.
Negative feedback rate of HE on Calcium	ζ	0.6	Est.
Basal current through IP3R	b	0.111	[3]
Maximum total Ca2+ flux through IP3R	k_1	23.1	[4]
Maximmum rate of Ca2+ pumping from the cytosol	k_2	5.7	[3]
Half maximum rate of Ca2+ pumping from the cytosol	k_3	0.14	[3]
Half maximum rate of DLL4 production	k_4	1.4	[5]
Association rate for dn complex	k_5	0.4	[5]
Disassociation rate for dn complex	k_6	0.002	[5]
Degradation rate of proteins	k_7	0.01	[5]
Catalyses rate for dn complex	k_8	0.2	[5]
Half maximum rate of NICD production	k_9	0.5	[5]

Table 4.2. Initial conditions used in the model were taken from [3, 5]. The initial values of c, and n variables provides the special conditions for the spatially observed wave dynamics in calcium transients. In addition, v value indicates DLL4 concentration preexist any external trigger of the DLL4 - Notch pathway.

Parameter	c	n	v	w	x	y	z
Initial Condition (A.U.)	0.200165	0.961477	0.1	0	0	0	0

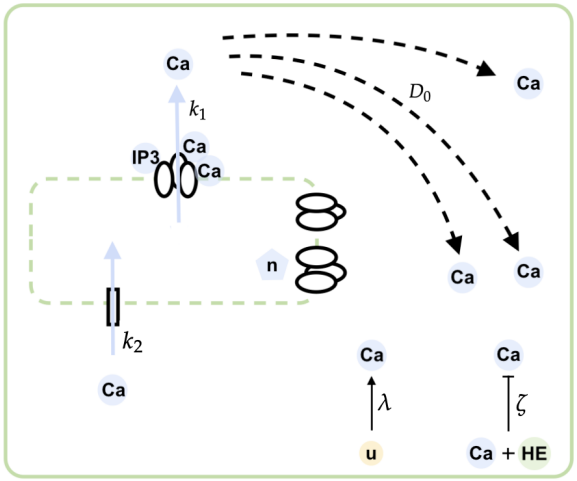

Figure 4.4. Calcium related events in cellular domain. IP3R and SERCA pump is shown in relation to their rate coefficients. Here, we illustrate cytosolic diffusion of calcium, the main contributor of the model IP3 receptor, the SERCA pump, and the angiogenic coupling terms assumed reaction. In this figure IP3 sites depicted to illustrate factors representing their behaviour. Therefore, we have 4 sites with 3 distinct behaviour: IP3 and calcium resulting a positive feedback, along with cooperative binding by calcium consequencing the negative feedback.

In the two-cell model equations depicted below, the subscript i specifies the cell while the subscript j specifies its neighbour. Calcium dynamics are governed by the following equations

$$\frac{\partial c_i}{\partial t} = D_0 \, \nabla^2 c_i + k_1 \, \mu_i \, n_i \left(\frac{b + c_i}{1 + c_i} \right) - k_2 \, \frac{c_i}{k_3 + c_i} - \zeta \, z_i \, c_i \tag{4.1}$$

$$\frac{dn_i}{dt} = 1 - \frac{c_i^2}{1 + c_i^2} - n_i. \tag{4.2}$$

where c, and n correspond to the cytosolic calcium concentration and the proportion of IP3 receptors not inactivated by calcium. The terms on the right-hand side of the calcium equation represent calcium diffusion inside the cytosol, endoplasmic Ca2+ flow by IP3 receptor, cytoplasmic calcium pumped out, and negative feedback by HE family proteins on calcium. Here, we examine a situation where calcium dynamics are activated only due to a VEGF-related increase in cytosolic IP3 levels. Concomitantly,

Ca2+ levels diminish by efflux from the cytosol and HE negative feedback. Repression to the signaling cascade is applied on Ca2+ rather than IP3 since inhibited signals are observed in Yokota et al. In addition, the right-hand side of Equation 4.2 denotes receptor inactivation by Ca and receptors.

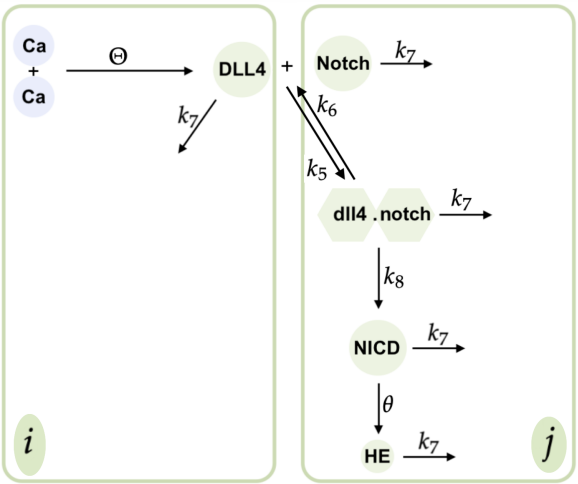

Figure 4.5. Angiogenic reaction schema in cascade direction, including calcium contribution, degradation term, k_7. Here it can be seen that dll4.nicd is a complex and for that reason it also has a back reaction which makes the system highly nonlinear. In this model only trans-interaction between transmembrane proteins is showed, for that reason we depict the interplay between different cells with varying subscripts i and j also showed in the schema. Here, we illustrated the reactions by following the cascade.

Stable configurations in EC (endothelial cell) phenotypes are usually distinguished by a specific gene expression of DLL4 [5, 147]. Here, we follow the same logic and consider DLL4 concentration as the sole determiner of expression of the tip cell phenotype. The equations describing the interaction between adjacent cells are as follows

$$\frac{dv_i}{dt} = \beta + \Theta \frac{c_i^2}{{k_4}^2 + c_i^2} - k_5\, v_i\, w_j + k_6\, x_j - k_7\, v_i \tag{4.3}$$

$$\frac{dw_i}{dt} = -k_5\, v_j\, w_i + k_6\, x_i - k_7\, w_i \tag{4.4}$$

$$\frac{dx_i}{dt} = k_5\, v_j\, w_i - k_6\, x_i - k_7\, x_i \tag{4.5}$$

where, v, w, and x describe concentrations of DLL4, Notch, and DLL-Notch complex respectively. The terms in Equation 4.3 are the basal DLL expression, the gene expression of DLL4 by Ca2+, DLL4 association by Notch of the adjacent cell, disassociation of the complex of the neighbour and DLL4 degradation. Respective terms in Equation 4.4 are an association of adjacent cell's DLL4 with Notch, disassociation of the DLL-Notch complex and Notch degradation. In addition, the terms on the right-hand side of the complex equation are an association of adjacent cell's DLL4 with Notch, disassociation of the complex and degradation of the complex.

Following DLL4-Notch signalling between neighbouring cells, the equations depicting NICD triggered secretion of HE family proteins are given by

$$\frac{dy_i}{dt} = k_8\, x_i - k_7\, y_i \tag{4.6}$$

$$\frac{dz_i}{dt} = \beta + \theta\, \frac{y_i^2}{y_i^2 + {k_9}^2} - k_7\, z_i \tag{4.7}$$

where y and z describe NICD and HE concentrations in the cell. The terms on the right-hand side of Equation 4.6 are the catalysis of the complex, and degradation of NICD. The terms in the last equation are the basal secretion of the factor, gene expression of HE by NICD, and HE degradation.

In the experiment by Yokota et al., both Ca2+ transients are observed across the cell, and cytosolic calcium changes are measured from the fluorescence of a calcium-related dye for a specific region of individual cells. Therefore, the experiment yields two types of information: spatial Ca2+ transients and temporal oscillations. Here, we aimed to reproduce both types with suitable approaches to the limitations of the model. Considering that DLL4 and Notch factors are trans-membrane proteins that should reside on the boundary of the surface, the setup of Venkatraman et al. [5] isn't suitable for a spatial domain simulation. Therefore, we used a spatial and temporal model. All initial conditions for PDE Ca2+ equation are taken the same as in the temporal case. Ca2+ is given an initial condition of a localized Gaussian peak at the center of the cell, capable of initiating the traveling wave dynamics.

4.4. Estimating Parameters

For the steady state analyses of the model in Equation 3.17 and 3.18 (β is taken 0)

$$0 = \mu k_{flux} n(x,t)(b + \frac{V_1 c(x,t)}{k_1 + c(x,t)}) - \gamma \frac{c(x,t)}{k_\gamma + c(x,t)} \tag{4.8}$$

$$0 = \frac{{k_2}^2}{{k_2}^2 + c(x,t)^2} - n(x,t) \tag{4.9}$$

from here we get an equilibrium curve between c and μ

$$\mu = \frac{\gamma c(x,t)({k_2}^2 + c(x,t)^2)}{{k_2}^2(k_\gamma + c(x,t))k_{flux}(b + \frac{V_1 c(x,t)}{k_1 + c(x,t)})}. \tag{4.10}$$

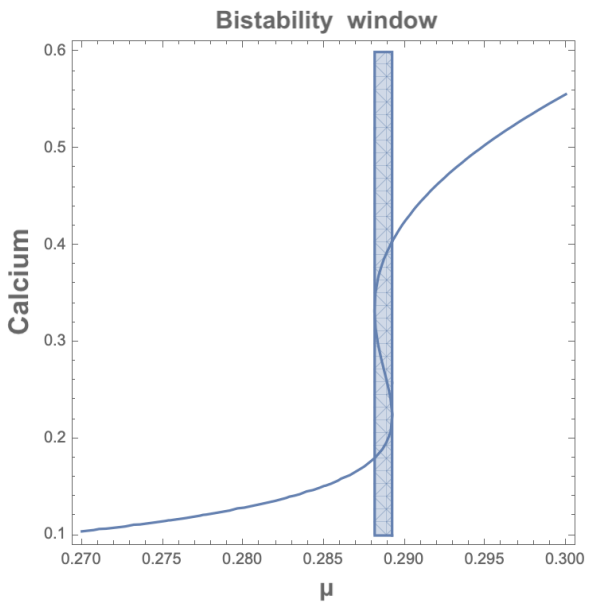

Figure 4.6. Nullcline for the dimensionless version of calcium Equation 3.17 showing the interval for oscillating behaviour. The nullcline is drawn from 4.10. In the equation all parameters of the Equation 3.18 is fully known. The model has been initiated from the steady states of the variables with a spatial perturbation, in order to create the desired dynamics. Steady states have been found from the ends of bistability window.

For a more detailed nonlinear inspection the Jacobian of the system has been computed below,

$$F = \mu k_{flux} n(x,t)(b + \frac{V_1 c(x,t)}{k_1 + c(x,t)}) - \gamma \frac{c(x,t)}{k_\gamma + c(x,t)} \tag{4.11}$$

$$G = \frac{{k_2}^2}{{k_2}^2 + c(x,t)^2} - n(x,t) \tag{4.12}$$

$$Tr = \partial_c F + \partial_n G \tag{4.13}$$

$$Det = \partial_c F \partial_n G - \partial_c G \partial_n F \tag{4.14}$$

$$Discr = (Tr)^2 - 4Det. \tag{4.15}$$

Travelling waves can have different dynamics and we can seek the proper dynamics with nonlinear analysis. From the beginning, we wanted to base our model on top of the calcium model. This is a calculative assumption since, investigating the oscillatory dynamics of a two variable system would be easier than inspection of the resulting 8 variable system. Also, to couple the models, we will be adding coupling terms including other variables to the calcium model. This will reflect as perturbations of the system away from the oscillating behaviour. Since we are interested with oscillating dynamics we will seek for parameters where the stability changes its nature and periodic oscillations emerges. For that reason, we search for Hopf bifurcations where the eigenvalue of the Jacobian becomes imaginary

$$\lambda = \frac{-Tr \pm \sqrt{(Tr)^2 - 4Det}}{2}. \tag{4.16}$$

For this to happen, the bifurcation parameter should satisfy $Tr = 0$ and $Det > 0$ conditions. With the existed parameters, we get that for the interval of $\mu = 0.29800 - 0.49500$ calcium concentration shows oscillatory dynamics. This sets us a reasonable interval where we might want to focus on. On the other hand, one should also take the nature of the problem into consideration. Our bifurcation parameter represents IP3 concentration in the cell, and its presence which will be given by hand is directly related with the concentration intake of the stimulant that we are interested in, VEGF. These cells are neighbours so we will focus on relatively similar range up to $\mu = 0.28 - 0.32$ in

scenarios. By choosing a range of parameters, we loosen the travelling wave conditions. This will lead waves profiles that is going to disperse and will die out easily.

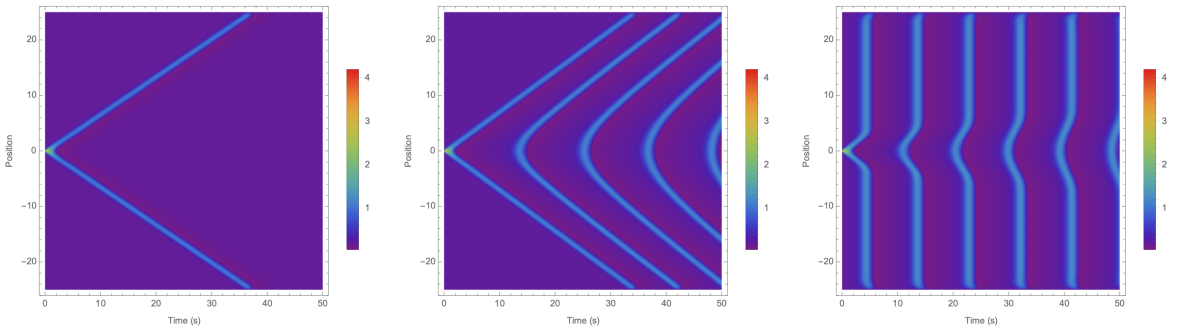

Figure 4.7. 1D example scenarios for depicting the dynamical effect of different IP3 μ levels. These graphics can be interpretable as if 1 dimensional domains that are glued to each other, creating a 2D domain. (This way of picturing chemical concentrations is particularly practical for observing the constant velocity of the wave.) In the left most figure, where $\mu = 0.288$, the wave is travelling faster than the center figure where $\mu = 0.289$. It can be seen that in the center figure the diffusion is beginning to take the control, therefore we have a rounding effect in the centre of the 1D domain.

4.5. Solution Method in Two-cell Spatio-temporal Coupling

A square domain with side length $x = 30AU$ for time $t = 4000s$ was considered for each cell when solving our model numerically. Characteristic variables for our model are $x = x_0\tilde{x}$ and $t = t_0\tilde{t}$ for nondimensionalization where $x_0 = 20\mu m$ and $t_0 = 2$. The spatial two-cell model is solved using a finite element method implemented using the FEniCS Project Software [148, 149]. A Crank-Nicolson time-stepping scheme is used to discretize the temporal domain for all equations. The Crank-Nicolson discretization method [150] for an heat equation,

$$k\frac{\partial \phi}{\partial t} = \frac{\partial^2 \phi}{\partial x^2} \tag{4.17}$$

for the above equation, k is any constant in the absence of sources

$$k\frac{\phi(i,j+1)-\phi(i,j)}{\Delta t}=\frac{1}{2}\left[\frac{\phi(i+1,j)-2\phi(i,j)+\phi(i-1,j)}{\Delta x^2}\right. \\ \left.+\frac{\phi(i+1,j+1)-2\phi(i,j+1)+\phi(i-1,j+1)}{\Delta x^2}\right] \tag{4.18}$$

is chosen to be applied with crossed triangle mesh element. Crank Nicolson is the de-facto solver for many PDEs due to it is unconditional stability and renders possible bigger time steps than explicit methods.

4.6. Results

To evaluate whether our model can present Ca2+ transients as observed in vivo in the experiments by Yokota et al [42], we performed simulations in a spatial domain with calcium diffusion. We focused on how wave dynamics change with IP3 and VEGF intake considering calcium transients influence filopodia and other migrational features of the cell. The model is capable of creating calcium transients on a spatial domain. We evaluated the model with Ca2+ diffusion and a localized Gaussian peak at the center of the domain to initiate the wave dynamics. The transients that our model predicts are consistent with observations. Notably, we also observed that before the calcium waves were suppressed by negative HE feedback, traveling waves were observed in cells with low levels of IP3. For cells with higher levels of IP3, the traveling waveform loses its interesting traveling features and becomes a step-like wave. Figure 4.8 depicts how Ca2+ waves propagate from the center of the cell toward its boundaries. When VEGF intake and therefore cytoplasmic IP3 concentration is high, the balance between diffusion and reaction dynamics is distorted on behalf of reaction, and the interesting features of the wave-front are lost.

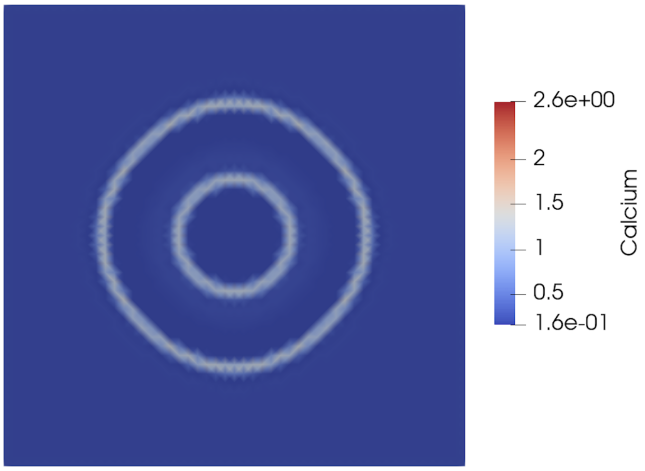

Figure 4.8. Spatial configuration for Ca2+ dynamics in the presence of diffusing from the Gaussian peak at the center. Configuration is estimated for $\mu = 0.28900$ in 4.8. At $\mu = 0.28900$, a Hopf bifurcation occurs, and relaxation oscillations are observed. Reaction of system to low IP3 levels and corresponding Ca2+ wave dynamics.

On of the questions we aimed to ask in the beginning of this model was "*Would dynamical features of the wave create a significant difference in cell guidance?*" Later, it occurred that dynamical features of calcium is irrelevant for the tip cell selection process and for that reason we did not discuss travelling waves regarding to angiogenic problem but confined ourselves to show that calcium is able to show transient waves and we will use these waves later in connection with the gelation solation extended model.

4.7. Solution Method in Two-cell Temporal Coupling

For the temporal model two-cell setup, the diffusion term in Equation 5.1 is excluded, such that the equation governing the Ca2+ dynamics becomes an ODE. This two-cell setup clearly shows the effect of DLL4 - Notch coupling. Without coupling, we do not have the resurrecting secondary oscillations resulting in the difference in phenotypes. The model simulations are performed using Method of Lines with a built-in adaptive solver NDSolve, in Mathematica 12. Method of lines (MOL) is a scheme combining both analytical and numerical methods. In MOL D-dimensional PDE is

discretized in D-1 dimensions with numerical discretization and uses the analytical solution of the PDE in the remaining dimension. It is numerically stable and due to its semi-analytical nature it reduces the computational time and effort [150].

4.8. Results

In the experiments by Yokota et al. [42], it is observed that DLL4 levels increase as a result of oscillating calcium dynamics and that cells who maintain their oscillatory behavior eventually present a tip phenotype. To demonstrate this phenomenon, temporal simulations are performed. Since tip cell behavior is linked to containing higher DLL4 concentration, Ca2+ has an essential role in gauging the direction such as cell polarization and filopodia stability. During migration, the spatial distribution of calcium is unrelated when phenotype destiny is considered. It is observed that both cells begin to oscillate; during this phase DLL4 concentration in both cells starts to increase. As it can be seen from Figure 4.9, Ca2+ oscillations become damped at later times. In some cases, damping may not cease the oscillating completely, but in all cases, it is damped for an interval following primary oscillations. This damping occurs as a result of the lateral inhibition related to HE negative feedback. On the other hand, lateral inhibition decreases the elevated DLL4 levels after oscillations ceased, and hence their contribution is stopped. Following the quiet period, n (i.e. the fraction of IP3 receptors which is not closed due to Ca2+) continues to decrease and rebounds oscillations over a certain threshold. DLL4 concentration of the oscillating cell notably increases in the secondary oscillation phase until reaching a steady state notably higher than the other cells. Therefore, the cell having notably higher DLL4 levels is defined as a tip cell.

Here we can observe that DLL4 has small gradual oscillations. This feature takes place since Ca2+ dynamics is much faster than DLL4-Notch interaction.

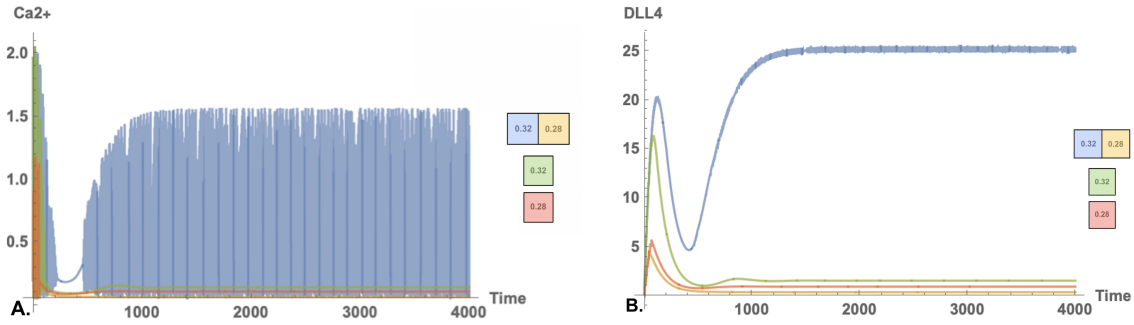

Figure 4.9. For $\mu_{left} = 0.29$ and $\mu_{right} = 0.32$ temporal calcium and DLL4 dynamics. In **A.,** we compared isolated case where cells don't communicate by DLL-Notch interaction with interaction case for Ca2+ levels. We observed that secondary oscillation phase rise from interaction dynamics. Similarly, in **B.,** DLL4 concentration elevates for the oscillating high μ interacting cell. Compared to high μ non-interacting cell, DLL4 levels are significantly higher.

4.9. Solution Method in Six-cell Temporal Coupling

In the multi-cell setup, the vessel is accepted as it consists of a total of six cells in a 2×3 setting. We perform simulations for all cells simultaneously. Since each cell has seven rate equations, we have 42 equations coupled through DLL4 - Notch signaling with different IP3 levels in a multi-cell scenario. Even though this model focuses only on temporal values, we placed cells such that an azimuthal cross-section of the vessel comprised two cells. The alignment and the enumeration of the cells are given in 4.10. Similar to the spatial calcium transient domain, cells in the multi-cell model are accepted as squares, and their placement is shifted. This arrangement enables equal contact sites with a different number of neighbors. This multi-cell setup depicts the result of cell-to-cell communication. Patterning in neighboring ECs is examined under different conditions, which cannot be created with a two-cell setup only. We use six cells for examining the effects in a small region of cells. We focus on this close neighborhood for investigating the effects of cell-to-cell contact on a cell rather than examining the collective behavior.

4.10. Results

To further elucidate the importance of the interaction dynamics, we simulated various multi-cell scenarios depicting the different levels for VEGF related IP3 intake, μ, and show that calcium oscillating cells remain in the tip character. We aimed to inspect relations between neighbours by a cylindrical vessel comprising 6 cells. Cells are placed as in Figure 4.10 where all contacting cells contact the same amount, and interactions are normalized according to the cell number to keep results levelled. We observe that the results of the six cell model agree qualitatively with the results from the two cell model. One small difference is that calcium reaches lower levels in the secondary oscillatory phase. Similarly, DLL4 dynamics reached a lower plateau than in the two-cell scenario.

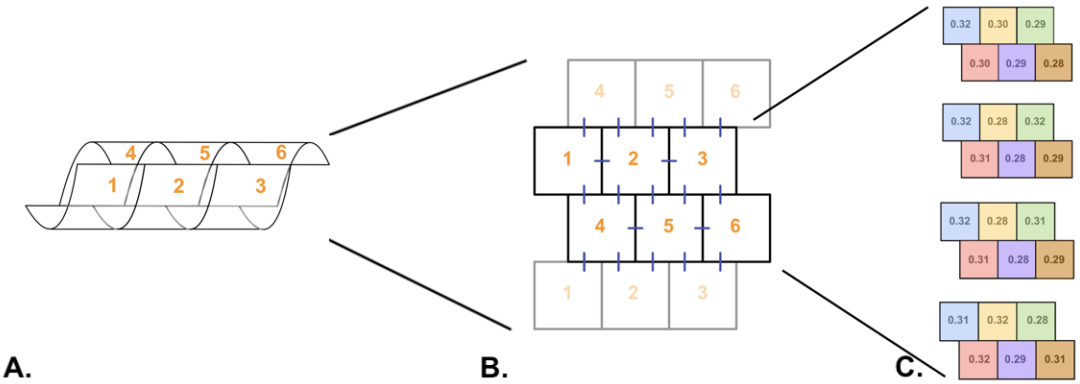

Figure 4.10. Cell enumeration and placement in the multi-cell scheme. **A.**, wrapped cylindrical vessel figure. **B.**, flat vessel with cell boundaries can be seen clearly. Blue lines indicate the cellular interactions, and the fainter cells are placed for depicting the cylindrical boundary. **C.**, applied stimulant configurations illustrated in color labeled cells with assigned IP3 concentrations are given inside. Cells are labeled in color such that calcium and DLL4 profiles will be demonstrated in matching colors.

For questioning the generalizability of the model, different μ distributions across cells are considered for the following situations. First, the model is evaluated with a decreasing μ gradient towards the cells on the right. Second, for understanding the contribution of cell's own μ level, we altered the μ level of the cell by increasing only a small amount and compared with the original result. For that, we run the simulation

with the configuration at Figure 4.14. Then, we increase the IP3 concentration for one of the cell that has been selected as a tip cell by the model. Finally, we analyze a μ distribution allowing the comparison of the cells in the extremities of the vessel. Here, we assigned two highest-in-concentration cells as neighbours and observe how lateral inhibition process takes place as illustrated in Figure 4.18.

Under a decreasing VEGF gradient in the axial direction, cells select a single cell as having the tip phenotype 4.11 B.. When the gradient is applied for higher levels, it is observed that cells reacted in the same manner. It can be observed that in Figure 4.11 B. there is a small change in the increase of the DLL4 level. The change occurs due to the relatively high VEGF intake of the neighbours so that the levels in neighbouring cells are decreased and the tip cell reaches its steady-state earlier.

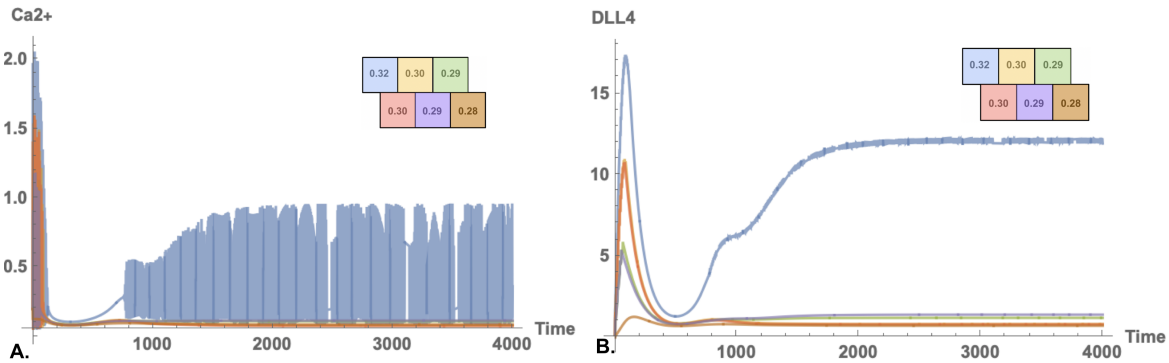

Figure 4.11. Example simulation for decreasing gradient μ. In **A.**, late calcium oscillations are observed initially in the cell having the highest concentration, $\mu = 0.32$. In **B.**, DLL4 concentrations reaching a plateau around t=1800.

In Figure 4.12 we also examine the contribution of cell μ levels under the same external conditions. In Figure 4.12 A and B the third (green) cell has $\mu = 0.31$ and in C and D has $\mu = 0.32$. First, it can be seen that the fourth (pink) cell which contains $\mu = 0.31$ as in third (green) cell in Figure 4.12 A and B, didn't select the tip cell phenotype under any circumstance. This is due to the higher μ level of the first (blue) cell which is its neighbour. We observed that having higher calcium levels induces higher DLL4 levels in the late period. Another important characteristic of Figure 4.12 A is that, although μ levels of third (green) cell are lower than the first,

Ca2+ oscillation of the third (green) cell started oscillation in an earlier time and from a higher level compared to the first cell. This depicts the influence of neighbour contribution on Ca2+ signalling.

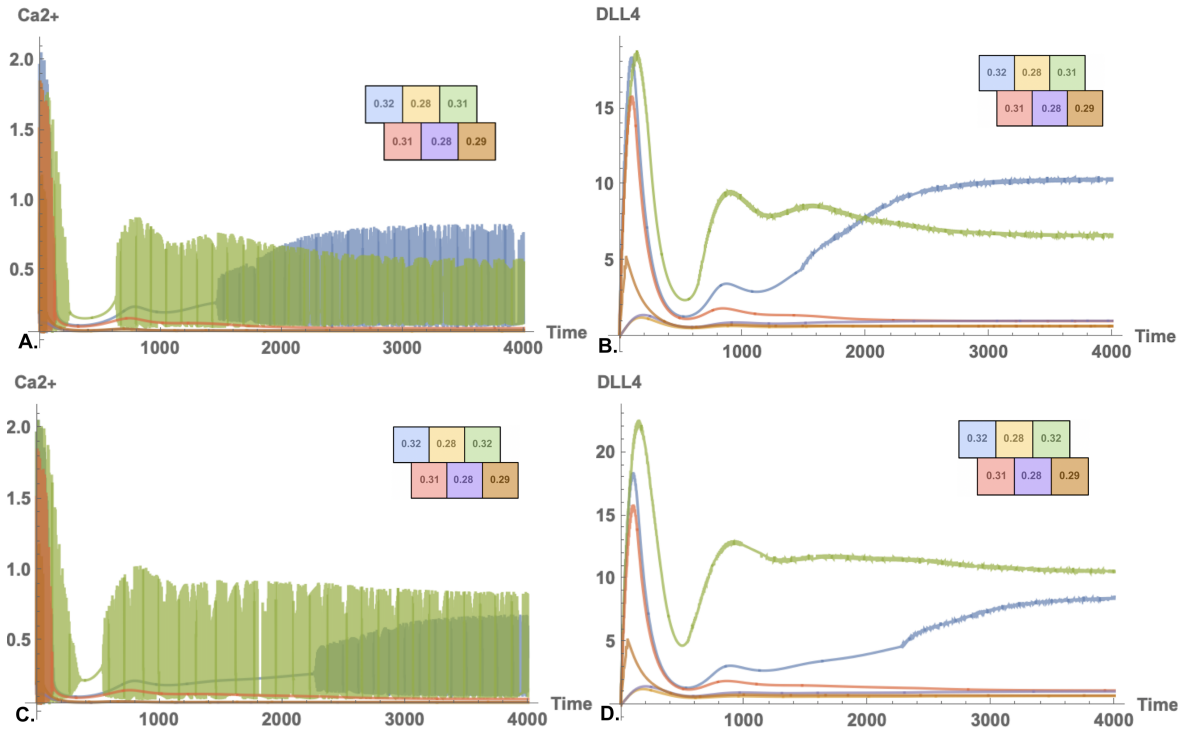

Figure 4.12. Example scenario in comparison of μ levels. In **A.**, cells containing high μ levels (green and blue) continued to oscillate. The cell with the highest concentration is shown to begin oscillating in a later time with lower Ca2+ levels. Although having the having the same amount of μ, the 4th cell (pink) doesn't posses continual oscillations as in the green cell. In **B.**, the late DLL4 concentration are higher in the blue cell relative to the green. However it is shown to increase later in accordance with late initiation of Ca2+ oscillation. In **C.**, the concentration in the green cell is increased and it is shown to influence the timing for blue cells secondary Ca2+ oscillation phase. In **D.**, DLL4 concentrations for the case where the blue and the green cells contains same amount of μ. It can be seen that the blue cell has lower DLL4 level for late times.

Lastly, to examine the case where the cells with the highest IP3 concentrations are adjacent, we used the distribution shown in Figure 4.13. Here cells depicted with yellow and pink colours contain the same highest IP3 levels. The yellow cell wins

the competition between the two, and the pink cell didn't regain Ca2+ oscillations. Although the yellow cell does resume oscillations, as can be observed in Figure 4.13 **A.**, calcium levels during the oscillation are lower than the levels in the orange cell. It shows the determinant influence of neighbouring dynamics on Ca2+ concentrations. On the other hand, μ levels of the yellow cell reach a higher steady-state than the orange cell similar to our prior observations. In addition, the pink cell oscillates in high levels during the initial oscillation period; however, it's oscillatory dynamics ceased due to influence by the blue cell. This clearly shows that cell-to-cell communication determines the phenotype decision. This is particularly important since lateral inhibition suggests that neighbouring cells are deterred to posses the tip phenotype altogether.

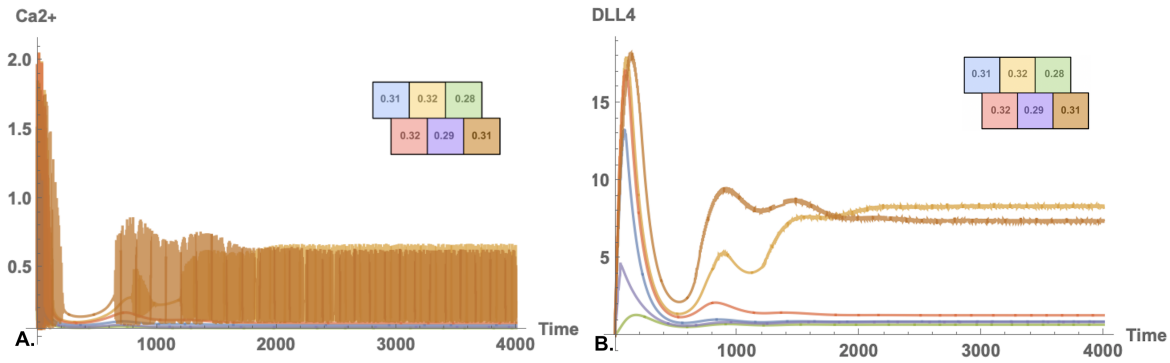

Figure 4.13. Example scenario where two high μ cell yellow and pink are neighbours. In **A.**, calcium oscillates for yellow and orange cells. One of the cells having the highest μ concentration doesn't regain it's oscillations. In **B.**, it can be seen from DLL4 concentrations is that the pink cell (the cell with stalk phenotype despite the high VEGF intake) increased to similar DLL4 levels with the yellow cell, yet unable to re-increase the concentration. However, the yellow cell whose neighbours have lower VEGF intake and consequently lower IP3 levels is shown to increase DLL4 levels in the secondary phase. Also, the late DLL4 levels are higher for the yellow cell than of orange cell.

4.11. Discussion

Calcium plays a crucial role in many steps of cell communication as a second messenger. However, the role of Ca2+ oscillations in EC decision-making has not

yet been entirely understood, but its importance as a key molecule is nevertheless clear. Here, by relating two experimentally validated models [3, 5], we conceptualized a calcium-angiogenesis model to describe the relationship between cytosolic Ca2+ and DLL4/Notch dynamics. We employ mathematical and computational models to investigate the significance of certain actors in the angiogenesis signaling pathway. We examine the role of calcium in the context of angiogenesis-related oscillations, which have been shown to play a significant role in early angiogenesis during the phenotype decision making process [42]. Investigation of pathway-specific events can serve as a framework for explaining the observed results.

In the experiments by Yokota et al. [42], some cells having a longer oscillation duration relative to their neighbors expressed a tip cell phenotype in response to VEGF concentration. For investigating this phenomenon, we simulated cells with the only difference being their cytosolic IP3 concentration, μ (which is related to VEGF concentration). These different IP3 levels determined the overall concentration of DLL4 levels which defines phenotypes. Throughout our simulations, the cell having a higher concentration of μ relative to its neighbors was selected as having a tip cell phenotype. Similarly, we observed that oscillating calcium levels lead to a higher DLL4 concentration and hence, classification as a tip cell. As shown in other studies [141, 142], all cells receiving VEGF signaling altered calcium levels. Cells oscillate initially, but their oscillations cease if a tip cell phenotype is not selected.

In Figure 4.8, we observed a directed wave in low μ for the initial oscillation. In contrast to Figure 4.8, for high IP3 levels, the initial wave structure is somewhat directionless, though, in later times, oscillations gained directional proceeding wave dynamics. Since Ca2+ is shown to gauge directional features on cell migration, such as filopodia or cytoskeletal remodeling [64], this observation might be related to complicated vascular configurations in tumor angiogenesis, where ECs are known to have higher levels of VEGF intake relative to healthy angiogenesis. Endothelial cells are known to expand their branches rather than elongating and branching [26] under high VEGF concentrations.

The relation between changing spatial calcium dynamics and obstruction in EC migration might be investigated as a future work. Here we developed a model where Notch, DLL4 and Notch-DLL4 complex is all treated as being cytosolic variables. This is only a modest approach on mechanistic quantitative modelling, such models are widely being used, and gives reasonable answers. However, for observing the spatial concentration change in Ca2+ during the resurrecting oscillation phase requires an upgraded version of the model, where Notch, DLL4 and Notch-DLL4 complex are placed on their real operation position: boundaries of the cells. On the other hand our main ambition in this project is depicting the decision process for the faith of the endothelial cells, and the model is confirmed to do so.

To our surprise, FEniCS platform simulated results slower than the Mathematica platform for this reason for future spatial simulations we preferred to proceed with the latter.

In Figure 4.11, it is observed that under a VEGF gradient, cells containing the highest levels of IP3 due to VEGF intake remain as a tip cell. However, other cells having relatively high IP3 levels fail to gain the phenotype. Another observation is the difference between the influence of neighboring and intrinsic μ levels.

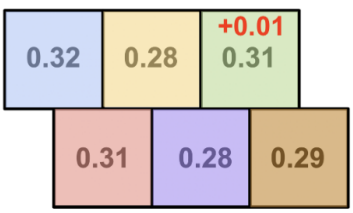

Figure 4.14. Illustrated applied stimulant configuration for the profiles in Figures 4.15, 4.16 and 4.17. Cells with assigned IP3 concentrations are given inside. Cells are labeled in color such that calcium and DLL4 profiles will be demonstrated in matching colors.

For the configuration illustrated in the above Figure 4.14, we first run the model with the assigned IP3 concentrations depicted in gray numbers. The DLL4 profiles in Figure 4.12 B displayed that cells labeled in blue and green colors are selected as

tip cells. Later, we increased the green cell's IP3 level as it can be seen in red font in Figure 4.14 and the model gave the DLL4 profile that can be seen in Figure 4.12 D. As expected, the green cell's tip features are strengthened due to increased DLL4 levels (Figure 4.15). Here, the direction of the arrows shows the resulting effect of the increment. Surprisingly, the increase at the IP3 concentrations of the green cell caused a decrease on the DLL4 levels of the blue cell as depicted in Figure 4.16. This effect is originated from the cell-to-cell communication through the pink cell. Such that its DLL4 profile in Figure 4.17 shows significant resemblance to the blue cell's temporal profile. Again here, arrow direction shows the resulting effect of the increment.

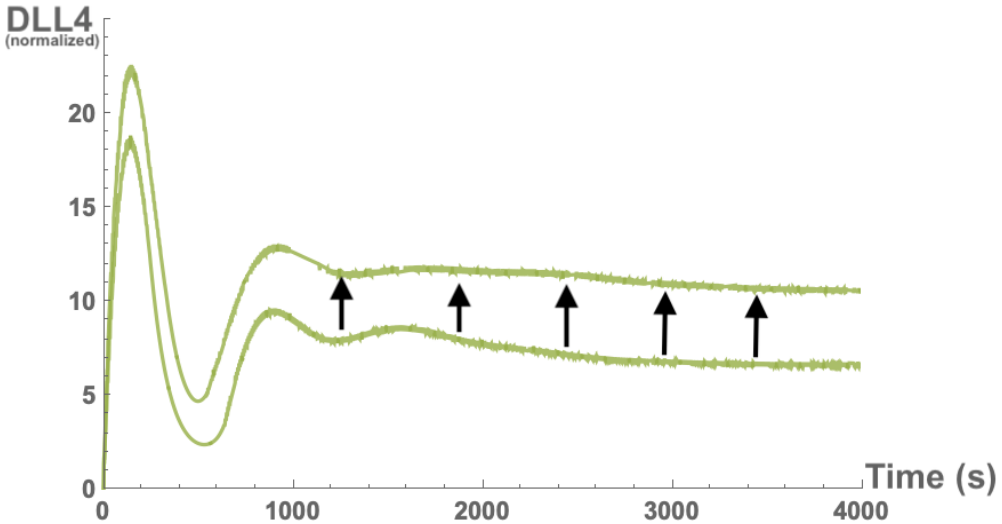

Figure 4.15. When the green tip cell's IP3 concentration is increased for the assigned IP3 concentrations illustrated in Figure 4.14 it's DLL4 level shows a significant increase. Due to DLL4's deterministic role in tip fate, this increment indicates stronger tip cell features.

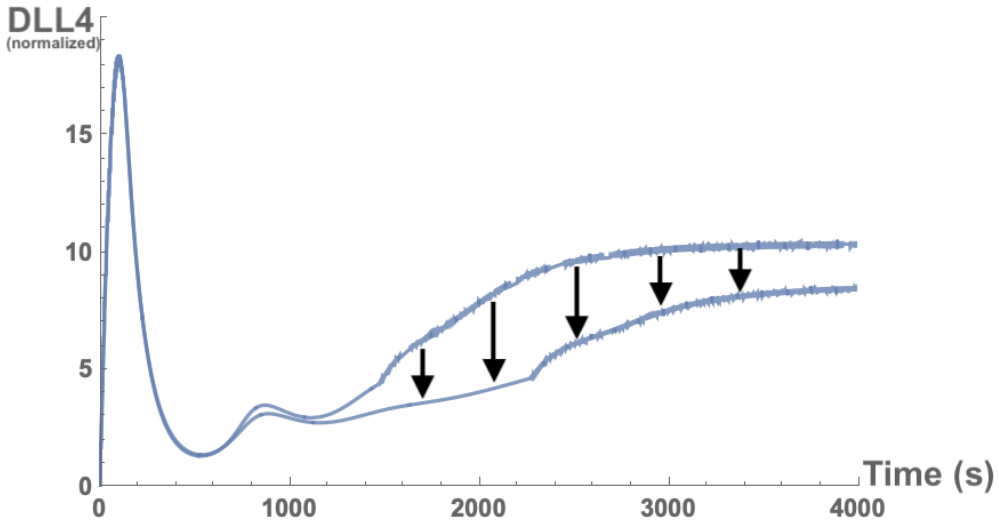

Figure 4.16. Resulting effect in the blue cell when the IP3 concentration for the green tip cells is increased for the assigned IP3 concentrations illustrated in Figure 4.14. Surprisingly DLL4 concentration for the blur labeled cell is decreased. This is due to cell-to cell communication observed through the pink labeled cell.

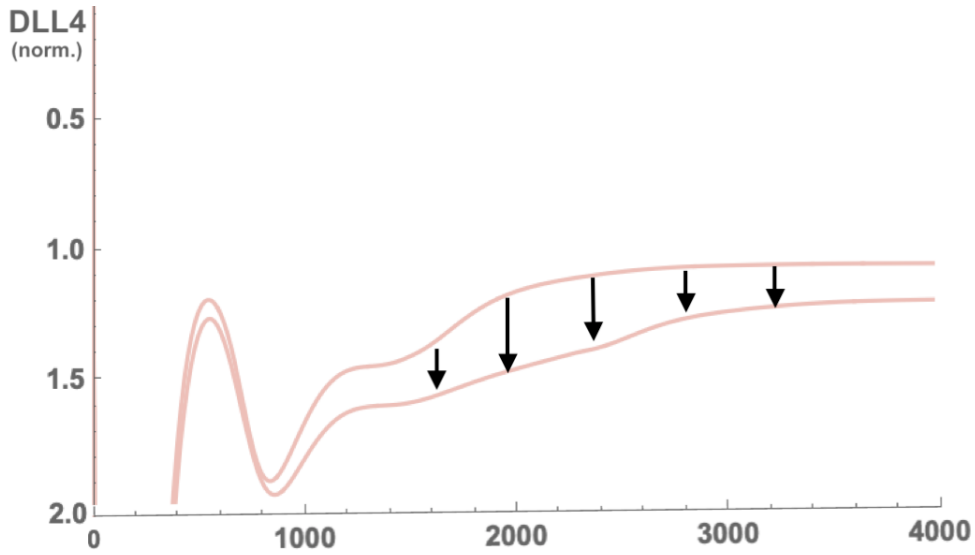

Figure 4.17. The pink cell's reaction when the IP3 concentration for the green tip cells is increased. The resemblance between the DLL4 profiles of the blue cell, Figure 4.16, and the pink cell shows that these two effect is related.

In Figure 4.12 B and D, it can be observed that tip selection is determined by cellular μ level. However, as observed from the 4th (pink) cell, high levels do not always guarantee that the tip character and neighboring cell IP3 levels become

decisive. Another observation is that in the calcium oscillations depicted in Figure 4.12 A and C , the first cell (blue), is shown to gain its oscillatory behavior in a later time than the third cell (green). This indicates that when resurrecting the oscillations, μ concentrations of the neighbors have higher importance than the cell's own μ level.

Figure 4.18. Illustrated applied stimulant configuration for the profiles in Figure 4.19. Cells with assigned IP3 concentrations are given inside. Cells are labeled in color such that calcium and DLL4 profiles will be demonstrated in matching colors.

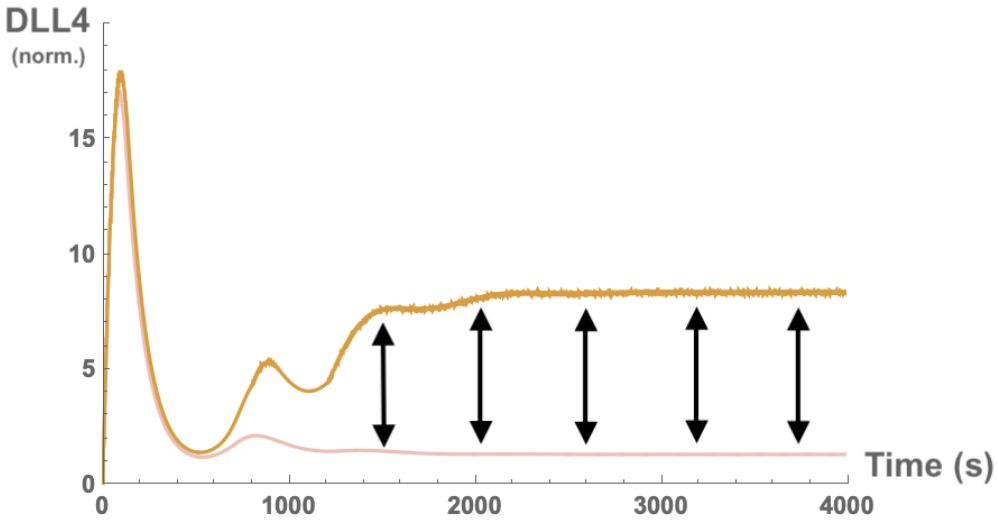

Figure 4.19. Pink and yellow cell's DLL4 levels are illustrated in matching colors. The pink cell is inhibited by lateral inhibition by the yellow cell. The self evidence difference between the DLL4 levels of highest-in-concentration cells for the configuration in Figure 4.18.

Finally, in Figure 4.13, we compare oscillations when the two cells having the same concentration for the assigned IP3 concentrations illustrated in 4.18 are adjacent to each other. Together with cell-to-cell interaction, lateral inhibition enabled only one of the cells to become a stalk cell. In Figure 4.19. DLL4 level of the yellow cell has increased substantially in comparison to the pink cell.

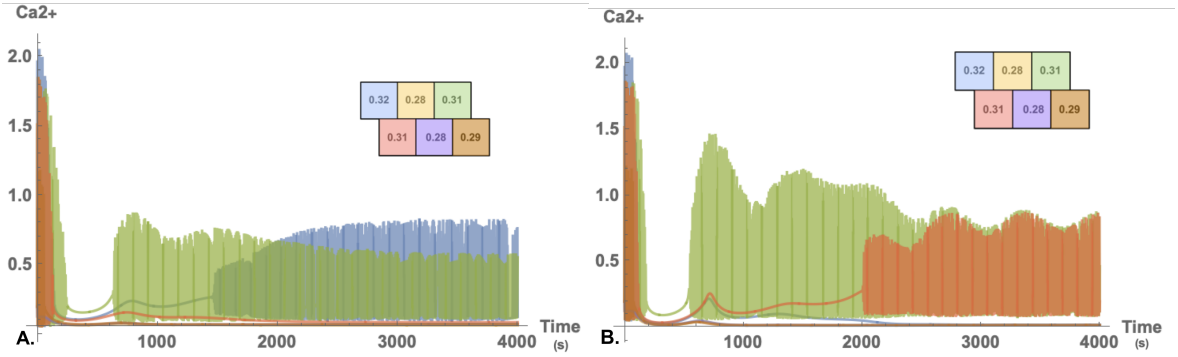

Figure 4.20. Comparison of linear vs nonlinear negative feedback for the IP3 (and relatively VEGF) distribution in Figure 4.12. In **A.**, the linear negative feedback scenario the cell with the highest level of IP3 (blue), become tip cell. On the other hand, the cell with the weakest neighbours and second highest concentration (green) selected as the tip phenotype. Around $t = 250s$ the calcium concentration amplitudes for the both cells remain the same with high IP3 high amplitude correlation. In **B.**, in the nonlinear scenario however, the blue cell is not selected despite having the highest concentration in IP3. On the other hand the cell with a high IP3 neighbor and low IP3 level (brown) becomes the tip cell. This situation is not compatible with the predictions of the model. Another key observation is the synchronized oscillation in calcium levels and the following matching in calcium levels.

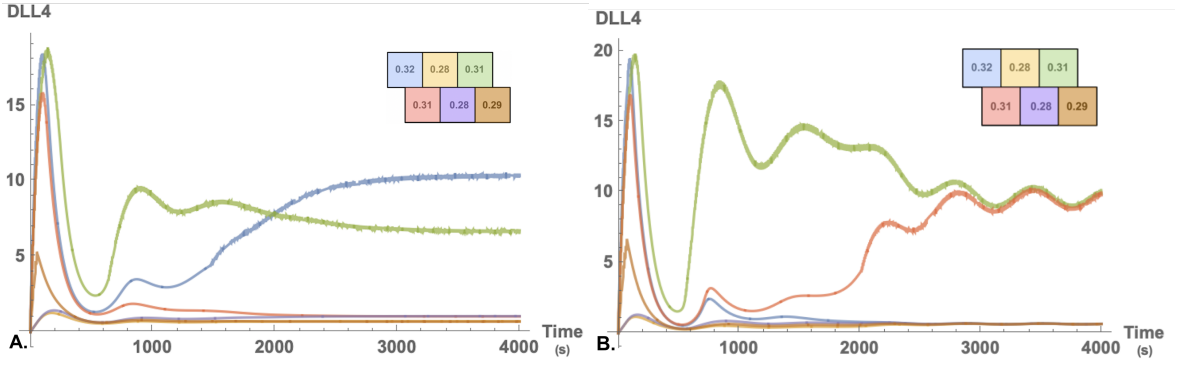

Figure 4.21. Comparison of linear vs nonlinear negative feedback for the IP3 (and relatively VEGF) distribution in Figure 4.12. In **A.**, the linear negative feedback scenario the cell with the highest level of IP3 (blue), along with a cell with high DLL4 but weak neighbor (green) become tip cell. It can be seen that there is a clear distinction between the cells' DLL4 levels. This scenario has been foreseen by the model. In **B.**, the nonlinear scenario however, the blue cell is not selected despite having the highest concentration in IP3. An the brown cell stand out from all the cells and become a tip cell. It can be seen that around $t = 2000s$ DLL4 levels of the brown cell increases by oscillating and around $t = 3200s$ reaches to the same DLL4 levels as the green cell.

In Section 3.2 we discuss the nonlinearity of the negative feedback of the original angiogenesis model. Here in Figure 4.20 and 4.21, we observe detailed comparison between linear (Figure 4.20 A and 4.21 A) and nonlinear (Figure 4.20 B and 4.21 B) negative feedback mechanisms. The main consequence of the choice in a linear mechanism comes from the consistence between high VEGF (hence IP3) $\rightarrow$ high DLL4 (tip phenotype). A nonlinear term induces results outside of this analogy, and contradicts with biological findings of Yokota et al. [42] indicating a correspondence between longer Ca2+ oscillation and high DLL4 concentrations. Another unwanted result of nonlinearity is overlapping/synchronized Ca2+ and DLL4 dynamics. The original model was designed for a two cell set-up, where both cells in physical contact. Synchronized oscillations in contacting cells are experimentally observed in the work of Ubezio et al. [26]. Our model also set to be used in multi-cell set ups, where synchronization

between neighbouring cells haven't been observed [42]. This type of overlapped values for the cells in contact induces incorrect predictions. For these reasons we proceeded with linear feedback mechanism.

Our model results show how calcium dynamics are a crucial part of phenotype selection. Significantly, calcium is involved in multiple ways in the process of cell migration. From gauging focal adhesion sites with local flickers to retracting the cell with cell-wide transients [64, 143, 151], understanding the action of calcium presents opportunities for therapeutic manipulation. Recently, a promising novel cancer therapy called calcium electroporation has been developed which aims to kill cancer cells by increasing cytosolic calcium levels [60]. In addition to eradicating tumor cells, it interferes with the migrational abilities of nearby endothelial cells, which results in anti-vascularization [61]. Models investigating the effects of Ca2+ in cell motility in angiogenesis can be built upon this model.

The widespread usage of the Ca2+ signalling allows it to be used in different areas of the fight against cancer. Although this study doesn't take into account the role of calcium in cell movement and focuses only on its interaction with DLL4, the fact that calcium signalling plays a role in almost every aspect of cell movement [64,152] is an element that should be carefully considered. In addition to angiogenesis, cell movement plays a very important role in another cancer related process, metastasis [24,153]. It allows cancer cells to spread to secondary sites after an Epithelial-to-Mesenchymal transition (EMT). The role of Ca2+ signalling in this transformation has been revealed in different types of cancer [154–156]. In addition, studies investigating the relation between DLL's and metastasis have revealed a possible link [157–159]. Furthermore, Mendonça et al. [160] showed that inhibition of endothelial specific DLL4/Notch interaction negatively regulates EMT and reduces the number of circulating metastatic cells. Considering these facts, the results in this work might be found interesting in terms of seeking potential therapeutic strategies on EMT prevention.

Nitric oxide (NO), a regulator of micro-vascular permeability [161] and apoptosis [162], is secreted by VEGF–mediated pathways triggered by DLL4 in ECs [163]. For monitoring different mediators of Ca2+, equations representing their kinetics could be added into the model. Along with investigating the permeability of the vessel, such a model would also be useful in commenting on the relation between vessel pruning and EC apoptosis by nitric oxide dependent factors [164, 165]. An intriguing extension of this model might also be adding another regulator of calcium homeostasis [53], mitochondria. It is also known to regulate apoptosis with certain proteins influencing Ca2+ homeostasis [166] and NO-related factors [167]. These interwoven relationships can be investigated with an additional feedback describing mitochondrial Ca2+ dynamics.

As no mathematical model perfectly represents the entirety of the complex biological interactions at play, our model has a few limitations worth noting. First, the model does not distinguish between the trans-membrane and cytosolic proteins; it treats all proteins the same. This enables us to focus only on temporal dynamics between variables. Another limitation is the nature of calcium oscillations: our oscillations have a strong periodic behavior; however, these oscillations have stochastic behaviors in reality. The last limitation is that external influences are implicitly included, such as VEGF concentration and membrane stretching. Since tip cells contain active protrusions, their stretched membranes trigger stretch-activated calcium channels. For that reason, we extend our model in the upcoming chapter.

The growth of a new vessel begins with phenotype selection at VEGF-activated dormant cells. VEGF activation leads to cell differentiation and concomitant competition between the cells. We focused on the calcium transients observed during these initial processes. By implementing different VEGF intake between the cells as different IP3 concentrations, we showed how VEGF explicitly influences DLL4 levels in cells. With the key elements of the calcium toolbox and cell-to-cell angiogenesis interactions, we made similar observations to experiments. By simulating the model, we showed that calcium oscillations maintained in the cells, which will be determined as tip phenotype, and cell-to-cell interaction between the neighbors influenced calcium levels and

phenotype destiny. However, the initial selection triggers migratory changes in the cell. In the future, the role of Ca2+ can be explored more by focusing on the effects of cytoskeletal remodeling during angiogenesis. These new features likely will bring about new feedbacks and pave the way for a more intriguing interplay between phenotype selection and calcium levels.

In this work we have seen that travelling waves plays a role only in the spatiotemporal domain in the dispersion of the concentration, however, for the phenotype definition they are irrelevant. There are two reasons for that, first, DLL4 itself is a trans-membrane ligand and this model completely ignores this fact. According to the logic at play, the ligand resides inside the cytosol along with the other transmembrane protein Notch and their complexes Dll4-Notch. In such case transmembrane proteins existing in the model only relevant in temporal assumptions. Making a spatiotemporal assumption by using proteins that should not exist in the cytosol would be unreasonable. Second, a tip cell phenotype is defined by a significant increase in temporal concentration of DLL4 in comparison to neighbor cells. Rather than the moving concentration wave the overall DLL4 concentration (by integrating on the spatial domain and normalizing to the area) come into prominence.

For these reasons we followed temporal solutions and made our remarks on temporal schemes, on the other hand, travelling waves will be definitely important in biological phenomenons including spatial orientation. For that we wanted to extend our model with cell elasticity such that we can see and compare the role of travelling waves in a phenomenon naturally occurring during angiogenesis.

5. THE EFFECT OF CALCIUM IN GELATED CELLS DURING PHENOTYPE SELECTION

In this chapter, we will combine the angiogenesis-calcium model of the prior chapter with the before-mentioned gelation-solation model. We will then run the model on the spatial domain for the two-cell model, and later, we will discuss our results.

5.1. Biological Motivation

Many cell types move to survive or response. According to the type of the cell various kinds of eukaryotic cell movement can be observed: some cells move by maintaining their orientation and their cellular shape [67]. This is especially advantageous for conditions where the cell avoid toxic material or other cells [168]. On the other hand, cells can also move with by involving podial parts (temporary cellular extensions occurring due to cytoskeletal reshaping) constantly extending retracting resulting an unoriented movement [169]. These various types of cellular movement occurs due to cytoskeletal organization. Cytoskeleton is a cellular structure composed of constantly production and degradation of actin filament proteins [170]. These structures are polarized and known to organize in ways to cause cellular protrusions extending out which cells rely on for motility, or to cause cytoskeleton-cytosol mixture to be squeezed [171].

Although, there is a tremendous effort to understand the aforementioned mechanisms both by theoretical and experimental studies [79, 172–176], the specific mechanism underlying cell-scale movement due to contraction of actin polymerization is still unknown.

Angiogenesis inheritedly includes cell mobilization. Especially, tip cells need to move away from the vessel axis and migrate to hypoxic sites. Tip cells should be able to orient it self and its follower stalk cells towards the hypoxic area for creating a supply to the area in need. However, due to the multifaceted nature of cell migration, this

process is usually disregarded in models. Here, we aim to combine our model with a simple element of cell mobility in relation to calcium machinery.

5.2. Introduction

According to the experiments of Yokota et al. [42], Ca2+ oscillation and DLL4 is connected and the cells maintaining oscillation dynamics contain higher levels of DLL4 and become tip cell. It is already known that tip cells have filopodia stretched out for reaching to extracellular medium normal to the mother vessel creating an information exchange between the extracellular medium and the cell [25, 177]. However, calcium is also known to be altered by stretching which results cytosolic contraction in cardiac cells [178] and epithelial cells [4]. Here, we want to combine these two ideas that might be seemed to be contradicting. If cells contracted by calcium how can they be elongated with their filopodias which is a result of maintaining the tip phenotype? To answer this question, one should point out at this moment the complex steps of cell mobility in relation to calcium. If a cell is moving in a direction, than the cell needs to elongate its filopodias, glue its cell membrane by adhesion points and, pull back its opposite end after releasing the adhesion points at the back of the cell [177]. Although mobility plays a role in angiogenesis the effect of cytosolic stretching/compressing the cell, it is usually disregarded by the models including sprout elongation [26]. Since we have a strong coupling with the calcium machinery in our model, disregarding a mechanism that occur naturally in our set up would mean losing information. Since, it would alter the Ca2+ signal causing different results and would even create an inherited cutoff to the tip cell selection.

Calcium has a multi-functional role in cell migration, and in this study, we will aim to trigger a global calcium transient with local calcium flickers from stretch sensitive calcium channels [179] and inspect the resulting influence on cytoskeletal remodeling. For this, we aimed to add a single equation for a humble integration of the mechanochemical effect of the cell. Our first aim to observe the stretching/compressing for that we might need to change coupling variable in the calcium model (ζ), and ex-

pect to observe regular waves and LI related loss of directionality at the later times. In this model we do not aim to kill the calcium signal with the mechanochemical coupling, but to observe the relation between the initial perturbation and the direction of the contraction wave. This feature is especially important since along with the direction of the stretched filopodias, cell contraction also has an effect on the cell's orientation.

This study aims to investigate the influence of calcium on cytoskeletal changes in a cell model in which dynamic actin polymerization in the calcium concentration controls the viscoelastic modeled cytosol-cytoskeleton mix [21]. In this model, the interwoven complexity of cell migration and phenotypic roles of calcium is combined in a computational model. We hope, it might pave the way for creation of more complex models that would question our understanding of biological events and may suggest new protocols or ideas for treatment.

5.3. Calcium Related Actin Polymerization for Angiogenic Phenotype Model

Investigating calcium in cell migration is important both for understanding the delicate balance and also for learning how to break it. Given the above considerations, we aimed to investigate cell contraction in relation to calcium. Cell contractions are demonstrated with a well-accepted gelation-solation mechanism [4, 21, 67]. In this mechanism actin and myosin factors generating traction influence the connectivity of the cytogel-cytoskeleton mixture. Changing features of connectivity control viscosity and elasticity [21]. The concept used in [4] is for a continuous model. In the work, the calcium model used is based on a model [3] which depicts CICR dynamics involving cytoplasmic calcium levels with the open ratio of IP3R that has not been inactivated by calcium. Traveling wave solutions of this model can be generated with initial conditions exceeding the required threshold in a spatially constricted region which is usually expressed as a Gaussian spike. This spatial construction shows similarities with the confined nature of microdomains which are small areas with high calcium concentrations [180]. Since filopodial extensions create Ca2+ flickers occurred

in microdomains [64], we will express these flickers as spatially distributed Gaussian. These flickers are spatially restricted, and will be our perturbations.

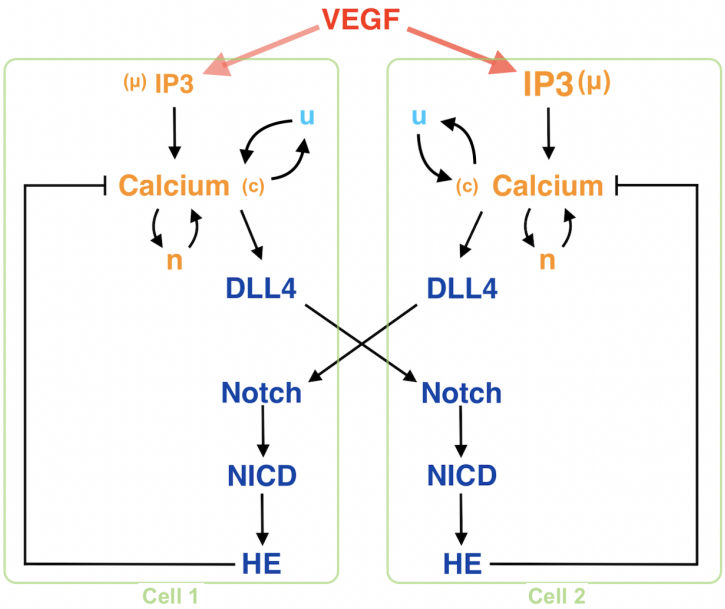

Figure 5.1. Schematic representation of the two cell model explaining the relevant factors and the interactions between them. Here we depicted the role of the dilation/contraction term in light blue along with angiogenic, and calcium models illustrated in navy and yellow font respectively.

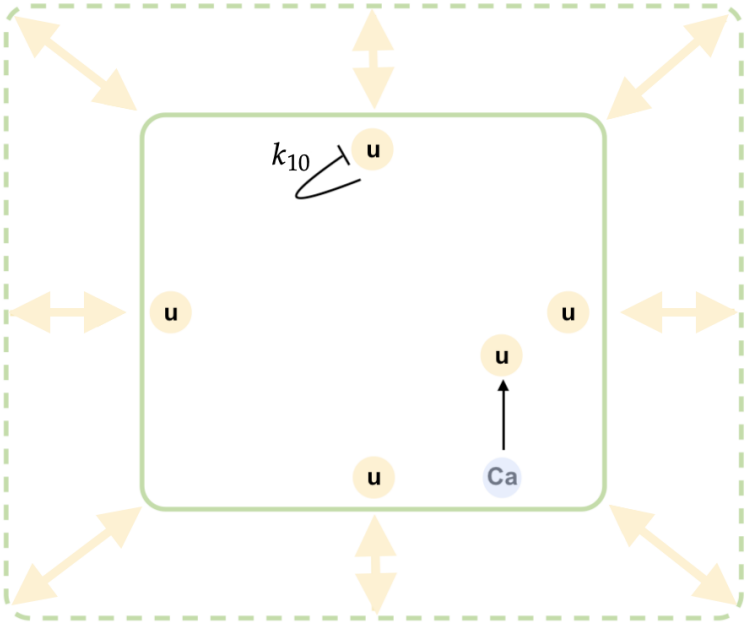

Figure 5.2. Dilatation/contraction related events in cellular domain. Calcium has a positive and u has a autonegative impact. It should be reminded that when we changed our notation to keep the integrity in notation with the calcium-angiogenesis model as previously explained.

As before, we use already existed models for building a detailed depiction of the desired effect. Below you can see the recent extension of the model with dilation/contraction variable u_i,

$$\frac{\partial c_i}{\partial t} = D_0\ \nabla^2 c_i + k_1\ \mu_i\ n_i \left(\frac{b + c_i}{1 + c_i}\right) - k_2\ \frac{c_i}{k_3 + c_i} - \zeta\ z_i\ c_i + \lambda u_i \tag{5.1}$$

$$\frac{dn_i}{dt} = 1 - \frac{c_i^2}{1 + c_i^2} - n_i \tag{5.2}$$

$$\frac{du_i}{dt} = -k_{10} u_i + \frac{k_{11} c_i}{1 + k_{11} c_i} \tag{5.3}$$

$$\frac{dv_i}{dt} = \beta + \Theta\ \frac{c_i^2}{{k_4}^2 + c_i^2} - k_5\ v_i\ w_j + k_6\ x_j - k_7\ v_i \tag{5.4}$$

$$\frac{dw_i}{dt} = -k_5\ v_j\ w_i + k_6\ x_i - k_7\ w_i \tag{5.5}$$

$$\frac{dx_i}{dt} = k_5\ v_j\ w_i - k_6\ x_i - k_7\ x_i \tag{5.6}$$

$$\frac{dy_i}{dt} = k_8\ x_i - k_7\ y_i \tag{5.7}$$

$$\frac{dz_i}{dt} = \beta + \theta \frac{y_i^2}{y_i^2 + {k_9}^2} - k_7 z_i. \tag{5.8}$$

The model has become slightly more complex with an additional player, u_i, which uses the same compartment. Stretching and shrinking of the cell cytosol is added and this model now relates gelation and solation mechanism in the cell cytosol with angiogenesis. Here we picked the traction term in Equation 5.3 as a linear Hill term. As it has been preferred in prior models [21]. But the principles are still the same, by only one variable, ζ, has been reparametrized. In the below table, you can see the changed and newly introduced or changed parameters.

Table 5.1. Altered or novel parameters used in the model were taken from [4] or estimated. As preferred in the previous model again we use Arbitrary Units (A.U.) for the qualitative, rather than quantitative portrayal of relative concentrations.

Parameter	Value	Explanation	Reference
μ	0.30 - 0.38	Bifurcation constant	Est.
λ	0.5	Mechanochemical contribution to calcium	[4]
ζ	0.8	Coupling term between calcium and angiogenesis	Est.
k_{10}	1.	Mechanochemical autofeedback	Est.
k_{11}	10.0	Strength of calcium contribution	Est.

Table 5.2. Initial conditions used in the model were taken from [3, 5]. The initial values of c, and n variables provides the special conditions for the spatially observed wave dynamics in calcium transients. In addition, v value indicates DLL4 concentration preexist any external trigger of the DLL4 - Notch pathway.

Parameter	c_0	n_0	u_0	v_0	w_0	x_0	y_0	z_0
Initial Condition (A.U.)	0.98602	0.50704	0.9079	0.1	0	0	0	0

5.4. Solution Method in Two-cell Spatiotemporal Coupling

For the spatiotemporal model in two-cell setup, the diffusion term in Equation 5.1 is included, such that the equation governing the Ca2+ dynamics becomes an PDE. This two-cell setup clearly shows the effect of dilatation/contraction. The model simulations are again performed by Method of Lines with a built-in adaptive solver NDSolve, in Mathematica 12. MOL is a scheme combining both analytical and numerical methods. The domain is set as $(-30, 30) \times (-30, 30)$ for $t = 4000\ s$. [150].

5.5. Results

To elucidate how the orientation of cell mobility effected by our calcium anagiogenesis model, we simulated a simple cytosolic gelation/solation model of Kaouri et al. [4] integrated to our previous calcium-angiogenesis model. We preferred to investigate this situation in a two-cell model where the coupling is only in between only two cells. In this study, we aim to create a basic model on which we can add more features in the future.

Usually models inspect cell elasticity merely in relation to angiogenic features [5, 34, 36, 44]. On the other hand, we aim here to add only one of the outstanding effects of calcium, cytosolic gelation, so that cell's orientation is also connected with in-cell directionality instead of focusing only filopodial orientation. Filopodias and other sources of microdomains for calcium will bring about spatially restricted calcium increments in the domain. These will reflect as perturbations in the initial conditions and initiate a travelling wave moving inside the cell.

For the following simulations we preferred to use the same domain parameters as in the Section 4.6. On the other hand, unlike Section 4.6, here we use Mathematica platform, since it completes simulations faster with its built-in numerical solver NDSolve. Here we focus on two cells which are side-by-side in theory, having rigid boundaries with no flux boundary conditions, and an initial condition with the follow-

ing perturbation on the calcium variable of both cells,

$$c_i(0, x, y) = 4 \exp\left(-50\left(x^2 + y^2\right)\right) + c_0 \tag{5.9}$$

In this extension, we are focused on the fate of in-cell orientation. For that, we proceed with parameters already used by other works in the literature by setting μ i.e., the stimulant intake, the only different variable between the cells. Before, we inspected the oscillating regime for the pure calcium model. Since couplings to the model will only perturb the calcium value, we expect the resulting behaviour to be the same. We selected our μ parameters within the oscillating range, and we will do the same in this model as well.

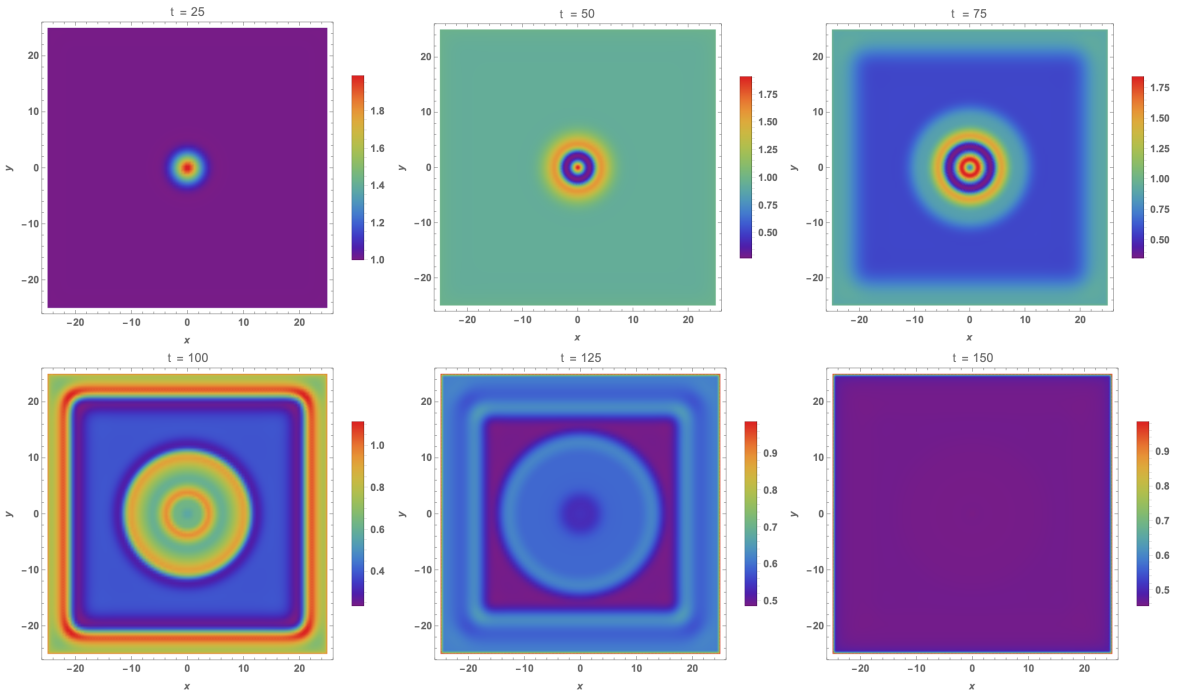

Figure 5.3. Cell1 cytosolic calcium for a single compartmental model. Here we observe the oriented initial wave dynamics at $\mu = 0.35$ the following instants time 25, 50, 75, 100, 125, and 150. Due to the gaussian perturbation we observe here that the concentration wave propagates in accordance to the initial trigger. This orientation turns into a gradual increase after the oscillation is killed.

In Figure 5.3, we observe spatial configuration cytosolic calcium for $\mu = 0.35$ at $t = 25,\ 50,\ 75,\ 100,\ 125,\ \text{and},\ 150s$ the perturbation given in Equation 5.9 initiates

a spherical wave from inside-out. The result of perturbation can be observed to occur at the center of the domain. By the diffusive impact of the calcium, the concentration wave proceed to move towards to the boundaries with time. On the other hand, the reaction terms surpasses diffusion and we can observe that at $t = 50s$ the overall domain concentration is increased. Since the concentration is oscillating at $t = 75 - 100s$, we see that decrease in the overall concentration initiate linear travelling waves due to the concentration difference around boundaries. At $t = 125s$, just before the collision both waves are nearly homogenized. The oriented wave structure decays when the concentration is homogenized after collapse.

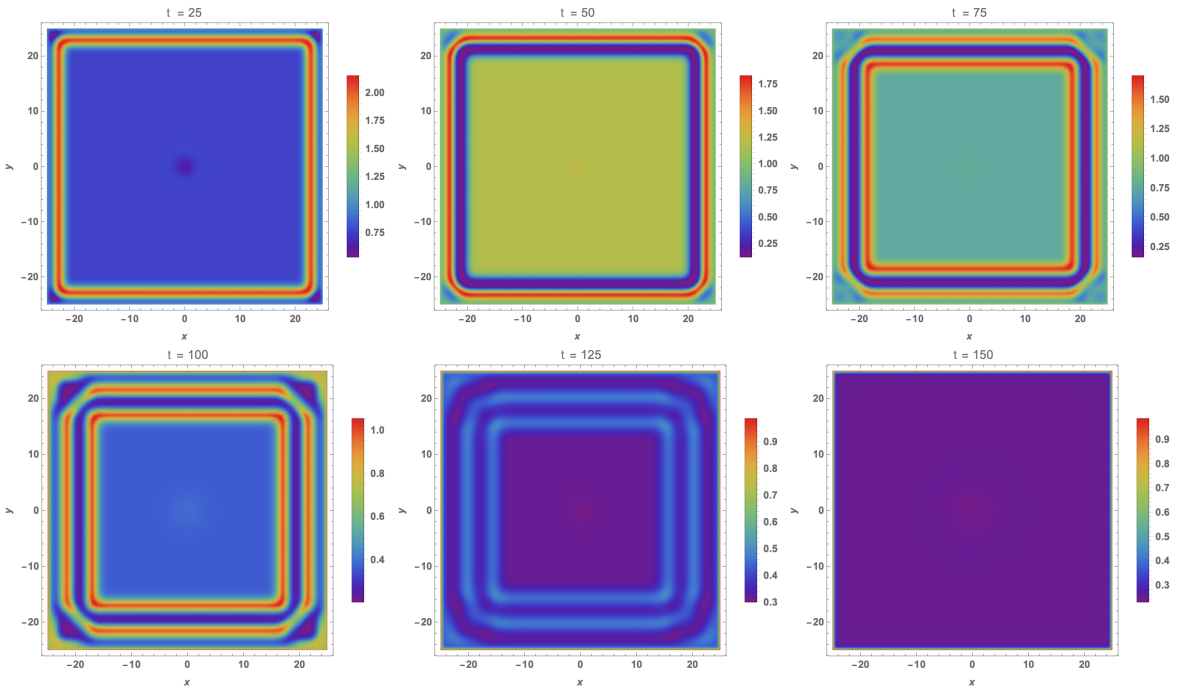

Figure 5.4. Cell2 cytosolic calcium for a single compartmental model. Here we observe the oriented initial wave dynamics at $\mu = 0.32$ the following instants time 25, 50, 75, 100, 125, and 150. We can observe here that due to the value difference between the boundary and the inner region of the cell wave propagates with the shape of boundaries. Here, we ignore the rounding effect on the corners. Also, the orientation turns into a gradual increase after the oscillation is killed which can be observed at $t = 150\ s$.

In Figure 5.4, we observe spatial configuration cytosolic calcium for $\mu = 0.32$ at $t = 25,\ 50,\ 75,\ 100,\ 125,\ \text{and},\ 150s$ the perturbation given in Equation 5.9 this time

doesn't initiate any spherical wave but we observe the wave starting from boundary towards the center of the domain. Here, we observe that at $t = 25s$ the initial perturbation suppressed by the overall increase of the domain. We see the effects of the perturbation at $t = 100s$ as well, however it is not enough to trigger a travelling wave. Again, we observe that the concentration difference diminishing with time, and the solution loses directionality around $t = 150s$

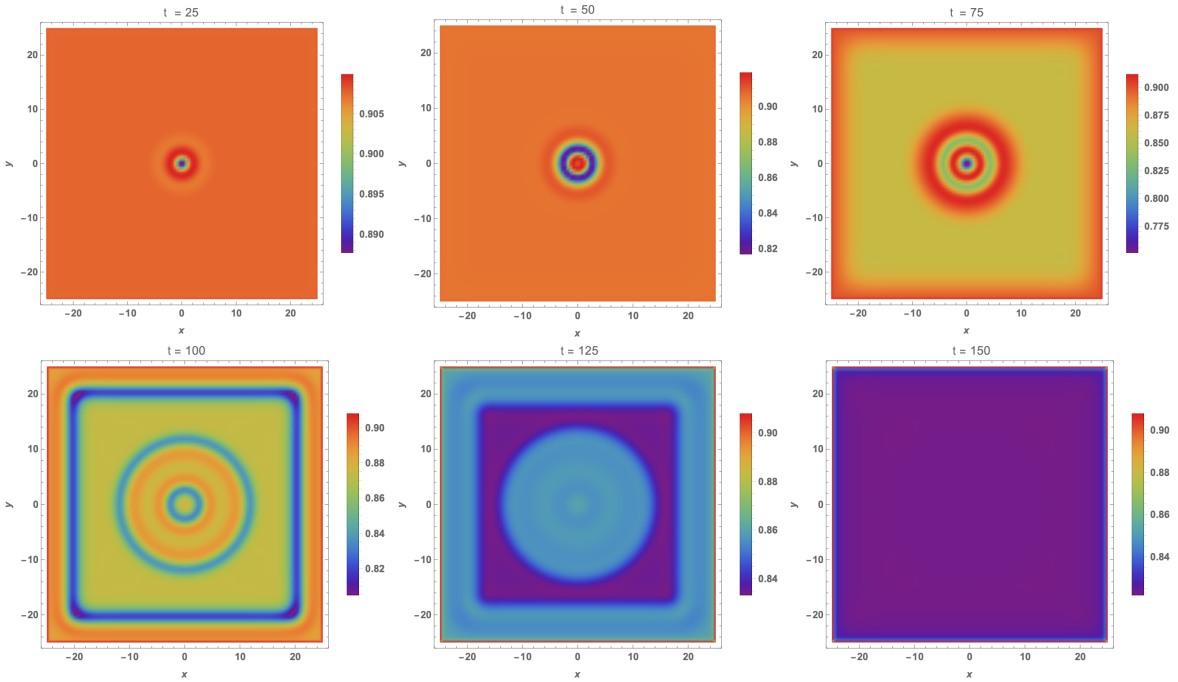

Figure 5.5. Cell1 cytosolic contraction/dilation wave for a single compartmental model. Here we observe the oriented initial wave dynamics at the following instants time 25, 50, 75, 100, 125, and 150. Due to the gaussian perturbation we observe here that the concentration wave propagates in accordance to the initial trigger. This orientation turns into a gradual increase after the oscillation is killed which can be observed at $t = 150\ s$.

In Figure 5.5 we observe u dynamics on the spatial domain for $\mu = 0.35$ at $t = 25,\ 50,\ 75,\ 100,\ 125,\ \text{and},\ 150s$. Similar to the calcium dynamics we observe both the spherical and the linear wave moving opposing directions and finally collapsing.

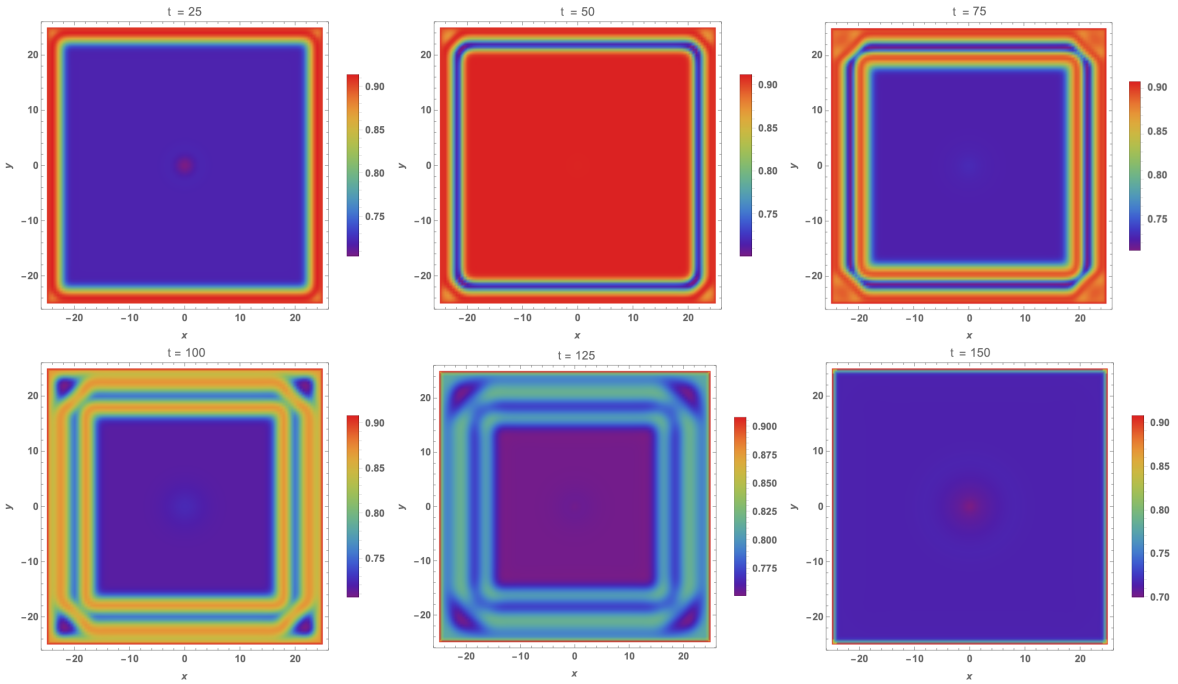

Figure 5.6. Cell2 cytosolic contraction/dilation wave for a single compartmental model. Here we observe the oriented initial wave dynamics at the following instants time 25, 50, 75, 100, 125, and 150. We can observe here that due to the value difference between the boundary and the inner region of the cell wave propagates with the shape of boundaries. Here, we ignore the rounding effect on the corners. Also, the orientation turns into a gradual increase after the oscillation is killed which can be observed at $t = 150\ s$.

In Figure 5.6 again we observe u dynamics on the spatial domain for this time $\mu = 0.32$ at $t = 25,\ 50,\ 75,\ 100,\ 125,$ and, $150s$. Similar to the calcium dynamics we observe don't observe the spherical waves but only the linear wave. Around $t = 125s$ again the difference between the wave and the rest of the domain become less apparent due to diffusive effects.

5.6. Discussion

Angiogenesis is a process where cells change their phenotypes and move towards the area of tissue or tumor growth orderly. In the prior study, we presented an ODE model for relating angiogenic cell alteration to calcium concentration. Since mobility

and phenotype alteration are two pillars of angiogenesis initialization, the next logical step seemed to explore whether we could apply the principles of the model to mobility or not. Very luckily, calcium is also an essential player in cell migration. Modeling a relationship between cell migration with Ca2+ requires being careful due to its multi-functional role in this multi-step process. Since modeling the total morphological effect of calcium is a very ambitious goal, we aim to start with the cytoskeleton's reaction with a relatively simple model. After solving this problem, in the future, we aim to develop new models by building further adjustments on this model, since modeling biological questions always aims through therapeutic applications.

In this model, the cell dilation is not coupled with any other variable. This is an assumption for simplifying the model. All variables, except n and u, are given in concentrations usually given or measured in molar units, which is an amount of substance in volume. However, it should be kept in mind that dilation exists due to changes in the size of the cell, which automatically should reflect its effect on the concentration levels of the factors included in the model. Besides, as one will remember, in this work, we treat all factors as cytosolic factors, and transmembrane variables would affect in different orders when compared with cytosolic factors. To avoid such complications, we accept this effect to be small.

On the other hand, assuming a small contraction resulted to a limited effect of dilatation to calcium concentration. On the contrary as it can be seen from the correlation between the spatial configuration of c (in Figure 5.3, Figure 5.4) and u (in Figure 5.5, Figure 5.6) calcium has an immense effect on the u configuration. However, experiments show that activity increases shear stress, like massage therapy, increased cytosolic calcium, and up-regulated other factors causing increased micro-circulation [127].

Directional waves cease to exist after $t = 150s$ because our initial perturbation sets the orientation for the following waveform. When the oriented wave train is stopped, the trigger setting, the form vanishes. Apparently, this situation is not

biologically correct since, during early angiogenesis, cells contain multiple filopodia continually triggering stretch-activated channels [177] and therefore create a continually existing external perturbation. At first glance, this would seem like this effect can be created with a simple addition to the existed model. However, one should take into account that there are usually multiple filopodia for one cell and their feedback with calcium depends on time. Time dependence between filopodia and calcium concentration is as the following up to threshold calcium makes positive feedback for filopodias and strengthens them, after the temporal threshold calcium creates an opposite effect and weaken the filopodias hence weaken the stretch-mediated calcium perturbation [181].

In this extended model, we aimed to inspect the orientation of the contraction/dilation wave due to its relation with the direction of the movement. In our scenario, all endothelial cells are objected to extracellular VEGF concentrations, and therefore all the cells should move towards to the VEGF source, the tumor. For that reason, cells must maintain their directional cytoplasmic contraction waves.

After $t = 150s$, the orientation of the waves does not resurrect even though the calcium oscillation re-surges. The absence of spatial perturbation creates only a gradual increase. In this scenario, a perturbation should arise by stretching sensitive receptors to keep the direction of the gelation-solation of the cell.

Novel treatments are trying to benefit from intricately balanced Ca2+. One of the recent cancer therapy options is calcium electroporation, where short electrical pulses accumulate cytosolic calcium levels by increasing the cell permeability. It is observed to kill malignant cells via toxic calcium levels while leaving healthy cells unharmed [13]. Calcium is very ubiquitously used by malignant and benign cells; therefore, fixing some "problems" during treatment may cause others. For example, calcium electroporation interferes with the migrational abilities of tissue nearby the tumor [182] and inhibits angiogenesis in healthy tissue [61]. The role of calcium in cell migration should be understood to avoid such secondary consequences. By simulating different scenarios, computational calcium models might help to understand how these problems should

be approached. However, calcium signaling should be chosen with utmost care to have a minimalist model creating the desired biological functions in the beginning. So that future models can be carefully built upon these base models for making more intricate models with increased predicted ability.

This model and other possible extensions to the calcium angiogenesis model rendered possible due to multi-functioning nature of the calcium. If we preferred to build the primary model with some other material with a few known/verified functions, we would not inspect features such as cell movement.

6. CONCLUSION

We began this thesis by introducing the biological and mathematical background. After a brief illustration of cancer, we focused on angiogenesis and elaborated on initial stages where the phenotype selection process called lateral inhibition was explained. Calcium signaling and its ubiquitous nature are explained in the next section. We especially emphasized its role as a second messenger. Moreover, cell movement has also been explained with actin-myosin polymerization. In this chapter, we also introduced how coordinated wave dynamics is being used by organisms. A brief biological summary of the problem studied on the thesis is also introduced where we tried to give an overview of how the work in the thesis might be relevant to these issues.

In following chapter, the mathematical background for the models and dynamics that has been used for building our model are given. We inspect the defining features of traveling waves and the underlying nonlinearity. Also, a famous nerve signaling model has been explained. Then, we delved in an angiogenesis model for cell phenotype selection via lateral inhibition initiated by an external stimulant, VEGF. We continued to our discussion through cytosolic calcium ion. Calcium oscillation and mechano-chemical reactions have been introduced and explained thoroughly. We closely examined receptor dynamics and a phenomenological model emerging from it. Also, we discussed cell motility mostly in relation to calcium. Mobility is a vast area for that reason, we limit our problem to a step of the cell migration: calcium-regulated cytogel solation and focus the model using the same calcium model we used throughout the thesis.

Later, we combined the models mentioned above and ran them on different setups. The two-cell model is solved both in spatiotemporal and temporal models. For the temporal model, we used Mathematica and the spatiotemporal model is being solved by a finite element model. Then, we used a six-cell model for mimicking the neighborly interactions between several cells. This model is solved by Mathematica as well. We

shared our results and discussed the consequences of the model.

Finally, we extend our calcium-angiogenesis model for cytosol gelation, where we observe biologically relevant traveling waves and discuss the extension's effects on the original model by commenting on the abilities and limitations of the model.

The most abundant metal in the human body, calcium, is ubiquitously used as a signaling molecule and a second messenger in the cell. Second, messengers initiate intracellular cascades to change cell physiology. Various processes, including gene expression, signal transmission, stimulus-secretion coupling, etc., requires calcium signaling [57], and many cellular features like organelles, receptors, transporters, etc. use calcium. The ubiquitous usage of calcium makes it a potent candidate for the treatment of many diseases like hypertension, atrial fibrillation, or diabetes [57]. In contrast to its wide usage and ubiquity, calcium is toxic for cells. Therefore it needed to be finely regulated. There are many components of calcium regulations, several pumps, exchangers, or receptors reside mostly on the endoplasmic reticulum (ER), mitochondria, and plasma membrane [53]. Calcium-induced calcium release (CICR) is based on Inositol trisphosphate receptor (IP3R) activation via cytosolic calcium-binding. It can also lead to a sequential increase in the cytosol, causing interesting wave dynamics. CICR can be evoked by local calcium intake due to membrane tension via transient receptor potential cation channels (TRPC) [58]. This autocatalytic process is balanced quickly by sarcoplasmic/endoplasmic reticulum calcium ATPase, (SERCA), which pumps excessive cytosolic calcium back to ER [53]. In this project, we were interested in calcium concentrations on cytosol and ER, with calcium perturbation in the intracellular domain, and inspected how calcium drives phenotype selection during vessel formation in angiogenesis and orient cell contraction at the same time.

The first model aims to simulate the relationship between tip cell selection and overall calcium transients in the cell. Although Ca2+ has a complex function in cell migration, our model meets the fundamental features of phenotype differentiation with a humble reference to calcium in cell migration. To our knowledge, this is the first

analytical model for investigating the role of calcium in phenotype characterization for angiogenesis. Here, we initiated a calcium-related lateral inhibition process in an unpatterned set of ECs.

The versatility of angiogenesis is built upon a delicate balance, usually depicted via the DLL/Notch pathway. We considered implicit VEGF intake by cells dictated by IP3 concentrations and explored the relationship between VEGF-related calcium oscillations and DLL4 levels. Our model results agree with experimental findings exploring a correlation between phenotype identity and calcium oscillations since cells containing high levels of VEGF sustained Ca2+ oscillations are categorized as having the tip phenotype. We further explored this idea in multiple-cell scenarios to compare how ECs are patterned by analyzing how cell-to-cell interaction between the neighbors influenced the calcium levels and phenotype selection outcome.

However, absent from the first model is the notion of migrating cells moving along the gradient of external signals. To incorporate more substantial migratory effects into the model, one must consider the multi-faceted roles of calcium in relation to the extracellular medium, which we preferred to abstain from all but the cytosolic gelation/ solation mechanism. We extended the calcium model with an accepted model equation depicting this mechanism. Eventually, we observed that a continual perturbation is necessary for sustaining the cell orientation.

Quantitative models in biology cannot explore every possible combination. By their nature, equations should guide the model to the essential parameters, and variables should respond as requested. One should keep in mind that no model is perfect and has limits. Selection of activated pathways, picking the important downstream agents, and holding them responsible for only some biological reactions requires excluding many features. For that reason, without creating new in silico replicas of the biological models, we carefully selected already proven models in the literature and built our computational setup by handpicking the essential variables and parametrizing for observing in our results what has been already observed by biology.

In this work, we wished to create a model that can be applied to many biological events with ease for inspecting possible scenarios. For example, VEGF therapy is a standard cancer treatment procedure. However, resistance to anti-vascular therapeutics or activation of compensatory pathways is common, creating a need for anti-angiogenic therapies which rely on novel substances [183, 184]. For example, calcium-regulating treatments have recently been explored as potential anti-angiogenic therapies [183]. We believe further inspections on calcium-angiogenesis relations will be held in the future.

REFERENCES

1. Hanahan, D. and R. A. Weinberg, "The Hallmarks of Cancer", *Cell*, Vol. 100, No. 1, pp. 57–70, 2000.

2. Hanahan, D. and R. A. Weinberg, "Hallmarks of Cancer: The Next Generation", *Cell*, Vol. 144, No. 5, pp. 646–674, 2011.

3. Atri, A., J. Amundson, D. Clapham and J. Sneyd, "A Single-Pool Model for Intracellular Calcium Oscillations and Waves in The Xenopus Laevis Oocyte", *Biophysical Journal*, Vol. 65, No. 4, pp. 1727–1739, 1993.

4. Kaouri, K., P. K. Maini, P. A. Skourides, N. Christodoulou and S. J. Chapman, "A Simple Mechanochemical Model for Calcium Signalling in Embryonic Epithelial Cells", *Journal of Mathematical Biology*, Vol. 78, No. 7, pp. 2059–2092, 2019.

5. Venkatraman, L., E. R. Regan and K. Bentley, "Time to Decide? Dynamical Analysis Predicts Partial Tip/Stalk Patterning States Arise During Angiogenesis", *PLoS One*, Vol. 11, No. 11, p. e0166489, 2016.

6. Medicine, Y., *Tumour*, 2021, `https://www.yalemedicine.org/conditions`, accessed in September 2021.

7. Organization, W. H., *Cancer*, 2021, `https://www.who.int/en/news-room`, accessed in September 2021.

8. Sung, H., J. Ferlay, R. L. Siegel, M. Laversanne, I. Soerjomataram, A. Jemal and F. Bray, "Global Cancer Statistics 2020: GLOBOCAN Estimates of Incidence and Mortality Worldwide for 36 Cancers in 185 Countries", *CA: A Cancer Journal for Clinicians*, Vol. 71, No. 3, pp. 209–249, 2021.

9. Institute, N. C., *Cancer Statistics*, 2021, `https://www.cancer.gov/about-cancer`,

accessed in September 2021.

10. Padmanabhan, R., N. Meskin and A.-E. Al Moustafa, *Mathematical Models of Cancer and Different Therapies: Unified Framework*, Springer Nature, 2021.

11. Fouad, Y. A. and C. Aanei, "Revisiting The Hallmarks of Cancer", *American Journal of Cancer Research*, Vol. 7, No. 5, p. 1016, 2017.

12. Schirrmacher, V., "From Chemotherapy to Biological Therapy: A Review of Novel Concepts to Reduce The Side Effects of Systemic Cancer Treatment", *International Journal of Oncology*, Vol. 54, No. 2, pp. 407–419, 2019.

13. Frandsen, S. K., M. Vissing and J. Gehl, "A Comprehensive Review of Calcium Electroporation—A Novel Cancer Treatment Modality", *Cancers*, Vol. 12, No. 2, p. 290, 2020.

14. Gatenby, R. A., K. Smallbone, P. K. Maini, F. Rose, J. Averill, R. B. Nagle, L. Worrall and R. J. Gillies, "Cellular Adaptations to Hypoxia and Acidosis During Somatic Evolution of Breast Cancer", *British Journal of Cancer*, Vol. 97, No. 5, pp. 646–653, 2007.

15. Parks, S. K., J. Chiche and J. Pouysségur, "Disrupting Proton Dynamics and Energy Metabolism for Cancer Therapy", *Nature Reviews Cancer*, Vol. 13, No. 9, pp. 611–623, 2013.

16. Lam, S. F., K. W. Bishop, R. Mintz, L. Fang and S. Achilefu, "Calcium Carbonate Nanoparticles Stimulate Cancer Cell Reprogramming to Suppress Tumor Growth and Invasion in An organ-on-a-chip System", *Scientific Reports*, Vol. 11, No. 1, pp. 1–12, 2021.

17. Adair, T. H. and J.-P. Montani, "Angiogenesis", *Colloquium Series on Integrated Systems Physiology: from Molecule to Function*, Vol. 2, pp. 1–84, Morgan & Claypool Life Sciences, 2010.

18. Ng, E. W. and A. P. Adamis, "Targeting Angiogenesis, The Underlying Disorder in Neovascular Age-related Macular Degeneration", *Canadian Journal of Ophthalmology*, Vol. 40, No. 3, pp. 352–368, 2005.

19. Heck, T., M.-M. Vaeyens and H. Van Oosterwyck, "Computational Models of Sprouting Angiogenesis and Cell Migration: Towards Multiscale Mechanochemical Models of Angiogenesis", *Mathematical Modelling of Natural Phenomena*, Vol. 10, No. 1, pp. 108–141, 2015.

20. Goel, S., D. G. Duda, L. Xu, L. L. Munn, Y. Boucher, D. Fukumura and R. K. Jain, "Normalization of The Vasculature for Treatment of Cancer and Other Diseases", *Physiological Reviews*, Vol. 91, No. 3, pp. 1071–1121, 2011.

21. Murray, J., *Mathematical Biology II: Spatial Models and Biomedical Applications*, Vol. 3, Springer-Verlag, 2001.

22. Folkman, J., "Angiogenesis", *Annual Review Medicine*, Vol. 57, pp. 1–18, 2006.

23. Mongiat, M., E. andreuzzi, G. Tarticchio and A. Paulitti, "Extracellular Matrix, A Hard Player in Angiogenesis", *International Journal of Molecular Sciences*, Vol. 17, No. 11, p. 1822, 2016.

24. Welch, D. R. and D. R. Hurst, "Defining The Hallmarks of Metastasis", *Cancer Research*, Vol. 79, No. 12, pp. 3011–3027, 2019.

25. Gerhardt, H., M. Golding, M. Fruttiger, C. Ruhrberg, a. Lundkvist, A. Abramsson, M. Jeltsch, C. Mitchell, K. Alitalo, D. Shima *et al.*, "VEGF Guides Angiogenic Sprouting Utilizing Endothelial Tip Cell Filopodia", *The Journal of Cell Biology*, Vol. 161, No. 6, pp. 1163–1177, 2003.

26. Ubezio, B., R. A. Blanco, I. Geudens, F. Stanchi, T. Mathivet, M. L. Jones, A. Ragab, K. Bentley and H. Gerhardt, "Synchronization of Endothelial Dll4-Notch Dynamics Switch Blood Vessels from Branching to Expansion", *Elife*,

Vol. 5, p. e12167, 2016.

27. Rao, N., Y. F. Lee and R. Ge, "Novel Endogenous Angiogenesis Inhibitors and Their Therapeutic Potential", *Acta Pharmacologica Sinica*, Vol. 36, No. 10, pp. 1177–1190, 2015.

28. Vasudev, N. S. and a. R. Reynolds, "Anti-Angiogenic Therapy for Cancer: Current Progress, Unresolved Questions and Future Directions", *Angiogenesis*, Vol. 17, No. 3, pp. 471–494, 2014.

29. Abdalla, A. M., L. Xiao, M. W. Ullah, M. Yu, C. Ouyang and G. Yang, "Current Challenges of Cancer Anti-Angiogenic Therapy and The Promise of Nanotherapeutics", *Theranostics*, Vol. 8, No. 2, p. 533, 2018.

30. Sosa, M. S., P. Bragado and J. A. Aguirre-Ghiso, "Mechanisms of Disseminated Cancer Cell Dormancy: An Awakening Field", *Nature Reviews Cancer*, Vol. 14, No. 9, pp. 611–622, 2014.

31. Bakri, S. J., M. R. Snyder, J. M. Reid, J. S. Pulido and R. J. Singh, "Pharmacokinetics of Intravitreal Bevacizumab (Avastin)", *Ophthalmology*, Vol. 114, No. 5, pp. 855–859, 2007.

32. Hussein, Z., H. Mizuo, S. Hayato, M. Namiki and R. Shumaker, "Clinical Pharmacokinetic and Pharmacodynamic Profile of Lenvatinib, An Orally Active, Small-Molecule, Multitargeted Tyrosine Kinase Inhibitor", *European Journal of Drug Metabolism and Pharmacokinetics*, Vol. 42, No. 6, pp. 903–914, 2017.

33. Eilken, H. M. and R. H. Adams, "Dynamics of Endothelial Cell Behavior in Sprouting Angiogenesis", *Current Opinion in Cell Biology*, Vol. 22, No. 5, pp. 617–625, 2010.

34. Carlier, A., L. Geris, K. Bentley, G. Carmeliet, P. Carmeliet and H. Van Oosterwyck, "MOSAIC: A Multiscale Model of Osteogenesis and Sprouting Angiogen-

esis with Lateral Inhibition of Endothelial Cells", *PLoS Computational Biology*, Vol. 8, No. 10, p. 1002724, 2012.

35. Laughlin, M. H., S. C. Newcomer and S. B. Bender, "Importance of Hemodynamic Forces as Signals for Exercise-Induced Changes in Endothelial Cell Phenotype", *Journal of Applied Physiology*, Vol. 104, No. 3, pp. 588–600, 2008.

36. Bentley, K. and S. Chakravartula, "The Temporal Basis of Angiogenesis", *Philosophical Transactions of The Royal Society B: Biological Sciences*, Vol. 372, No. 1720, p. 20150522, 2017.

37. Ferrara, N., H.-P. Gerber and J. LeCouter, "The Biology of VEGF and Its Receptors", *Nature Medicine*, Vol. 9, No. 6, pp. 669–676, 2003.

38. Neufeld, G., T. Cohen, S. Gengrinovitch and Z. Poltorak, "Vascular Endothelial Growth Factor (VEGF) and Its Receptors", *The FASEB Journal*, Vol. 13, No. 1, pp. 9–22, 1999.

39. Collier, J. R., N. A. Monk, P. K. Maini and J. H. Lewis, "Pattern Formation by Lateral Inhibition with Feedback: A Mathematical Model of Delta-Notch Intercellular Signalling", *Journal of Theoretical Biology*, Vol. 183, No. 4, pp. 429–446, 1996.

40. Zakirov, B., G. Charalambous, R. Thuret, I. M. Aspalter, K. Van-Vuuren, T. Mead, K. Harrington, E. R. Regan, S. P. Herbert and K. Bentley, "Active Perception During Angiogenesis: Filopodia Speed Up Notch Selection of Tip Cells in Silico and in Vivo", *Philosophical Transactions of The Royal Society B*, Vol. 376, No. 1821, p. 20190753, 2021.

41. McLaughlin, A. and G. de Vries, "Role of PLCγ and Ca2+ in VEGF-and FGF-Induced Choroidal Endothelial Cell Proliferation", *American Journal of Physiology-Cell Physiology*, Vol. 281, No. 5, pp. C1448–C1456, 2001.

42. Yokota, Y., H. Nakajima, Y. Wakayama, A. Muto, K. Kawakami, S. Fukuhara and N. Mochizuki, "Endothelial Ca2+ Oscillations Reflect VEGFR Signaling-Regulated Angiogenic Capacity in Vivo", *eLife*, Vol. 4, p. e08817, 2015.

43. Lobov, I., R. Renard, N. Papadopoulos, N. Gale, G. Thurston, G. Yancopoulos and S. Wiegand, "Delta-Like Ligand 4 (Dll4) Is Induced by VEGF as A Negative Regulator of Angiogenic Sprouting", *Proceedings of The National Academy of Sciences*, Vol. 104, No. 9, pp. 3219–3224, 2007.

44. Page, D. J., R. Thuret, L. Venkatraman, T. Takahashi, K. Bentley and S. P. Herbert, "Positive Feedback Defines The Timing, Magnitude, and Robustness of Angiogenesis", *Cell Reports*, Vol. 27, No. 11, pp. 3139–3151, 2019.

45. Margadant, C., "Positive and Negative Feedback Mechanisms Controlling Tip/Stalk Cell Identity During Sprouting Angiogenesis", *Angiogenesis*, Vol. 23, No. 2, pp. 75–77, 2020.

46. Pontes-Quero, S., M. Fernández-Chacón, W. Luo, F. F. Lunella, V. Casquero-Garcia, I. Garcia-Gonzalez, A. Hermoso, S. F. Rocha, M. Bansal and R. Benedito, "High Mitogenic Stimulation Arrests Angiogenesis", *Nature Communications*, Vol. 10, No. 1, pp. 1–16, 2019.

47. Fischer, A. and M. Gessler, "Delta–Notch—and Then? Protein Interactions and Proposed Modes of Repression by Hes and Hey BHLH Factors", *Nucleic Acids Research*, Vol. 35, No. 14, pp. 4583–4596, 2007.

48. Hellström, M., L.-K. Phng, J. J. Hofmann, E. Wallgard, L. Coultas, P. Lindblom, J. Alva, A.-K. Nilsson, L. Karlsson, N. Gaiano *et al.*, "Dll4 Signalling Through Notch1 Regulates Formation of Tip Cells During Angiogenesis", *Nature*, Vol. 445, No. 7129, pp. 776–780, 2007.

49. Suchting, S., C. Freitas, F. Le Noble, R. Benedito, C. Bréant, A. Duarte and

A. Eichmann, "The Notch Ligand Delta-Like 4 Negatively Regulates Endothelial Tip Cell Formation and Vessel Branching", *Proceedings of The National Academy of Sciences*, Vol. 104, No. 9, pp. 3225–3230, 2007.

50. Liu, Z.-J., T. Shirakawa, Y. Li, A. Soma, M. Oka, G. P. Dotto, R. M. Fairman, O. C. Velazquez and M. Herlyn, "Regulation of Notch1 and Dll4 by Vascular Endothelial Growth Factor in Arterial Endothelial Cells: Implications for Modulating Arteriogenesis and Angiogenesis", *Molecular and Cellular Biology*, Vol. 23, No. 1, pp. 14–25, 2003.

51. Kuhnert, F., J. R. Kirshner and G. Thurston, "Dll4-Notch Signaling as A Therapeutic Target in Tumor Angiogenesis", *Vascular Cell*, Vol. 3, No. 1, pp. 1–8, 2011.

52. Ridgway, J., G. Zhang, Y. Wu, S. Stawicki, W.-C. Liang, Y. Chanthery, J. Kowalski, R. J. Watts, C. Callahan, I. Kasman *et al.*, "Inhibition of Dll4 Signalling Inhibits Tumour Growth by Deregulating Angiogenesis", *Nature*, Vol. 444, No. 7122, pp. 1083–1087, 2006.

53. Dupont, G., M. Falcke, V. Kirk and J. Sneyd, *Models of Calcium Signalling*, Vol. 43, Springer, 2016.

54. Gil, D., A. H. Guse and G. Dupont, "Three-Dimensional Model of Subplasmalemmal Ca2+ Microdomains Evoked by The Interplay Between ORAI1 and InsP3 Receptors", *Frontiers in Immunology*, Vol. 12, p. 659790, 2021.

55. Olson, M. F. and E. Sahai, "The Actin Cytoskeleton in Cancer Cell Motility", *Clinical & Experimental Metastasis*, Vol. 26, No. 4, p. 273, 2009.

56. Carafoli, E., "Calcium Signaling: A Tale for All Seasons", *Proceedings of The National Academy of Sciences*, Vol. 99, No. 3, pp. 1115–1122, 2002.

57. Islam, M. S., "Calcium Signaling: from Basic to Bedside", *Calcium Signaling*,

pp. 1–6, 2020.

58. Chen, J.-P., Y. Luan, C.-X. You, X.-H. Chen, R.-C. Luo and R. Li, "TRPM7 Regulates The Migration of Human Nasopharyngeal Carcinoma Cell by Mediating Ca2+ Influx", *Cell Calcium*, Vol. 47, No. 5, pp. 425–432, 2010.

59. Efremov, A. K., M. Yao, M. P. Sheetz, A. D. Bershadsky, B. Martinac and J. Yan, "Mechanosensitive Calcium Signaling in Filopodia", *bioRxiv*, 2020.

60. Frandsen, S. K., H. Gissel, P. Hojman, T. Tramm, J. Eriksen and J. Gehl, "Direct Therapeutic Applications of Calcium Electroporation to Effectively Induce Tumor Necrosis", *Cancer Research*, Vol. 72, No. 6, pp. 1336–1341, 2012.

61. Staresinic, B., T. Jesenko, U. Kamensek, S. K. Frandsen, G. Sersa, J. Gehl and M. Cemazar, "Effect of Calcium Electroporation on Tumour Vasculature", *Scientific Reports*, Vol. 8, No. 1, pp. 1–14, 2018.

62. de Menorval, M.-A., F. M. andre, A. Silve, C. Dalmay, O. Français, B. Le Pioufle and L. M. Mir, "Electric Pulses: A Flexible Tool to Manipulate Cytosolic Calcium Concentrations and Generate Spontaneous-Like Calcium Oscillations in Mesenchymal Stem Cells", *Scientific Reports*, Vol. 6, No. 1, pp. 1–9, 2016.

63. Pauly, R. R., C. Bilato, S. J. Sollott, R. Monticone, P. T. Kelly, E. G. Lakatta and M. T. Crow, "Role of Calcium/Calmodulin-Dependent Protein Kinase II in The Regulation of Vascular Smooth Muscle Cell Migration", *Circulation*, Vol. 91, No. 4, pp. 1107–1115, 1995.

64. Wei, C., X. Wang, M. Chen, K. Ouyang, L.-S. Song and H. Cheng, "Calcium Flickers Steer Cell Migration", *Nature*, Vol. 457, No. 7231, pp. 901–905, 2009.

65. Wei, C., X. Wang, M. Zheng and H. Cheng, "Calcium Gradients Underlying Cell Migration", *Current Opinion in Cell Biology*, Vol. 24, No. 2, pp. 254–261, 2012.

66. Huttenlocher, A., S. P. Palecek, Q. Lu, W. Zhang, R. L. Mellgren, D. A. Lauffenburger, M. H. Ginsberg and A. F. Horwitz, "Regulation of Cell Migration by The Calcium-Dependent Protease Calpain", *Journal of Biological Chemistry*, Vol. 272, No. 52, pp. 32719–32722, 1997.

67. Bray, D., *Cell Movements: from Molecules to Motility*, Garland Science, 2000.

68. Fletcher, D. A. and R. D. Mullins, "Cell Mechanics and The Cytoskeleton", *Nature*, Vol. 463, No. 7280, pp. 485–492, 2010.

69. Janmey, P. A., "The Cytoskeleton and Cell Signaling: Component Localization and Mechanical Coupling", *Physiological Reviews*, Vol. 78, No. 3, pp. 763–781, 1998.

70. Mitchison, T. and L. Cramer, "Actin-based Cell Motility and Cell Locomotion", *Cell*, Vol. 84, No. 3, pp. 371–379, 1996.

71. Rayment, I., H. M. Holden, M. Whittaker, C. B. Yohn, M. Lorenz, K. C. Holmes and R. A. Milligan, "Structure of The Actin-Myosin Complex and Its Implications for Muscle Contraction", *Science*, Vol. 261, No. 5117, pp. 58–65, 1993.

72. Mitra, S. K., D. A. Hanson and D. D. Schlaepfer, "Focal Adhesion Kinase: in Command and Control of Cell Motility", *Nature Reviews Molecular Cell Biology*, Vol. 6, No. 1, pp. 56–68, 2005.

73. Mogilner, A., "Mathematics of Cell Motility: Have We Got Its Number?", *Journal of Mathematical Biology*, Vol. 58, No. 1, pp. 105–134, 2009.

74. Ridley, A. J., M. A. Schwartz, K. Burridge, R. A. Firtel, M. H. Ginsberg, G. Borisy, J. T. Parsons and A. R. Horwitz, "Cell Migration: Integrating Signals from Front to Back", *Science*, Vol. 302, No. 5651, pp. 1704–1709, 2003.

75. Hammad, A. S. and K. Machaca, "Store Operated Calcium Entry in Cell Migra-

tion and Cancer Metastasis", *Cells*, Vol. 10, No. 5, p. 1246, 2021.

76. Loose, M., K. Kruse and P. Schwille, "Protein Self-Organization: Lessons from The Min System", *Annual Review of Biophysics*, Vol. 40, pp. 315–336, 2011.

77. Parker, K. K., A. L. Brock, C. Brangwynne, R. J. Mannix, N. Wang, E. Ostuni, N. A. Geisse, J. C. Adams, G. M. Whitesides and D. E. Ingber, "Directional Control of Lamellipodia Extension by Constraining Cell Shape and Orienting Cell Tractional Forces", *The FASEB Journal*, Vol. 16, No. 10, pp. 1195–1204, 2002.

78. Mallavarapu, A. and T. Mitchison, "Regulated Actin Cytoskeleton Assembly At Filopodium Tips Controls Their Extension and Retraction", *Journal of Cell Biology*, Vol. 146, No. 5, pp. 1097–1106, 1999.

79. Dreher, A., I. S. Aranson and K. Kruse, "Spiral Actin-Polymerization Waves Can Generate Amoeboidal Cell Crawling", *New Journal of Physics*, Vol. 16, No. 5, p. 055007, 2014.

80. Allard, J. and A. Mogilner, "Traveling Waves in Actin Dynamics and Cell Motility", *Current Opinion in Cell Biology*, Vol. 25, No. 1, pp. 107–115, 2013.

81. Taylor, C., "The Contractile Vacuole in Euplotes: An Example of The Sol-gel Reversibility of Cytoplasm", *Journal of Experimental Zoology*, Vol. 37, No. 3, pp. 259–289, 1923.

82. Murray, J. and G. Oster, "Generation of Biological Pattern and Form", *Mathematical Medicine and Biology: A Journal of The IMA*, Vol. 1, No. 1, pp. 51–75, 1984.

83. Oster, G. F. and G. Odell, "Mechanics of Cytogels I: Oscillations in Physarum", *Cell Motility*, Vol. 4, No. 6, pp. 469–503, 1984.

84. Janson, L. W., J. Kolega and D. L. Taylor, "Modulation of Contraction by Gelation/Solation in A Reconstituted Motile Model.", *The Journal of Cell Biology*, Vol. 114, No. 5, pp. 1005–1015, 1991.

85. Bendix, P. M., G. H. Koenderink, D. Cuvelier, Z. Dogic, B. N. Koeleman, W. M. Brieher, C. M. Field, L. Mahadevan and D. A. Weitz, "A Quantitative Analysis of Contractility in Active Cytoskeletal Protein Networks", *Biophysical Journal*, Vol. 94, No. 8, pp. 3126–3136, 2008.

86. Pava, J. A., *Nonlinear Dispersive Equations: Existence and Stability of Solitary and Periodic Travelling Wave Solutions*, 156, American Mathematical Society, 2009.

87. Winfree, A. T., "Spiral Waves of Chemical Activity", *Science*, Vol. 175, No. 4022, pp. 634–636, 1972.

88. Tyson, J. J. and J. P. Keener, "Singular Perturbation Theory of Traveling Waves in Excitable Media (a Review)", *Physica D: Nonlinear Phenomena*, Vol. 32, No. 3, pp. 327–361, 1988.

89. Allbritton, N. L., T. Meyer and L. Stryer, "Range of Messenger Action of Calcium Ion and Inositol 1, 4, 5-trisphosphate", *Science*, Vol. 258, No. 5089, pp. 1812–1815, 1992.

90. Prahlad, V., M. Yoon, R. D. Moir, R. D. Vale and R. D. Goldman, "Rapid Movements of Vimentin on Microtubule Tracks: Kinesin-Dependent Assembly of Intermediate Filament Networks", *The Journal of Cell Biology*, Vol. 143, No. 1, pp. 159–170, 1998.

91. Hall, J. E. and M. E. Hall, *Guyton and Hall Textbook of Medical Physiology E-Book*, Elsevier Health Sciences, 2020.

92. Hursh, J., "Conduction Velocity and Diameter of Nerve Fibers", *American Jour-*

nal of Physiology-Legacy Content, Vol. 127, No. 1, pp. 131–139, 1939.

93. FitzHugh, R., "Impulses and Physiological States in Theoretical Models of Nerve Membrane", *Biophysical Journal*, Vol. 1, No. 6, pp. 445–466, 1961.

94. Chang, J. B. and J. E. Ferrell Jr, "Mitotic Trigger Waves and The Spatial Coordination of The Xenopus Cell Cycle", *Nature*, Vol. 500, No. 7464, pp. 603–607, 2013.

95. Cornell-Bell, A. H., S. M. Finkbeiner, M. S. Cooper and S. J. Smith, "Glutamate Induces Calcium Waves in Cultured Astrocytes: Long-range Glial Signaling", *Science*, Vol. 247, No. 4941, pp. 470–473, 1990.

96. Bauer, A. L., T. L. Jackson and Y. Jiang, "Topography of Extracellular Matrix Mediates Vascular Morphogenesis and Migration Speeds in Angiogenesis", *PLoS Computational Biology*, Vol. 5, No. 7, p. e1000445, 2009.

97. Trepat, X., Z. Chen and K. Jacobson, "Cell Migration", *Comprehensive Physiology*, Vol. 2, No. 4, p. 2369, 2012.

98. Shahi, P. K. and I. F. Pineda, "Tumoral Angiogenesis: Review of The Literature", *Cancer Investigation*, Vol. 26, No. 1, pp. 104–108, 2008.

99. Otrock, Z. K., R. A. Mahfouz, J. A. Makarem and A. I. Shamseddine, "Understanding The Biology of Angiogenesis: Review of The Most Important Molecular Mechanisms", *Blood Cells, Molecules, and Diseases*, Vol. 39, No. 2, pp. 212–220, 2007.

100. Tahergorabi, Z. and M. Khazaei, "A Review on Angiogenesis and Its Assays", *Iranian Journal of Basic Medical Sciences*, Vol. 15, No. 6, p. 1110, 2012.

101. Auerbach, W. and R. Auerbach, "Angiogenesis Inhibition: A Review", *Pharmacology & Therapeutics*, Vol. 63, No. 3, pp. 265–311, 1994.

102. Deneke, V. E. and S. Di Talia, "Chemical Waves in Cell and Developmental Biology", *Journal of Cell Biology*, Vol. 217, No. 4, pp. 1193–1204, 2018.

103. Deneke, V. E., A. Melbinger, M. Vergassola and S. Di Talia, "Waves of Cdk1 Activity in S Phase Synchronize The Cell Cycle in Drosophila Embryos", *Developmental Cell*, Vol. 38, No. 4, pp. 399–412, 2016.

104. Hughes, J. R., "The Phenomenon of Travelling Waves: A Review", *Clinical Electroencephalography*, Vol. 26, No. 1, pp. 1–6, 1995.

105. Muller, L., F. Chavane, J. Reynolds and T. J. Sejnowski, "Cortical Travelling Waves: Mechanisms and Computational Principles", *Nature Reviews Neuroscience*, Vol. 19, No. 5, pp. 255–268, 2018.

106. Turing, A. M., "The Chemical Basis of Morphogenesis", *Bulletin of Mathematical Biology*, Vol. 52, No. 1, pp. 153–197, 1990.

107. Zeeman, E., "Differential Equations for The Heartbeat and Nerve Impulse", *Dynamical Systems*, pp. 683–741, Elsevier, 1973.

108. Otte, S., S. Berg, S. Luther and U. Parlitz, "Bifurcations, Chaos, and Sensitivity to Parameter Variations in The Sato Cardiac Cell Model", *Communications in Nonlinear Science and Numerical Simulation*, Vol. 37, pp. 265–281, 2016.

109. Nagumo, J., S. Arimoto and S. Yoshizawa, "An Active Pulse Transmission Line Simulating Nerve Axon", *Proceedings of The IRE*, Vol. 50, No. 10, pp. 2061–2070, 1962.

110. Hodgkin, A. L. and a. F. Huxley, "A Quantitative Description of Membrane Current and Its Application to Conduction and Excitation in Nerve", *The Journal of Physiology*, Vol. 117, No. 4, pp. 500–544, 1952.

111. Fuchs, A., *Nonlinear Dynamics in Complex Systems*, Springer, 2014.

112. Keener, J. P. and J. Sneyd, *Mathematical Physiology*, Vol. 1, Springer, 1998.

113. Wilkins, M. and J. Sneyd, "Intercellular Spiral Waves of Calcium", *Journal of Theoretical Biology*, Vol. 191, No. 3, pp. 299–308, 1998.

114. Olson, S. D., S. S. Suarez and L. J. Fauci, "A Model of CatSper Channel Mediated Calcium Dynamics in Mammalian Spermatozoa", *Bulletin of Mathematical Biology*, Vol. 72, No. 8, pp. 1925–1946, 2010.

115. Kobayashi, Y., Y. Sanno, A. Sakai, Y. Sawabu, M. Tsutsumi, M. Goto, H. Kitahata, S. Nakata, J. Kumamoto, M. Denda *et al.*, "Mathematical Modeling of Calcium Waves Induced by Mechanical Stimulation in Keratinocytes", *PLoS One*, Vol. 9, No. 3, p. e92650, 2014.

116. Kobayashi, Y., Y. Sawabu, H. Kitahata, M. Denda and M. Nagayama, "Mathematical Model for Calcium-Assisted Epidermal Homeostasis", *Journal of Theoretical Biology*, Vol. 397, pp. 52–60, 2016.

117. Estrada, J., N. andrew, D. Gibson, F. Chang, F. Gnad and J. Gunawardena, "Cellular Interrogation: Exploiting Cell-to-cell Variability to Discriminate Regulatory Mechanisms in Oscillatory Signalling", *PLoS Computational Biology*, Vol. 12, No. 7, p. e1004995, 2016.

118. Pantazaka, E. and C. W. Taylor, "Differential Distribution, Clustering, and Lateral Diffusion of Subtypes of The Inositol 1, 4, 5-trisphosphate Receptor", *Journal of Biological Chemistry*, Vol. 286, No. 26, pp. 23378–23387, 2011.

119. Taufiq-Ur-Rahman, A. S., M. Falcke and C. W. Taylor, "Clustering of IP3 Receptors by IP3 Retunes Their Regulation by IP3 and Ca2+", *Nature*, Vol. 458, No. 7238, p. 655, 2009.

120. Mataragka, S. and C. W. Taylor, "All Three IP3 Receptor Subtypes Generate Ca2+ Puffs, The Universal Building Blocks of IP3-evoked Ca2+ Signals", *Journal*

of Cell Science, Vol. 131, No. 16, p. jcs220848, 2018.

121. Arguin, G., Y. Regimbald-Dumas, M.-O. Fregeau, A. Z. Caron and G. Guillemette, "Protein Kinase C Phosphorylates The Inositol 1, 4, 5-trisphosphate Receptor Type 2 and Decreases The Mobilization of Ca2+ in Pancreatoma AR4-2J Cells", *Journal of Endocrinology*, Vol. 192, No. 3, pp. 659–668, 2007.

122. Saleem, H., S. C. Tovey, T. F. Molinski and C. W. Taylor, "Interactions of Antagonists with Subtypes of Inositol 1, 4, 5-trisphosphate (IP 3) Receptor", *British Journal of Pharmacology*, Vol. 171, No. 13, pp. 3298–3312, 2014.

123. Miyakawa, T., A. Maeda, T. Yamazawa, K. Hirose, T. Kurosaki and M. Iino, "Encoding of Ca2+ Signals by Differential Expression of IP3 Receptor Subtypes", *The EMBO Journal*, Vol. 18, No. 5, pp. 1303–1308, 1999.

124. Stern, M., "Buffering of Calcium in The Vicinity of A Channel Pore", *Cell Calcium*, Vol. 13, No. 3, pp. 183–192, 1992.

125. Mo, P. and S. Yang, "The Store-Operated Calcium Channels in Cancer Metastasis: from Cell Migration, Invasion to Metastatic Colonization", *Frontiers in Bioscience (Landmark Edition)*, Vol. 23, p. 1241, 2018.

126. Brundage, R. A., K. E. Fogarty, R. A. Tuft and F. S. Fay, "Calcium Gradients Underlying Polarization and Chemotaxis of Eosinophils", *Science*, Vol. 254, No. 5032, pp. 703–706, 1991.

127. Yang, W., J.-Y. Chen and L. Zhou, "Effects of Shear Stress on Intracellular Calcium Change and Histamine Release in Rat Basophilic Leukemia (RBL-2H3) Cells", *Journal of Environmental Pathology, Toxicology and Oncology*, Vol. 28, No. 3, 2009.

128. Tsutsumi, M., K. Inoue, S. Denda, K. Ikeyama, M. Goto and M. Denda,

"Mechanical-Stimulation-evoked Calcium Waves in Proliferating and Differentiated Human Keratinocytes", *Cell and Tissue Research*, Vol. 338, No. 1, pp. 99–106, 2009.

129. Bereiter-Hahn, J., "Mechanics of Crawling Cells", *Medical Engineering & Physics*, Vol. 27, No. 9, pp. 743–753, 2005.

130. Narciso, C. E., N. M. Contento, T. J. Storey, D. J. Hoelzle and J. J. Zartman, "Release of Applied Mechanical Loading Stimulates Intercellular Calcium Waves in Drosophila Wing Discs", *Biophysical Journal*, Vol. 113, No. 2, pp. 491–501, 2017.

131. Landau, L. D., E. M. Lifshitz, R. Atkin and N. Fox, "The Theory of Elasticity", *Physics of Continuous Media*, pp. 167–178, CRC Press, 2020.

132. Barbolosi, D., J. Ciccolini, B. Lacarelle, F. Barlési and N. andré, "Computational Oncology—mathematical Modelling of Drug Regimens for Precision Medicine", *Nature Reviews Clinical Oncology*, Vol. 13, No. 4, pp. 242–254, 2016.

133. Powathil, G. G., M. Swat and M. A. Chaplain, "Systems Oncology: Towards Patient-Specific Treatment Regimes Informed by Multiscale Mathematical Modelling", *Seminars in Cancer Biology*, Vol. 30, pp. 13–20, Elsevier, 2015.

134. Chowdhury, S., P. K. Roy and R. J. Smith, "Mathematical Modelling of Enfuvirtide and Protease Inhibitors as Combination Therapy for HIV", *International Journal Nonlinear Scientific Numerical Simulations*, Vol. 17, No. 6, pp. 259–275, 2016.

135. Van Noorden, R., "Software Beats Animal Tests At Predicting Toxicity of Chemicals", *Nature*, Vol. 559, No. 7713, pp. 163–164, 2018.

136. van Leeuwen, C. J. and T. G. Vermeire, *Risk Assessment of Chemicals: An Introduction*, Springer Science & Business Media, 2007.

137. Lamon, L., D. Asturiol, A. Vilchez, J. Cabellos, J. Damásio, G. Janer, A. Richarz and A. Worth, "Physiologically Based Mathematical Models of Nanomaterials for Regulatory Toxicology: A Review", *Computational Toxicology*, Vol. 9, pp. 133–142, 2019.

138. Bullen, C. K., H. T. Hogberg, A. Bahadirli-Talbott, W. R. Bishai, T. Hartung, C. Keuthan, M. M. Looney, a. Pekosz, J. C. Romero, F. C. Sillé *et al.*, "Infectability of Human Brain Sphere Neurons Suggests Neurotropism of SARS-CoV-2", *ALTEX-Alternatives to Animal Experimentation*, Vol. 37, No. 4, pp. 665–671, 2020.

139. Reardon, S., "'Organs-on-chips' Go Mainstream", *Nature News*, Vol. 523, No. 7560, p. 266, 2015.

140. Weiss, J. N., "The Hill Equation Revisited: Uses and Misuses", *The FASEB Journal*, Vol. 11, No. 11, pp. 835–841, 1997.

141. Savage, A. M., S. Kurusamy, Y. Chen, Z. Jiang, K. Chhabria, R. B. MacDonald, H. R. Kim, H. L. Wilson, F. J. Van Eeden, A. L. Armesilla *et al.*, "tmem33 Is Essential for VEGF-Mediated Endothelial Calcium Oscillations and Angiogenesis", *Nature Communications*, Vol. 10, No. 1, pp. 1–15, 2019.

142. Noren, D. P., W. H. Chou, S. H. Lee, A. A. Qutub, A. Warmflash, D. S. Wagner, A. S. Popel and a. Levchenko, "Endothelial Cells Decode VEGF-Mediated Ca2+ Signaling Patterns to Produce Distinct Functional Responses", *Science Signaling*, Vol. 9, No. 416, pp. ra20–ra20, 2016.

143. Monteith, G. R., N. Prevarskaya and S. J. Roberts-Thomson, "The Calcium–Cancer Signalling Nexus", *Nature Reviews Cancer*, Vol. 17, No. 6, p. 367, 2017.

144. Iamshanova, O., A. Fiorio Pla and N. Prevarskaya, "Molecular Mechanisms of Tumour Invasion: Regulation by Calcium Signals", *The Journal of Physiology*,

Vol. 595, No. 10, pp. 3063–3075, 2017.

145. Harvey, E., V. Kirk, M. Wechselberger and J. Sneyd, "Multiple Timescales, Mixed Mode Oscillations and Canards in Models of Intracellular Calcium Dynamics", *Journal of Nonlinear Science*, Vol. 21, No. 5, pp. 639–683, 2011.

146. Shi, X., Y. Zheng, Z. Liu and W. Yang, "A Model of Calcium Signaling and Degranulation Dynamics Induced by Laser Irradiation in Mast Cells", *Chinese Science Bulletin*, Vol. 53, No. 15, pp. 2315–2325, 2008.

147. Stepanova, D., H. M. Byrne, P. K. Maini and T. Alarcón, "A Multiscale Model of Complex Endothelial Cell Dynamics in Early Angiogenesis", *PLOS Computational Biology*, Vol. 17, No. 1, p. e1008055, 2021.

148. Logg, A., G. N. Wells and J. Hake, *DOLFIN: A C++/Python Finite Element Library*, chap. 10, Springer, 2012.

149. Alnæs, M. S., J. Blechta, J. Hake, A. Johansson, B. Kehlet, A. Logg, C. Richardson, J. Ring, M. E. Rognes and G. N. Wells, "The FEniCS Project Version 1.5", *Archive of Numerical Software*, Vol. 3, No. 100, 2015.

150. Sadiku, M. N., *Numerical Techniques in Electromagnetics*, CRC Press, 2000.

151. Marchi, S., C. Giorgi, L. Galluzzi and P. Pinton, "Ca2+ Fluxes and Cancer", *Molecular Cell*, Vol. 78, No. 6, pp. 1055–1069, 2020.

152. Lee, J., A. Ishihara, G. Oxford, B. Johnson and K. Jacobson, "Regulation of Cell Movement Is Mediated by Stretch-Activated Calcium Channels", *Nature*, Vol. 400, No. 6742, pp. 382–386, 1999.

153. Stuelten, C. H., C. A. Parent and D. J. Montell, "Cell Motility in Cancer Invasion and Metastasis: Insights from Simple Model organisms", *Nature Reviews Cancer*, Vol. 18, No. 5, pp. 296–312, 2018.

154. Davis, F. M., I. Azimi, R. A. Faville, A. A. Peters, K. Jalink, J. Putney, G. J. Goodhill, E. W. Thompson, S. J. Roberts-Thomson and G. R. Monteith, "Induction of Epithelial–Mesenchymal Transition (EMT) in Breast Cancer Cells Is Calcium Signal Dependent", *Oncogene*, Vol. 33, No. 18, pp. 2307–2316, 2014.

155. Norgard, R. J., J. R. Pitarresi, R. Maddipati, N. M. Aiello-Couzo, D. Balli, J. Li, T. Yamazoe, M. D. Wengyn, I. D. Millstein, I. W. Folkert *et al.*, "Calcium Signaling Induces A Partial EMT", *EMBO Reports*, p. e51872, 2021.

156. Qi, L., W. Song, L. Li, L. Cao, Y. Yu, C. Song, Y. Wang, F. Zhang, Y. Li, B. Zhang *et al.*, "FGF4 Induces Epithelial-Mesenchymal Transition by Inducing Store-Operated Calcium Entry in Lung Adenocarcinoma", *Oncotarget*, Vol. 7, No. 45, p. 74015, 2016.

157. Wieland, E., J. Rodriguez-Vita, S. S. Liebler, C. Mogler, I. Moll, S. E. Herberich, E. Espinet, E. Herpel, A. Menuchin, J. Chang-Claude *et al.*, "Endothelial Notch1 Activity Facilitates Metastasis", *Cancer Cell*, Vol. 31, No. 3, pp. 355–367, 2017.

158. Huang, Q. B., X. Ma, H. Z. Li, Q. Ai, S. W. Liu, Y. Zhang, Y. Gao, Y. Fan, D. Ni, B. J. Wang *et al.*, "Endothelial Delta-Like 4 (DLL4) Promotes Renal Cell Carcinoma Hematogenous Metastasis", *Oncotarget*, Vol. 5, No. 10, p. 3066, 2014.

159. Kuramoto, T., H. Goto, A. Mitsuhashi, S. Tabata, H. Ogawa, H. Uehara, A. Saijo, S. Kakiuchi, Y. Maekawa, K. Yasutomo *et al.*, "Dll4-Fc, An Inhibitor of Dll4-notch Signaling, Suppresses Liver Metastasis of Small Cell Lung Cancer Cells Through The Downregulation of The NF-κB Activity", *Molecular Cancer Therapeutics*, Vol. 11, No. 12, pp. 2578–2587, 2012.

160. Mendonça, L., A. Trindade, C. Carvalho, J. Correia, M. Badenes, J. Gigante and A. Duarte, "Metastasis Is Impaired by Endothelial-Specific Dll4 Loss-of-Function Through Inhibition of Epithelial-to-Mesenchymal Transition and Reduction of Cancer Stem Cells and Circulating Tumor Cells", *Clinical & Experimental Metas-*

tasis, Vol. 36, No. 4, pp. 365–380, 2019.

161. Kubes, P. and D. N. Granger, "Nitric Oxide Modulates Microvascular Permeability", *the American Journal of Physiology-Heart and Circulatory Physiology*, Vol. 262, No. 2, pp. H611–H615, 1992.

162. Kim, P. K., R. Zamora, P. Petrosko and T. R. Billiar, "The Regulatory Role of Nitric Oxide in Apoptosis", *International Immunopharmacology*, Vol. 1, No. 8, pp. 1421–1441, 2001.

163. Miloudi, K., M. Oubaha, C. Ménard, A. Dejda, V. Guber, G. Cagnone, A. M. Wilson, N. Tétreault, G. Mawambo, F. Binet *et al.*, "NOTCH1 Signaling Induces Pathological Vascular Permeability in Diabetic Retinopathy", *Proceedings of The National Academy of Sciences*, Vol. 116, No. 10, pp. 4538–4547, 2019.

164. Snyder, C. M., E. H. Shroff, J. Liu and N. S. Chandel, "Nitric Oxide Induces Cell Death by Regulating Anti-Apoptotic BCL-2 Family Members", *PloS one*, Vol. 4, No. 9, p. e7059, 2009.

165. Watson, E., L. Whitehead, R. Adams, G. Dewson and L. Coultas, "Endothelial Cell Survival During Angiogenesis Requires The Pro-Survival Protein MCL1", *Cell Death & Differentiation*, Vol. 23, No. 8, pp. 1371–1379, 2016.

166. Bock, F. J. and S. W. Tait, "Mitochondria as Multifaceted Regulators of Cell Death", *Nature Reviews Molecular Cell Biology*, Vol. 21, No. 2, pp. 85–100, 2020.

167. Boyd, C. S. and E. Cadenas, "Nitric Oxide and Cell Signaling Pathways in Mitochondrial-Dependent Apoptosis", *Biological Chemistry*, Vol. 383, pp. 411–423, 2002.

168. Svitkina, T. M., A. B. Verkhovsky, K. M. McQuade and G. G. Borisy, "Analysis of The Actin–Myosin II System in Fish Epidermal Keratocytes: Mechanism of Cell Body Translocation", *Journal of Cell Biology*, Vol. 139, No. 2, pp. 397–415,

1997.

169. Iglesias, P. A. and P. N. Devreotes, "Navigating Through Models of Chemotaxis", *Current Opinion in Cell Biology*, Vol. 20, No. 1, pp. 35–40, 2008.

170. Pollard, T. D. and G. G. Borisy, "Cellular Motility Driven by Assembly and Disassembly of Actin Filaments", *Cell*, Vol. 112, No. 4, pp. 453–465, 2003.

171. Charras, G. and E. Paluch, "Blebs Lead The Way: How to Migrate without Lamellipodia", *Nature Reviews Molecular Cell Biology*, Vol. 9, No. 9, pp. 730–736, 2008.

172. Recho, P., T. Putelat and L. Truskinovsky, "Contraction-Driven Cell Motility", *Physical Review Letters*, Vol. 111, No. 10, p. 108102, 2013.

173. Callan-Jones, A. and R. Voituriez, "Active Gel Model of Amoeboid Cell Motility", *New Journal of Physics*, Vol. 15, No. 2, p. 025022, 2013.

174. Tjhung, E., D. Marenduzzo and M. E. Cates, "Spontaneous Symmetry Breaking in Active Droplets Provides A Generic Route to Motility", *Proceedings of The National Academy of Sciences*, Vol. 109, No. 31, pp. 12381–12386, 2012.

175. Gerisch, G., T. Bretschneider, A. Müller-Taubenberger, E. Simmeth, M. Ecke, S. Diez and K. anderson, "Mobile Actin Clusters and Traveling Waves in Cells Recovering from Actin Depolymerization", *Biophysical Journal*, Vol. 87, No. 5, pp. 3493–3503, 2004.

176. Reymann, A.-C., R. Boujemaa-Paterski, J.-L. Martiel, C. Guérin, W. Cao, H. F. Chin, M. Enrique, M. Théry and L. Blanchoin, "Actin Network Architecture Can Determine Myosin Motor Activity", *Science*, Vol. 336, No. 6086, pp. 1310–1314, 2012.

177. Fischer, R. S., P.-Y. Lam, A. Huttenlocher and C. M. Waterman, "Filopodia

and Focal Adhesions: An Integrated System Driving Branching Morphogenesis in Neuronal Pathfinding and Angiogenesis", *Developmental Biology*, Vol. 451, No. 1, pp. 86–95, 2019.

178. Kamp, T. J. and J. W. Hell, "Regulation of Cardiac L-type Calcium Channels by Protein Kinase A and Protein Kinase C", *Circulation Research*, Vol. 87, No. 12, pp. 1095–1102, 2000.

179. Li, F., C. Yang, F. Yuan, D. Liao, T. Li, F. Guilak and P. Zhong, "Dynamics and Mechanisms of Intracellular Calcium Waves Elicited by Tandem Bubble-Induced jetting Flow", *Proceedings of The National Academy of Sciences*, Vol. 115, No. 3, pp. E353–E362, 2018.

180. McIvor, E., S. Coombes and R. Thul, "Three-Dimensional Spatio-Temporal Modelling of Store Operated Ca2+ Entry: Insights Into ER Refilling and The Spatial Signature of Ca2+ Signals", *Cell Calcium*, Vol. 73, pp. 11–24, 2018.

181. Ademuyiwa, O. M., *The Role of Calcium Flux in The Regulation of Filopodia Dynamics*, Bowling Green State University, 2019.

182. Kiełbik, A., W. Szlasa, O. Michel, A. Szewczyk, M. Tarek, J. Saczko and J. Kulbacka, "In Vitro Study of Calcium Microsecond Electroporation of Prostate Adenocarcinoma Cells", *Molecules*, Vol. 25, No. 22, p. 5406, 2020.

183. Brossa, A., L. Buono, S. Fallo, A. Fiorio Pla, L. Munaron and B. Bussolati, "Alternative Strategies to Inhibit Tumor Vascularization", *International Journal of Molecular Sciences*, Vol. 20, No. 24, p. 6180, 2019.

184. Haibe, Y., M. Kreidieh, H. El Hajj, I. Khalifeh, D. Mukherji, S. Temraz and A. Shamseddine, "Resistance Mechanisms to Anti-Angiogenic Therapies in Cancer", *Frontiers in Oncology*, Vol. 10, p. 221, 2020.